SEQUENCE STRATIGRAPHY, PALAEOGEOGRAPHY AND PETROLEUM PLAYS OF THE CENOMANIAN – TURONIAN SUCCESSION OF THE ARABIAN PLATE: AN UPDATED SYNTHESIS

JPG Journal of Petroleum Geology www.jpg.co.uk

Journal of Petroleum Geology, Vol. 45(2), April 2022, pp 119-162

SEQUENCE STRATIGRAPHY, PALAEOGEOGRAPHY AND PETROLEUM PLAYS OF THE CENOMANIAN – TURONIAN SUCCESSION OF THE ARABIAN PLATE: AN UPDATED SYNTHESIS

A. D. Bromhead[1*], F.S.P. van Buchem[2], M.D. Simmons[1] and R.B. Davies[3]

In order to facilitate the search for new play concepts and exploration opportunities, a sequence stratigraphic synthesis of the Cenomanian–Turonian interval of the Arabian Plate has been compiled. The synthesis is based on published datasets which have been analysed within a temporal framework constrained by biostratigraphy and isotope stratigraphy. The high stratigraphic resolution allows the palaeogeography of the study area to be mapped within 3rd order depositional sequences, and the relative influence of eustacy and tectonics on basin development to be evaluated. This significantly improves the prediction of stratigraphic architecture and depositional morphology at the scale of the entire tectonic plate.

Conceptual models informed by outcrop and subsurface observations have been applied to characterize the development of intrashelf basins in depositional settings that are either isolated from siliciclastics (symmetric intrashelf basin model) or influenced by siliciclastics (asymmetric intrashelf basin model). The application of a sequence stratigraphic model across regional well log transects facilitates an understanding of stratigraphic architecture and acts as an important control for the generation of a new suite of gross depositional environment (GDE) maps. These maps characterize the palaeogeography at a previously unprecedented resolution and scale during both periods of high relative sea level (maximum flooding surface and highstand systems tract) and low relative sea level (lowstand systems tract). The maps are complemented by sequence isopachs which reveal changes in accommodation through time and space.

This approach helps characterize the preserved distribution and stratigraphic configuration of petroleum systems elements. In the Shilaif (UAE), Natih (Oman) and Sarvak (Iran) intrashelf basins, condensed, organic-rich carbonate source rocks were deposited in restricted, anoxic conditions. These basins resulted from differential aggradation of the carbonate platform during the transgressive systems tract. Grainy, rudist-debris –rich carbonate reservoir rocks developed along the margins of the intrashelf basins during highstand progradation. Claystones in the overlying sequence may form intraformational seals and were deposited during retrogradation of the shoreline associated with sea-level rise.

[1]Halliburton, 97 Jubilee Avenue, Milton Park, Abingdon, OX14 4RW, UK.
[2] King Abdullah University of Science and Technology, Thuwal 23955, Saudi Arabia.
[3] Davies Geoconsulting Limited, London.
* Corresponding author:
alex.bromhead@halliburton.com

Key words: Mid-Cretaceous, Arabian Plate, sequence stratigraphy, Gross Depositional Environment, intrashelf basins, reservoir, source rock, seal, subcrop trap.

By contrast in the Najaf intrashelf basin (Iraq), there is a significant siliciclastic component sourced from the Arabian Shield. This influx resulted in a mixed carbonate-siliciclastic ramp depositional system on the proximal, western margin of the basin, and an apparent absence of organic-rich intervals within the central basin succession. Grainy carbonate reservoir rocks are restricted to the eastern margin and are charged by older source rocks within the underlying stratigraphy.

The GDE maps record the configuration of these petroleum systems elements within the Cenomanian–Turonian interval and form the basis for play screening. The Cenomanian–Turonian interval is punctuated by the major mid-Turonian unconformity which is a tectonostratigraphic boundary of considerable geological and economic significance. In the southern and eastern part of the Arabian Plate, this unconformity has a differential erosion profile that facilitates a subcrop play with exploration potential. Identifying subtle stratigraphic traps is challenging, but by combining GDE facies with the mapped preservation limit for each sequence, it is possible to identify areas where rudist-rich reservoir facies with potential karst enhancement are overlain by a regional claystone seal, high-grading areas with subcrop trap potential.

INTRODUCTION

The Cenomanian–Turonian stratigraphic interval in the Arabian Plate contains prolific, high-quality conventional carbonate reservoirs in the Mishrif Formation and equivalent units such as the Sarvak and Natih Formations which are distributed from Oman to SE Turkey (Fig. 1). Most hydrocarbon accumulations associated with these reservoirs occur in structural closures, and undrilled structures are now scarce within what is a mature petroleum province. Future exploration opportunities within this interval are therefore likely to be restricted to stratigraphic traps. This is highlighted by some of the stratigraphic trapping concepts proposed for Mishrif reservoirs in the UAE which include diagenetic traps (Taher *et al.*, 2010), porosity pinch-outs (Loutfi *et al.*, 1987; Lü *et al.*, 2018) and subcrop traps (Burchette and Britton, 1985; Al-Zaabi *et al.*, 2010; Franco *et al.*, 2018), as well as isolated patch reefs in Iraq (Sadooni, 2005; Mahdi and Aqrawi, 2014). The Dujaila field in SE Iraq is interpreted as a stratigraphic trap (Sadooni, 2005; Khawaja and Thabit, 2021) and a similar trapping style has been suggested for the recently-discovered Eridu field located to the south, ca. 120 km west of Basra (Lukoil, 2017).

The Cenomanian–Turonian of the Arabian Plate has been extensively investigated at the outcrop scale (e.g. van Buchem *et al.*, 2002; Homewood *et al.*, 2008; Razin *et al.*, 2010; Kalanat *et al.*, 2021), at the field scale (e.g. Jordan *et al.*, 1985; Videtich *et al.*, 1988; Neo, 1996; Cantrell *et al.*, 2020), and at the scale of individual intrashelf basins (e.g. Droste and Van Steenwinkel, 2004; Aqrawi and Horbury, 2008; Al-Zaabi *et al.*, 2010; Vahrenkamp *et al.*, 2015; Franco *et al.*, 2018). However, studies that consider the interval at the scale of the Arabian Plate are scarce. As outlined in van Buchem *et al.* (2011), regional correlation of the interval based on lithostratigraphy is challenging as lithostratigraphic terms change across provincial boundaries and are used inconsistently (Fig. 2). This paper expands on van Buchem *et al.*'s (2011) study and attempts to apply a consistent sequence stratigraphic framework which enables the recognition and correlation of stratigraphic patterns across the entire Arabian Plate independent of lithostratigraphy (Fig. 2).

Despite the importance of regional palaeogeography to hydrocarbon exploration, the most recent plate-scale palaeogeographic maps published for the mid-Cretaceous of the Arabian Plate are those of Murris (1980), Burchette (1993) and Ziegler (2001) which provide useful regional context. However, an increase in both spatial and temporal resolution is required for purposes of exploration and field appraisal. This contribution therefore aims to provide a series of data-supported gross depositional environment (GDE) maps at the scale of the Arabian Plate within a high-resolution sequence stratigraphic framework. The GDE maps are supported by sequence isopachs generated from the interpretation of well and outcrop data. These two sets of maps offer new insights and demonstrate significant variations in thicknesses and depositional patterns across the Arabian Plate, and in combination help to unravel the competing influences of eustacy and tectonics on intrashelf basin development.

METHODOLOGY

This study uses published datasets to characterize the Cenomanian–Turonian stratigraphic interval across the Arabian Plate. These datasets, which include well logs and outcrop logs (Fig. 3) together with sparse 2D seismic data plus supporting studies, are integrated within a consistent biostratigraphically age-constrained sequence stratigraphic framework (Fig. 2) derived from the Arabian Plate Sequence Stratigraphic model of Sharland *et al.* (2001).

The sequence stratigraphic model was applied to a stratigraphic dataset consisting of 626 published wells and 176 published outcrop sections from the Arabian Plate (Fig. 3). This dataset was supported by sedimentological and petrographic descriptions, biostratigraphic and carbon isotope data, rock property and organic geochemistry datasets, a tectonic elements map, a dataset for the known distribution of hydrocarbon occurrences, and a limited number

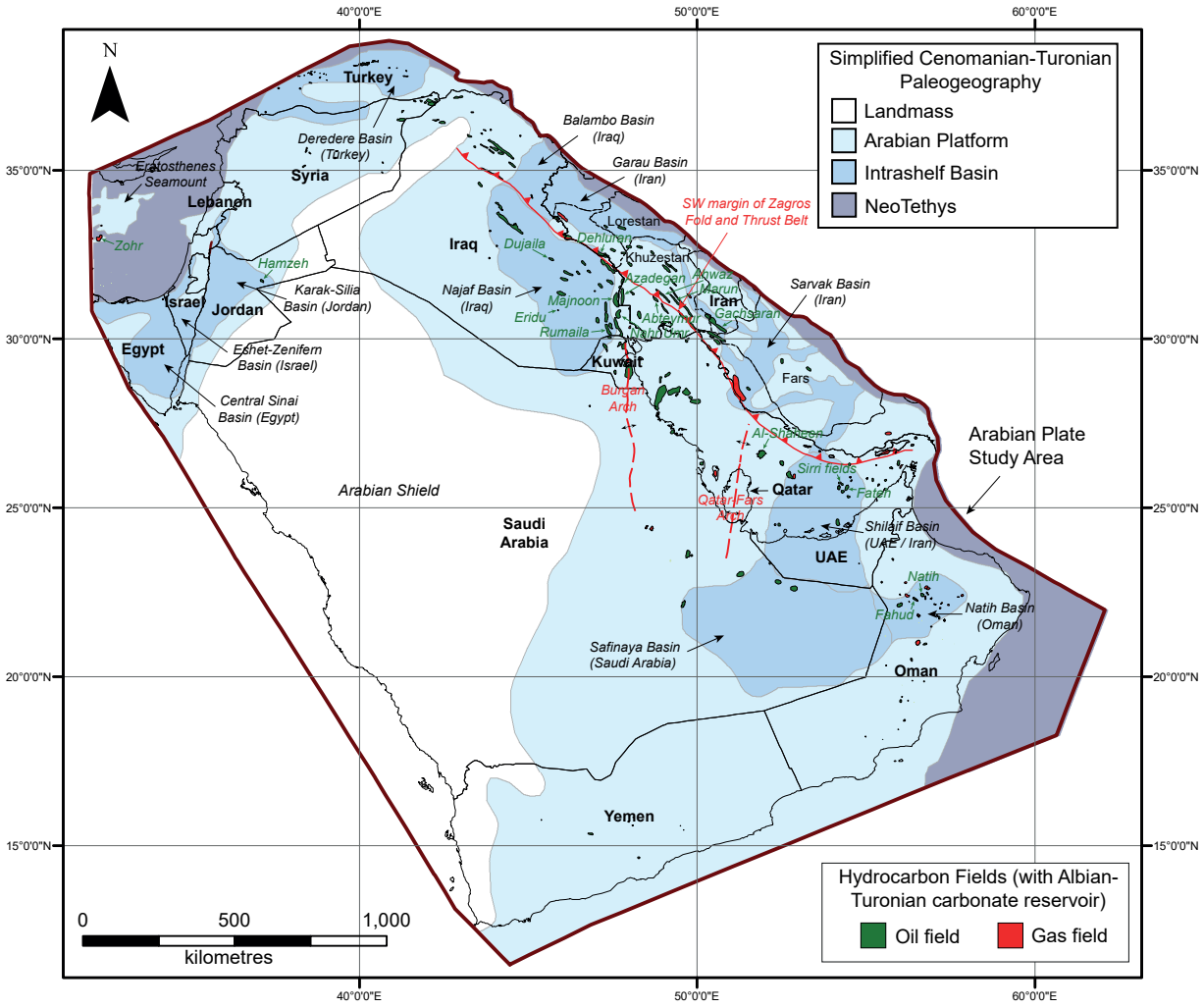

Fig. 1. Location map of the Arabian Plate showing key geological and palaeogeographic features, along with the distribution of oil and gas fields with a producing Albian–Turonian carbonate reservoir interval. The palaeogeography has been generalized to show the maximum extent of Cenomanian–Turonian intrashelf basins within the Arabian Platform. The configuration of the intrashelf basins in each depositional sequence within the Cenomanian–Turonian is shown in Fig. 12 (page 141). Oil and gas fields discussed in the text are labelled.

of published 2D seismic transects. The quality and completeness of stratigraphic sections derived from the public domain was found to be highly variable.

The sequence stratigraphic model was first applied to high-quality sections with age constraint from biostratigraphy and/or carbon isotope curves (Fig. 4). This enabled characteristic sequences to be established and correlated into other data based on wireline log patterns and changes in sedimentology and depositional facies. From this, conceptual models for the creation and infill of Cenomanian–Turonian intrashelf basins were established (Fig. 5).

Not all of the stratigraphic sections used in this study are directly age constrained. However, the application of the sequence stratigraphic model provides a proxy age attribution for each sequence stratigraphic surface interpreted within the dataset, regardless of data quality. This is key to unlocking value as it creates a consistent, structured and temporally precise dataset that can offer new geological insight when integrated into a variety of regional mapping and exploration workflows.

A series of regional stratigraphic transects were constructed across the Arabian Plate which demonstrate variations in sequence preservation, thickness and morphological expression. These transects cover the southern plate (Oman, Saudi Arabia and the UAE) (Fig. 6), southern Iraq (Fig. 7), central Iraq (Fig. 8), southwest Iran (Fig. 9) and the northern plate (Egypt, Jordan, Lebanon, Turkey and northern Iraq (Fig. 10). This was valuable in the assessment of the tectonostratigraphic evolution of the mid-Cretaceous interval, particularly in the absence of seismic data. In any case the length of the correlation transects substantially exceeds that which could be obtained from seismic data, and the large length scale, combined with the stratigraphic detail in vertical sections, is valuable in recognising the geometric evolution of the stratigraphic architecture.

The sequence stratigraphic framework formed the basis for the generation of GDE maps for specific time

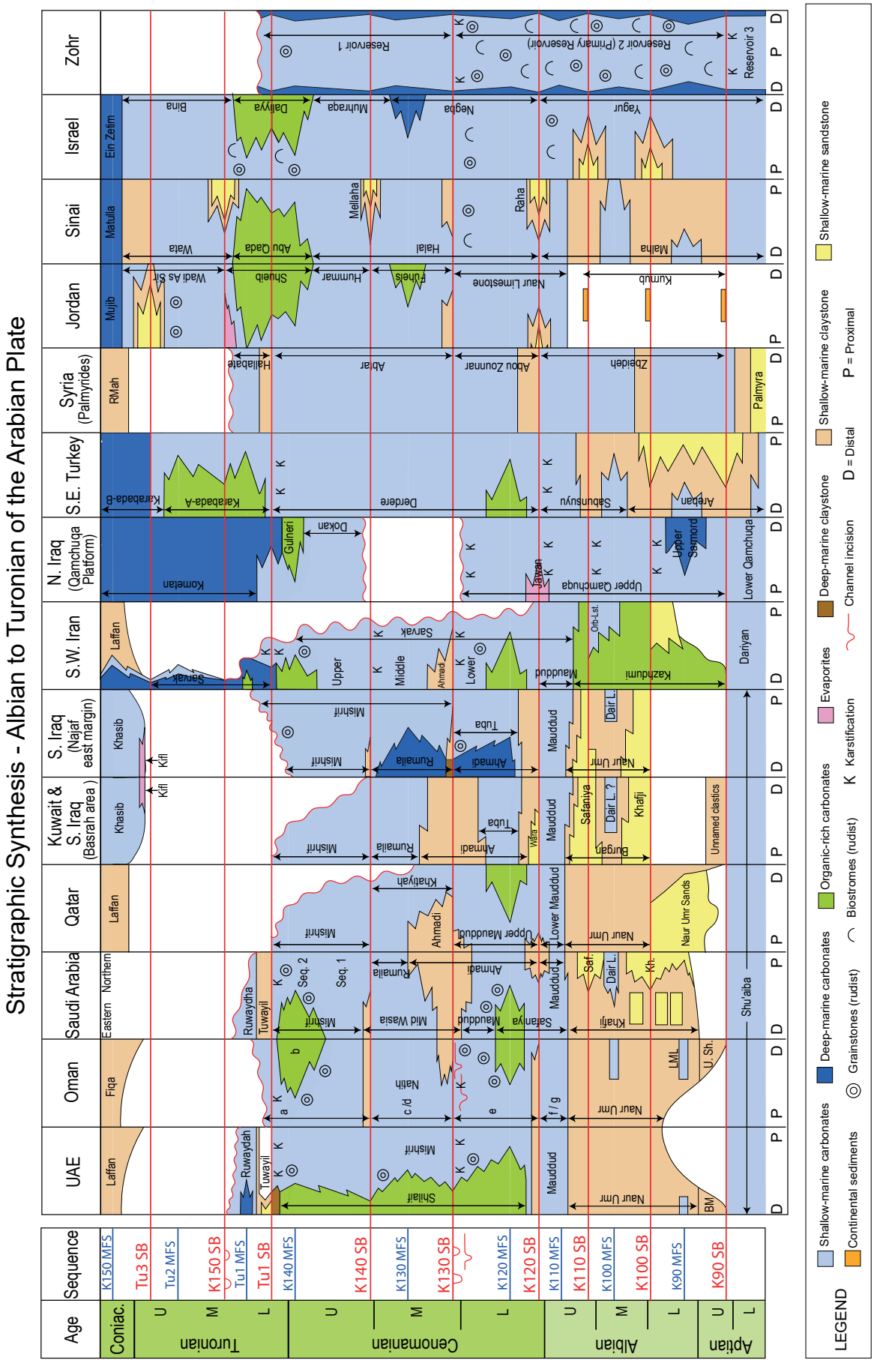

Fig. 2. Stratigraphic synthesis for the middle Cretaceous of Arabia. The consistent, age-attributed sequence stratigraphic framework clarifies the disjointed lithostratigraphy. Modified after van Buchem *et al.* (2011).

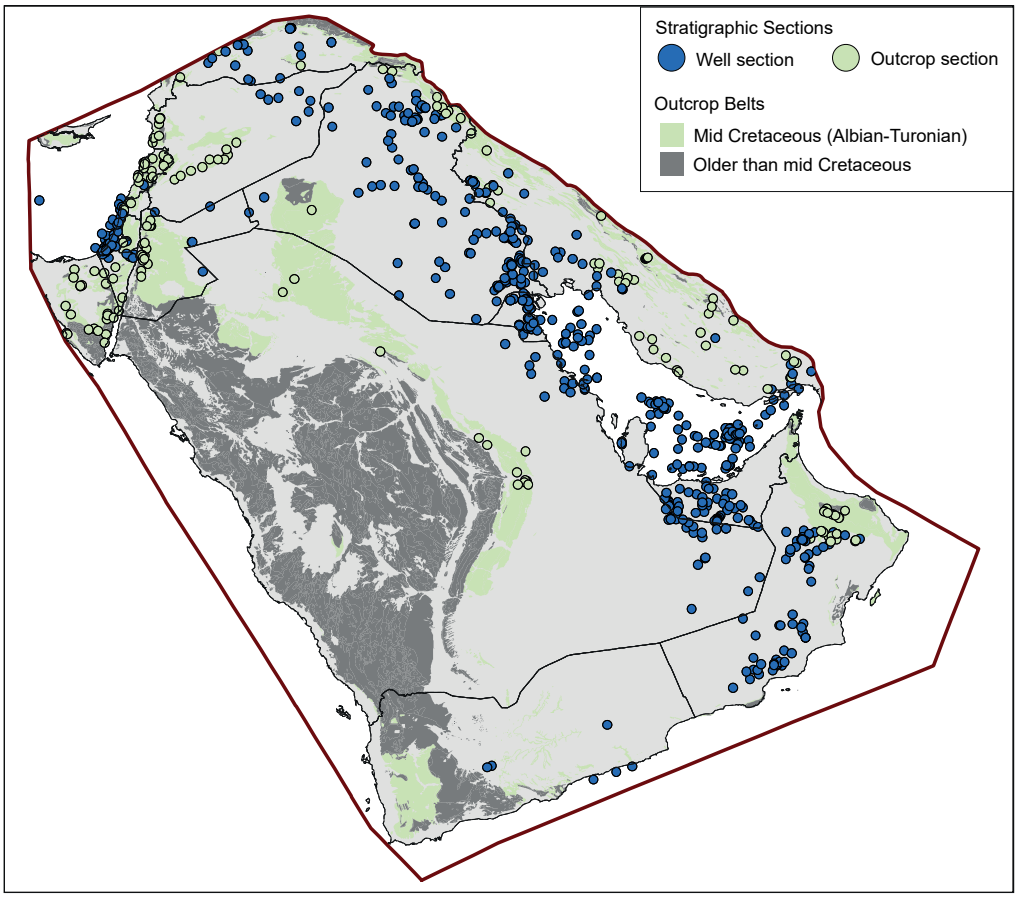

Fig. 3. Location map showing the distribution of stratigraphic sections (wells and outcrops) interpreted within this study. The configuration of outcrop belts is shown for the mid-Cretaceous (Albian–Turonian) and the older pre– mid-Cretaceous stratigraphy.

intervals during the late Albian to Turonian. These maps illustrate the palaeogeography and depositional settings across the Arabian Plate related to either the Maximum Flooding Surface (MFS), Highstand Systems Tract (HST) or Lowstand Systems Tract (LST) of each depositional sequence. A combination of these three mapping surfaces enables the depositional system to be represented throughout a full sea-level cycle at relatively high temporal resolution (Fig. 11). The configuration of petroleum systems elements, such as organic-rich carbonate source rocks and grainstone carbonate reservoirs, can be represented on these maps and serves as a basis for regional play screening. The MFS maps for each depositional sequence characterize palaeogeography and the evolution of depocentres from the late Albian to the middle Turonian (Fig. 12). The GDE maps are supplemented by sequence-level isopach maps that support the palaeogeographic and tectonostratigraphic trends depicted (Fig. 13).

TECTONOSTRATIGRAPHIC OVERVIEW

During the mid-Cretaceous, the Arabian Plate lay on the southern margin of NeoTethys in a position close to the equator (Sharland *et al.*, 2001; Scotese, 2021). Relatively high sea levels (Miller *et al.*, 2005; Haq, 2014; Simmons *et al.*, 2020; Wright *et al.*, 2020) led to inundation of the plate and the widespread deposition of shallow-marine carbonates, although siliciclastic units were deposited proximal to the Arabian Shield and prograded basinwards during lowstands (Davies *et al.*, 2002; 2019; van Buchem *et al.*, 2011). Carbonates and siliciclastics within the mid-Cretaceous interval form some of the most prolific conventional petroleum reservoirs in the world.

Significant plate-scale depositional and tectonostratigraphic trends are evident through the mid-Cretaceous of the Arabian Plate (Fig. 2) and are summarised briefly below:

Albian

The latest Aptian to Albian interval represents a significant break in the over- and underlying carbonate-dominated stratigraphy (Davies *et al.*, 2019). A combination of eustatic sea-level fall (Haq, 2014) and uplift of the Arabian Shield related to far-field stresses generated by accelerated South Atlantic opening (Stampfli and Borel, 2002), along with the humid climatic conditions (Poinar *et al.*, 2004), caused large volumes of siliciclastic sediment to be shed from the exposed Arabian Shield in an easterly direction. These siliciclastics were deposited across much of the Arabian

Plate within a broad, muddy ramp system. Deltaic sedimentation resulted in the deposition of highly porous and permeable siliciclastic reservoir rocks in proximal areas (e.g. Burgan Formation; Strohmenger *et al.*, 2006; Datta *et al.*, 2011, 2019), with source rocks developed more distally (e.g. Kazhdumi Formation; Davies *et al.*, 2002; Bordenave, 2014; Sfidari *et al.*, 2016). In the late Albian, these siliciclastic systems were suppressed during a transgression (K110 MFS *sensu* Sharland *et al.*, 2001) and a broad carbonate ramp (Mauddud Formation and regional equivalents) was established across the plate (Davies *et al.*, 2002, 2019; Strohmenger *et al.*, 2006; Cross *et al.*, 2010; van Buchem *et al.*, 2011).

Cenomanian

The Cenomanian interval of the Arabian Plate is characterized by intrashelf basin development within a broad carbonate platform (Sharland *et al.*, 2001; van Buchem *et al.*, 2011) (Fig. 1). Characterizing the evolving configuration and depositional evolution of these intrashelf basins through the mid-Cretaceous is paramount for exploration success, as they exert a strong control on the distribution of source, reservoir and seal rocks (*see below*). Some of these basins such as the Shilaif Basin (centred around the United Arab Emirates: Al-Zaabi *et al.*, 2010; Vahrenkamp *et al.*, 2015) and the Najaf Basin (centred around southern Iraq: Aqrawi and Horbury, 2008; Aqrawi *et al.*, 2010a, b) were relatively long-lived and spanned the entire Cenomanian; others such as the Natih E and Natih B Basins in northern Oman were created and infilled within a single depositional sequence (van Buchem *et al.*, 2002) (locations in Fig. 1).

During the Cenomanian, low frequency retrogradation of the Albian siliciclastic systems occurred as the Arabian Shield hinterland was denuded. Siliciclastic units within the Cenomanian became less areally extensive through time (Davies *et al.*, 2002, 2019) but occur particularly along the western margin of the Arabian Platform. These units include the Wara sandstones and Ahmadi shales in Kuwait, southern Iraq and Saudi Arabia (van Bellen *et al.*, 1959; Davies *et al.*, 2002; Alsharhan *et al.*, 2014; Youssef *et al.*, 2014, 2019; Al-Anzi and Tourqui, 2019) and fine-grained siliciclastics within the Natih Formation of Oman (Droste and Van Steenwinkel, 2004; Homewood *et al.*, 2008). In southern Iraq and Kuwait, the Upper Ahmadi Member represents the last significant siliciclastic pulse within the Cenomanian before the Mishrif carbonate platform became established (Davies *et al.*, 2002, 2019). Cenomanian siliciclastic pulses may have been related to relative sea-level falls which may have coincided with more humid climatic intervals (Davies *et al.*, 2002, 2019).

Turonian

The Turonian is associated with uplift across the southern part of the Arabian Plate, and a major erosional unconformity in the mid-Turonian (Harris *et al.*, 1984; Droste and Van Steenwinkel, 2004; Ghabeishavi *et al.*, 2009, 2010) forms the top of the early-mid Cretaceous AP8 tectonostratigraphic megasequence of Sharland *et al.* (2001). This unconformity marks a transition from a passive to an active margin along the eastern edge of the Arabian Plate. The initiation of a subduction zone within the central NeoTethys and progressive closure of the southern branch of the ocean resulted in compression within the southern and eastern Arabian Plate (Robertson and Searle, 1990) as a precursor to Late Cretaceous ophiolite obduction (Searle *et al.*, 2014). As a result of this uplift, the preservation of Turonian stratigraphy, and in some areas Cenomanian stratigraphy, is variable across the southern part of the plate (Fig. 2).

Petroleum Systems

The Cenomanian–Turonian petroleum system in the Arabian Plate in general refers to the carbonate reservoirs in the Mishrif Formation (and its regional equivalents) (Fig. 2), and is one of the most prolific and volumetrically significant petroleum systems known. Numerous giant and supergiant hydrocarbon fields produce from these reservoirs within structural and stratigraphic traps (Fig. 1). Conventional reservoirs typically occur within grainy rudist-rich carbonates developed at the margins of intrashelf basins (Jordan *et al.*, 1985; Burchette and Britton, 1985; Burchette, 1993; Perrotta *et al.*, 2017). The reservoir properties of the Mishrif carbonates may be enhanced as a result of karstification and meteoric diagenesis (Wagner, 1990; Sharp *et al.*, 2010; Hajikazemi *et al.*, 2017; Malekzadeh *et al.*, 2020), fracturing and/or dolomitisation (Sharp *et al.*, 2006; 2010; Lapponi *et al.*, 2011).

The late Albian Mauddud Formation is generally a relatively minor carbonate reservoir compared to the Mishrif Formation. The main exception to this is in Kuwait, where the Mauddud Formation is a much more prolific reservoir as the shales of the overlying Ahmadi Formation form an effective seal preventing charge to the Mishrif Formation (Al-Anzi, 1995; Strohmenger *et al.*, 2006; Cross *et al.*, 2010; Vincent *et al.*, 2020). The early Turonian Tuwayil Formation is recognized as a siliciclastic reservoir (Azzam, 1995), although volumes are relatively minor compared to production from the Mishrif Formation and equivalents.

Source rocks for the hydrocarbons reservoired in the Cenomanian–Turonian carbonate reservoirs include mid-Cretaceous organic-rich carbonates and marls deposited within the intrashelf basins, such as the Kazhdumi (Iran), Shilaif (UAE), Safinaya (Saudi Arabia) and Natih (Oman) Formations. They

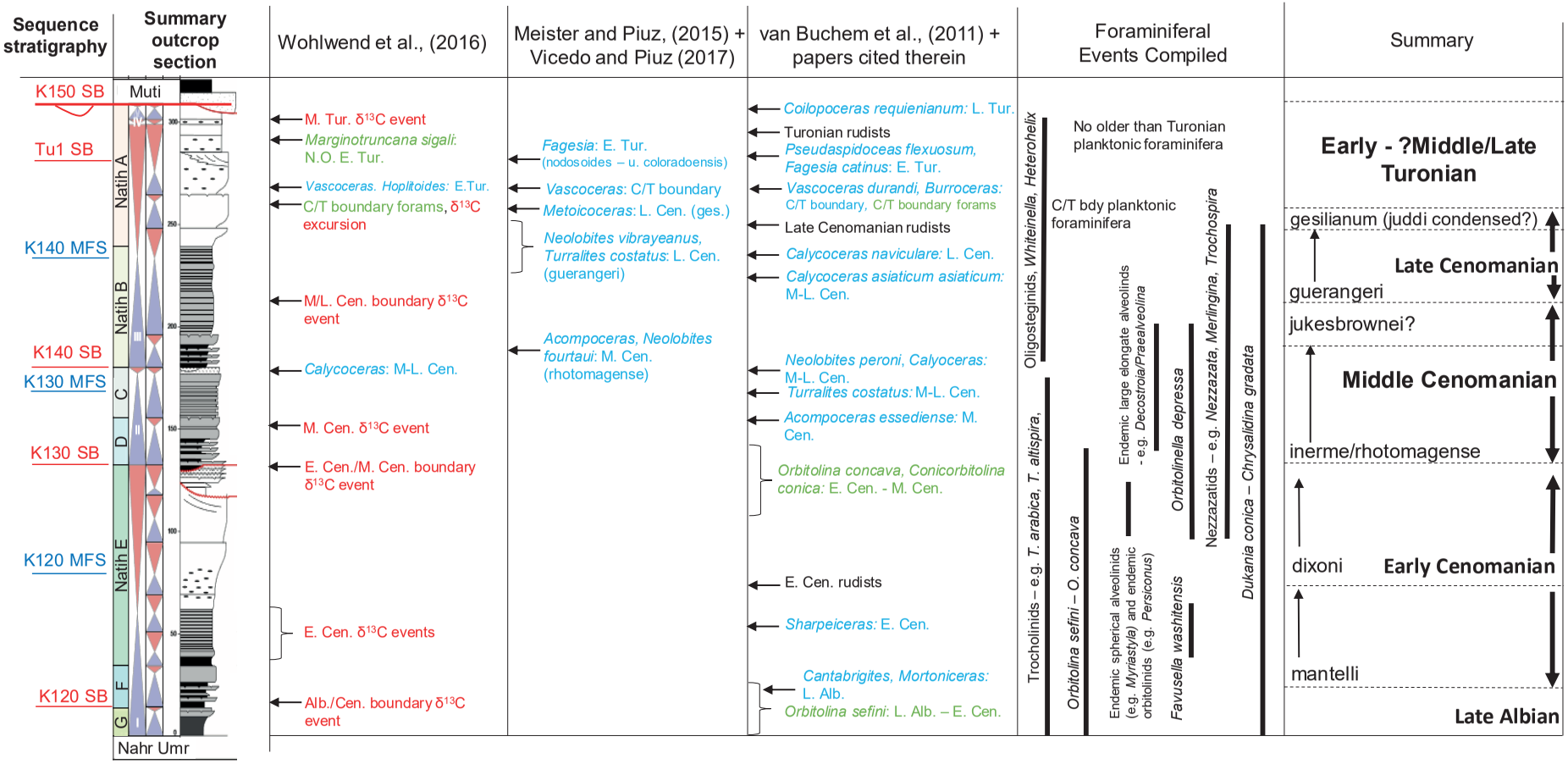

Fig. 4. Type outcrop section through the Natih Formation in Oman indicating the age constraints used to establish the Arabian Plate Sequence Stratigraphic Model surfaces used in this study. Blue text = ammonites, green text = foraminifera, and red text = δ^{13}C isotope events.

also include major source rocks in the underlying succession such as the Upper Jurassic – Lower Cretaceous Sulaiy and Yamama Formations (SE Iraq) (Abeed *et al.*, 2012); the Middle – Upper Jurassic Sargelu and Naokelekan Formations (Iraq) (Pitman *et al.*, 2004; Al Ameri and Zumberge, 2012; Grabowski, 2014; Al-Khafaji *et al.*, 2018); the Middle Jurassic Sargelu and Lower Cretaceous Garau Formations in the Abadan Plain (SW Iran) (Bordenave and Huc, 1995; Dehyadegari, 2019); and intervals in the Precambrian–Cambrian Huqf Group (Oman) (Terken, 1999).

SEQUENCE STRATIGRAPHIC FRAMEWORK

Sequence Stratigraphic Model Definition

The sequence stratigraphic model used in this study is a derivation of the Arabian Plate Sequence Stratigraphic Model of Sharland *et al.* (2001) as updated by Davies *et al.* (2002) and van Buchem *et al.* (2011). The model divides the stratigraphy into 3rd order depositional sequences bounded by sequence boundaries. These sequences have a global signature and are therefore likely to be related to eustacy (Scott *et al.*, 2000; Simmons *et al.*, 2007). The sequences display a marked cyclicity (Davies *et al.*, 2002); typically, platform successions begin with a sequence boundary which may show variable evidence for subaerial exposure and karstification (Wagner, 1990), overlain by transgressive facies which initially consist of claystones or marls passing up into clean carbonates during the maximum flooding interval and subsequent highstand. This succession represents a backstepping facies pattern in which clay-rich inner platform sediments were followed by cleaner, mid-outer platform deposits that were carbonate-dominated. Carbonate deposition occurred away from the influence of clays which suppressed the carbonate factory. Lowstands may be recognised in intrashelf basins and along the platform margin and often contain a significant siliciclastic component.

The third-order sequences recognised are as follows (from oldest to youngest) (Fig. 2):

K110 (late Albian): This sequence is associated with a transgression that led to widespread carbonate deposition typified by the Mauddud Formation. This followed mostly siliciclastic deposition across the Arabian Plate during the late Aptian – middle Albian.

K120 (early Cenomanian): The sequence boundary (SB) at the base of this sequence lies close to the Albian–Cenomanian boundary and was followed by a transgression which created intrashelf basins such as the Shilaif Basin in the UAE and the Natih E Basin in Oman. There is varying evidence at the K120 sequence boundary for exposure and erosion of the underlying K110 sequence; it can be clearly demonstrated in Kuwait (Strohmenger *et al.*, 2006; Vincent *et al.*, 2020) but is not evident in Oman (van Buchem *et al.*, 2002).

K130 (middle – late Cenomanian): A major sequence boundary occurs around the lower/middle Cenomanian boundary and is associated with erosion and channel incision (e.g. Grelaud *et al.*, 2006, 2010; Homewood *et al.*, 2008; Sharp *et al.*, 2010). This was followed by sea-level rise associated with a middle Cenomanian maximum flooding surface and its subsequent highstand.

K140 (late Cenomanian – earliest Turonian): This depositional cycle is mostly late Cenomanian in age with a maximum flooding surface coincident with the onset of OAE2 (e.g. Wohlwend *et al.*, 2016). A capping sequence boundary occurs within the early Turonian. This sequence is associated with the Mishrif Formation in many parts of the Arabian Plate.

K150 (middle Turonian – middle Coniacian): The middle Turonian sequence boundary (K150 SB of Sharland *et al.*, 2001) represents a major tectonically enhanced boundary which defines the top of early – middle Cretaceous tectonostratigraphic megasequence AP8 and which is associated with major erosion and truncation (Jordan *et al.*, 1985; Droste and Van Steenwinkel, 2004; Soroka *et al.*, 2005; Ghabeishavi *et al.*, 2009, 2010). Incised valleys up to 65 m deep have been described from Oman (Droste and Van Steenwinkel, 2004) and Khuzestan, SW Iran (Azar *et al.*, 2009). The K150 MFS occurs within the early Coniacian, and is therefore younger than the stratigraphic interval which is the focus of this study. It records widespread transgression across the southern and eastern parts of the Arabian Plate that post-dates regional uplift. Fine-grained siliciclastic and carbonate mudstones (e.g. Laffan Formation) deposited during this transgression form an important regional top-seal for Cenomanian–Turonian carbonate reservoirs beneath the mid-Turonian unconformity.

In addition to the Arabian Plate Sequence Stratigraphic model surfaces of Sharland *et al.* (2001), this study recognizes two additional sequences within the Turonian (Fig. 2):

Tu1 (early – middle Turonian): This sequence precedes the mid-Turonian erosional unconformity (K150 SB) and is only variably preserved across the southern and eastern portions of the Arabian Plate. It is associated with the Tuwayil and Ruwaydah Formations.

Tu2 (middle – late Turonian): The base of this sequence is represented by the K150 SB (*sensu* Sharland *et al.*, 2001) and corresponds to the mid-Turonian tectonostratigraphic megasequence boundary. The sequence is coincident with regional uplift across the southern and eastern parts of the Arabian Plate and is therefore only typically recognized along the

northern and NW plate margins. Middle-late Turonian stratigraphy corresponding to this sequence is also recognized in the lower part of the Surgah Formation in the Garau Basin, southwest Iran (Moghaddam, 2017; Raziani *et al.*, 2018), which appears to have been preserved despite mid-Turonian inversion. The top of this sequence corresponds to the Tu3 SB which is positioned within the upper Turonian. The Tu3 SB pre-dates the Coniacian K150 MFS of Sharland *et al.* (2001), and hence the Tu2 sequence can be considered as an additional division within the K150 sequence of Sharland *et al.* (2001).

Recognizing and Age Constraining Sequences at Outcrop

Outcrops of the mid-Cretaceous stratigraphic interval occur in the Al Hajar Mountains and the Jebel Akhdar area in northern Oman and in the Zagros Mountains of SW Iran, and provide an opportunity to build a reference model that can be applied in the subsurface and regionally across the Arabian Plate. These outcrops have been studied extensively: in Oman by van Buchem *et al.* (1996, 2002), Grelaud *et al.*, (2006, 2010); Homewood *et al.* (2008) and Razin *et al.* (2017); and in Iran by Razin *et al.* (2010), Vincent *et al.* (2015), Navidtalab et al (2019), Navidtalab *et al.* (2020) and Kalanat *et al.* (2021). The outcrops are valuable for reference as they enable depositional sequences to be identified in age-constrained sections and correlated into the subsurface, and allow the depositional morphology to be characterized in three dimensions. In addition, the outcrops provide detailed sedimentological profiles where vertical evolution of depositional facies can be characterized.

The Natih Formation is well exposed in northern Oman, allowing detailed stratigraphic calibration of the sequences present from a mixture of microfossil, macrofossil and stable-isotope –based data. The outcrops represent an excellent location for the age calibration of the mid-Cretaceous sequences (Fig. 4), whose correlation to other successions on the Arabian Plate is shown in Fig. 2. Much of the Natih succession is rich in shallow-marine benthic foraminifera (e.g. Simmons and Hart, 1987; Smith *et al.*, 1990; Kennedy and Simmons, 1991; Piuz *et al.*, 2014; Vicedo and Piuz, 2017; Piuz and Vicedo, 2020) and rudists (Philip *et al.*, 1995). More open-marine sediments are also present, especially in those parts of the succession which were deposited in intrashelf basinal conditions (van Buchem *et al.*, 2002, 2011; Droste, 2010), and contain ammonites and planktonic foraminifera (e.g. Kennedy and Simmons, 1991, van Buchem *et al.*, 2002, 2011; Meister and Piuz, 2015, Wohlwend *et al.*, 2016; Vicedo and Piuz, 2017). Detailed carbon isotope studies of the formation have also been carried out (e.g. Vahrenkamp, 2013; Wohlwend *et al.*, 2016), and in combination this stratigraphic information allows a fairly accurate calibration of the Natih succession to the standard NeoTethyan ammonite zonation for the late Albian – Turonian (Wright *et al.*, 2017; Gale *et al.*, 2020) (Fig. 4).

The Natih Formation is divided into seven members, lettered A-G from top to bottom (Tschopp, 1967), which have distinctive wireline log characteristics (Forbes *et al.*, 2010). Notwithstanding that lateral facies variations due to the presence of intrashelf basins may cause uncertainty in the precise position of lithostratigraphic boundaries (Vicedo and Piuz, 2017), these seven members can be traced from the subsurface into the outcrop belt with fairly high confidence (van Buchem *et al.*, 2002; Homewood *et al.*, 2008; Razin *et al.*, 2017) and can be correlated regionally (Fig. 2). The seven Natih Members are summarised briefly below.

The Natih G Member represents the uppermost part of the K110 sequence and is late Albian in age based on the presence of a carbon isotope event around the boundary with the Natih F Member which is interpreted to be associated with the Albian–Cenomanian boundary (Wohlwend *et al.*, 2016). The presence of the benthic foraminifera *Orbitolina seifini* (e.g. Simmons and Hart, 1987) supports this age assignment as the species has a late Albian – early Cenomanian age range (Simmons *et al.*, 2000).

The Natih F Member marks the base of the K120 Sequence. Near the base of the member is the Albian–Cenomanian boundary carbon isotope event (Wohlwend *et al.*, 2016). The member begins with transgressive marls which pass up into the intrashelf basin facies of the Natih E comprising open-marine, chalky and organic-rich limestones. The K120 MFS is located at the turnaround point into cleaning- and shallowing-up carbonates of the upper Natih E, with a sequence boundary located at the top of the member expressed as a prominent exposure surface (van Buchem *et al.*, 2002; Grélaud *et al.*, 2006, 2010; Homewood *et al.*, 2008; Razin *et al.*, 2017). Late Albian ammonites (*Cantabrigites, Mortoniceras*) have been reported from within the Natih F and the lowest part of the Natih E (van Buchem *et al.*, 2011; Luc Bulot, *pers. comm.* 2021). The Natih F is therefore most likely to be latest Albian to earliest Cenomanian in age.

The Natih E Member is almost entirely early Cenomanian in age. The lower part of the member, which consists of deep-water intrashelf basin facies, contains carbon isotope events correlated to those within the *mantelli* zone of the early Cenomanian. This age assignment is supported by the presence of the ammonite *Sharpeiceras* (van Buchem *et al.*, 2011). The boundary between the *mantelli* and *dixoni* zones of the early Cenomanian is uncertain in the Natih E succession, but the early–middle Cenomanian boundary carbon isotope event has been detected at the

top of the member. Support for an early Cenomanian age assignment for the upper part of the Natih E comes from the benthic foraminifera and rudists present (e.g. Simmons and Hart, 1987; Philip *et al.*, 1995), although it is now known that much of the distinctive benthic foraminifera fauna in the uppermost Natih E is in fact endemic (e.g. Piuz *et al.*, 2014; Vicedo and Piuz, 2017; Schlagintweit and Yazdi-Moghadam, 2020) and thus offers no direct age calibration. K120 is thus dated as early Cenomanian.

Sequence K130 begins at the clear sequence boundary between the Natih D and E Members and extends up to the sequence boundary at the Natih C-B transition. The Natih D Member contains transgressive shales and marls which pass up into the cleaning- and shallowing-up highstand carbonates of the Natih C, within which an MFS is located. The Natih D and C Members can be assigned to the *rhotomagense* zone of the middle Cenomanian. The short duration *inerme* zone may be present within the Natih D, but there is no direct evidence for its presence. Assignment to the *rhotomagense* zone is supported by the presence of the middle Cenomanian carbon isotope event in the upper part of the Natih D Member (Wohlwend *et al.*, 2016). The ammonites *Acompoceras* and *Neolobites fourtaui* which have been found in the lower part of the Natih B Member suggest an age no younger than the *rhotomagense* zone (Meister and Piuz, 2015). Sequence K130 is thus of middle Cenomanian age (*rhotomagense* zone).

Sequence K140 extends from the base of the Natih B to an erosion surface within the Natih A. The Natih B consists of intrashelf basin facies, with the K140 MFS located approximately at the downlap surface which introduces the highstand progradational carbonates of the Natih A. The lowest part of the Natih B belongs to the *rhotomagense* zone of the middle Cenomanian. No definitive evidence for the presence of the *jukesbrowni* zone of the middle Cenomanian is present. However the zone is assumed to occur within the Natih B, below the middle/late Cenomanian boundary carbon isotope event which occurs within the middle of the member (Wohlwend *et al.*, 2016). Above this, the upper part of the Natih B contains late Cenomanian (*guerangeri* zone) ammonites including a distinctive *Neolobites vibrayeanus* fauna (Meister and Piuz, 2015).

The lower part of the Natih A Member contains evidence for both the *guerangeri* and *geslinianum* ammonite zones (e.g. *Metoicoceras*) (e.g. Meister and Piuz, 2015). Overlying this within the lower Natih A is the Cenomanian/Turonian boundary carbon isotope event (Wohlwend *et al.*, 2016), suggesting that the *juddi* zone of the latest Cenomanian is condensed. The location of the boundary is supported by the presence of ammonites and planktonic foraminifera typical of the Cenomanian–Turonian transition (Kennedy and Simmons, 1991; Meister and Piuz, 2015; Wohlwend *et al.*, 2016). Sequence K140 is thus of middle Cenomanian – early Turonian age with an MFS located in the uppermost *guerangeri* zone of the late Cenomanian.

The upper part of the Natih A is clearly Turonian in age, although how young it ranges within the Turonian is uncertain. Early Turonian (*nodosoides* – upper *coloradoensis* zone) ammonite faunas (e.g. *Fagesia*) are present within the upper Natih A (Kennedy and Simmons, 2001; Meister and Piuz, 2015). Wohlwend *et al.* (2016) found a carbon isotope event towards the top of the Natih A that they associated with a middle Turonian event. A late Turonian ammonite *Coilopoceras requienianum* has been reported from near the top of the formation (van Buchem *et al.*, 2002) but this has been disputed (Luc Bulot, *pers. comm.* 2021) and the specimen may be *Choffaticeras* of early – middle Turonian age. A Turonian age for at least part of Natih A is indicated from the foraminiferal fauna (*Dohia planata, Dictyoconella minima*) reported from the subsurface (Forbes *et al.*, 2010).

Conceptual models for the development of Cenomanian intrashelf basins

Cenomanian–Turonian intrashelf basins on the Arabian Plate have been extensively studied. van Buchem *et al.* (1996) proposed a model for the development of intrashelf basins in a carbonate platform setting based on a study of the Natih Formation in Oman. This model was expanded by van Buchem *et al.* (2002) and Razin *et al.* (2017), and is consistent with studies of the Sarvak Formation in SW Iran (Razin *et al.*, 2010). The model is considered to be broadly applicable to Cenomanian–Turonian intrashelf basins developed in the southern part of the Arabian Plate, in tectonically quiescent settings which are largely isolated from siliciclastic input. Under these conditions, the intrashelf basins which develop are symmetric and are characterized by margins that are broadly comparable along their entire perimeter in terms morphology, thickness and depositional facies. In addition to the Natih intrashelf basin, the Shiliaf intrashelf basin (UAE, Saudi Arabia and offshore Iran) and the Sarvak intrashelf basin (SW Iran) (Fig. 1) conform to this category.

An alternative model is required for areas more proximal to the Arabian Shield where the input of siliciclastic material was more significant. The "Migratory Carbonate Suppressed Belt" model presented by Davies *et al.* (2002) and Davies *et al.* (2019) characterizes the mid-Cretaceous depositional system near the western margin of the Arabian Shield in northern Saudi Arabia, Kuwait and southern Iraq. In these settings, the siliciclastic input mostly impacts the inboard basin margin while the outboard margin remains relatively unaffected, resulting in the development of a strongly asymmetric intrashelf

basin or homoclinal ramp system. The asymmetric intrashelf basin model is typified by the Najaf Basin in southern Iraq. The deposition of the early Turonian Tuwayil Formation (K150 LST) in the Shilaif Basin also conforms to the lowstand component of this model, although there is a tectonic overprint related to hinterland uplift.

Herein, we consider the development of Cenomanian–Turonian intrashelf basins in terms of these two end-member models (Fig. 5 and Table 1). This has significant implications for the prediction of petroleum systems elements. For instance, asymmetric intrashelf basins such as the Najaf Basin (SE Iraq) exhibit significant variations between the inboard and outboard basin margins in terms of carbonate reservoir presence and quality. In addition, siliciclastic input within the asymmetric intrashelf basin model impedes source rock development, with the intraformational shales and marls forming important seals.

Both the symmetric and asymmetric intrashelf basin models assume a relatively quiescent tectonic setting, and this is the case for the majority of the Cenomanian intrashelf basins considered. However, sectors of the Sarvak intrashelf basin in SW Iran appear to have developed in an extensional setting with structurally controlled margins (e.g. Navidtalab *et al.*, 2020). Structural control on the Garau Basin in western Iran and NE Iraq (Fig. 1), which was a long-lived intrashelf basin lasting throughout the Cretaceous (van Buchem *et al.*, 2010), has also been proposed (Navidtalab *et al.*, 2014). Water depths in the Garau Basin likely reached several hundreds of metres and were significantly greater than those in more short-lived Cenomanian basins such as the adjacent Najaf Basin (Aqrawi and Horbury, 2008). A NW-SE trending transtensional margin through central Iraq into southwest Iran is likely to have formed the transition zone between the Garau and Najaf intrashelf basins (Buday, 1980).

LATE ALBIAN –TURONIAN DEPOSITIONAL SEQUENCES

The results of the sequence stratigraphic analysis of the late Albian –Turonian interval of the Arabian Plate are presented in the following paragraphs. Large scale depositional geometries and lateral facies changes are illustrated in regional well and outcrop correlations in Figs 6 to 10. Palaeogeography and depocentre evolution are shown in GDE maps (Figs 11, 12) and isopach maps (Fig. 13). The main palaeogeographical and morphological features of each depositional sequence are summarised below with a focus on the southern and central parts of the Arabian Plate. Table 2 (page 160) presents a comparison of the depositional sequences and includes additional observations from SW Iran and the northern margin part of the plate.

Late Albian (K110) (Fig. 12a)

The late Albian marks a transition from a siliciclastic-dominated muddy ramp system to a broad, low-angle carbonate ramp across much of the Arabian Plate. The K110 MFS is the most extensive of the three Albian transgressions documented on the plate by Sharland *et al.* (2001), with waning siliciclastic influence throughout the transgression (van Buchem *et al.*, 2011). The carbonate ramp is represented by the Mauddud Formation in the UAE, Kuwait and south Iraq (van Bellen *et al.*, 1959; Strohmenger *et al.*, 2006; Cross *et al.*, 2010; Alsharhan *et al.*, 2014; Vincent *et al.*, 2020), the lower part of the Mauddud Formation in Qatar, the Mauddud Member or basal part of the Sarvak Formation in Iran, and the Natih G in Oman (Fig. 2).

Early Cenomanian (K120) (Figs 11 a,b, 12b and 13a,b)

During the transgression of the early Cenomanian K120 sequence, a fundamental change in the palaeogeography of the Arabian Plate occurred with the initiation of several intrashelf basins which were in general surrounded by flat-topped, shallow-water carbonate platforms (Fig. 12b). Significant bathymetric relief was established, resulting in lateral facies changes from the shallow-water, mixed muddy and grainy carbonate platform tops and margins to deeper-water, basinal carbonate mudstones which may have had significant organic matter contents. Thus organic-rich carbonates of the Shilaif Formation were deposited in the Shilaif Basin (UAE and offshore Iran), in which deposition occurred throughout the Cenomanian (Burchette, 1993; Burchette and Briton, 1985; Vahrenkamp *et al.*, 2015; Perrotta *et al.*; 2017; Franco *et al.*, 2018; Alipour *et al.*, 2021) (Figs 6 and 11). Within these carbonates, three Cenomanian depositional cycles have been recognized (e.g. Perrotta *et al.*; 2017; van Laer *et al.*, 2019) and relate to the K120, K130 and K140 depositional sequences (see Fig. 6, Shilaif Basin well).

The early Cenomanian intrashelf basin in the southern Arabian Plate extends beyond the UAE into the Rub'Al Khali area of Saudi Arabia and into Oman and southwest Iran (Fig. 11a). In Saudi Arabia, the equivalent of the basal part of the Shilaif Formation is the Safinaya Formation which is composed of organic-rich carbonates and marls (Fig. 6) (van Laer *et al.*, 2019) and which has TOC contents of up to 14 wt% (Newell and Hennington, 1983). The equivalent organic-rich interval in Oman is the Natih E (Fig. 6) which was deposited in maximum water depths of ~60 m as determined by clinoform heights (van Buchem *et al.*, 1996; Droste, 2010).

In Iraq, the Cenomanian Najaf intrashelf basin has been described by various authors (Aqrawi *et al.*, 1998; Aqrawi *et al.*, 2010a, b; Aqrawi and Horbury,

Table 1. Summary of the phases of development for symmetric intrashelf basins with minor siliciclastic influence, and asymmetric intrashelf basins with a more significant siliciclastic influence.

Model Stage (Systems Tract)	Symmetric intrashelf basin e.g. Natih Basin (Oman), Shiliaf Basin (UAE, offshore Iran and Saudi Arabia), Sarvak Basin (onshore Iran)	Asymmetric intrashelf basin e.g. Najaf Basin (southern Iraq and Kuwait)
1. Early Transgressive Sytstems Tract	The model starts at the SB assuming a relatively flat carbonate platform top. This is broadly representative of the Mauddud/Natih F-G carbonate platform. Fine-grained siliciclastics retrograde across the platform before aggradational carbonates re-establish as the siliciclastics retrograde inboard.	The model starts at the SB assuming a relatively flat carbonate platform top. Siliciclastics mostly influence the inboard margin proximal to the Arabian Shield hinterland (e.g. southwestern margin of the Najaf intrashelf basin). Aggradational carbonates are established on the outboard isolated margin, but are suppressed as a result of silici lastic influence on the inboard margin.
2. Late Transgressive Systems Tract	The rate of sea-level rise accelerates and intrashelf basin areas begin to differentiate from the platform. The carbonate system within the areas which become the intrashelf basin are unable to keep pace with sea-level rise and are drowned. However, the carbonate system within the platform interior continues to aggrade throughout the TST. This differential aggradation along the perimeter margins of the intrashelf basin creates a symmetric morphology, assuming relative tectonic quintessence (Razin et al., 2010, 2017). The intrashelf basins become restricted and anoxic, resulting in the deposition of organic-rich carbonates.	Carbonate production is also suppressed within intrashelf basin areas. This reflects the dual factors of sea-level rise and siliciclastic input. The basinal facies are characterized by oligosteginid-rich marls with an apparent lack of organic-rich horizons, presumably due to siliciclastic dilution. The isolated outboard carbonate margin demonstrates differential aggradation akin to the symmetric basin model. However, carbonate production is more suppressed on the inboard margin adjacent to the sediment supply, resulting in a mixed carbonate-siliciclastic homoclinal ramp system. The contrasting rates of carbonate production between the inboard and outboard margins result in the asymmetric morphology of the basin.
3. Highstand Systems Tract	Progradation of the carbonate margins occurs as carbonate production outpaces accommodation. Grainy carbonate shoals with rudist-rich grainstones and rudstones are characteristic of the HST along the margins of the intrashelf basins and track the trajectory of the shelf break. In single-sequence intrashelf basins e.g. the Natih A-B basin (K140 sequence), the HST carbonate progrades may completely infill accommodation.	On the isolated outboard margin, progradational rudist-rich shoals characterize the HST (e.g. Mishrif shoals on the eastern margin of the Najaf intrashelf basin). On the inboard margin, homoclinal ramp carbonates are established as the siliciclastic influence is diminished by high relative sea-level. The inboard and outboard margins exhibit different morphological styles and carbonate depositional facies.
4. Lowstand Systems Tract	In long-lived multi-sequence intrashelf basins such as the Shilaif basin, there is remaining accommodation during the LST. In these instances, the LST is typically suppressed as exposure of the platform dramatically reduces the areal extent of carbonate productivity and the amount of shedding into the basin. The LST wedge is areally limited and basinal LST deposits are often condensed. Exposure of the platform top gives the potential for karstification of HST carbonate shoals.	Exposure of the homoclinal ramp on the inboard margin enables siliciclastic bypass into the intrashelf basin. This is expressed as a siliciclastic LST wedge that has the potential to infill accommodation along the inboard margin of the basin. On the outboard margin, the carbonate LST wedge is areally limited as carbonate productivity is suppressed during platform exposure. The LST deposits are envisaged to be highly asymmetric in terms of morphology, thickness and depositional facies.

2008; Mahdi *et al.*, 2013; and Mahdi and Aqrawi, 2014) However, the configuration and morphology of the basin and the depositional facies are not well understood (e.g. see Fig. 12a of Aqrawi *et al.*, 1998 versus Fig. 7.34 of Aqrawi *et al.*, 2010a). Within the basin succession, mudstone-wackestones characterized by simple, non-keeled planktonic foraminifera and calcispheres are present in the Rumaila Formation (Al-Naqib, 1967; Aqrawi and Khaiwka, 1989; Mahdi *et al.*, 2013) and indicate deposition in sub-basinal water depths of ~40-60 m. Locally, the fauna recognized within the Rumaila Formation is dwarven implying some environmental restriction (Jassim and Buday, 2006).

These facies contrast with the rudist-rich, shallow-marine carbonates of the Mishrif Formation on the eastern basin margin (e.g. Aqrawi *et al.*, 2010a, b; Cantrell *et al.*, 2020). However the westward extent of the intrashelf basin facies is not clear. Palaeogeographic maps and well correlations (Aqrawi and Horbury, 2008) indicate that these facies extended as far as the Fallujah-1 well in the NW of the basin

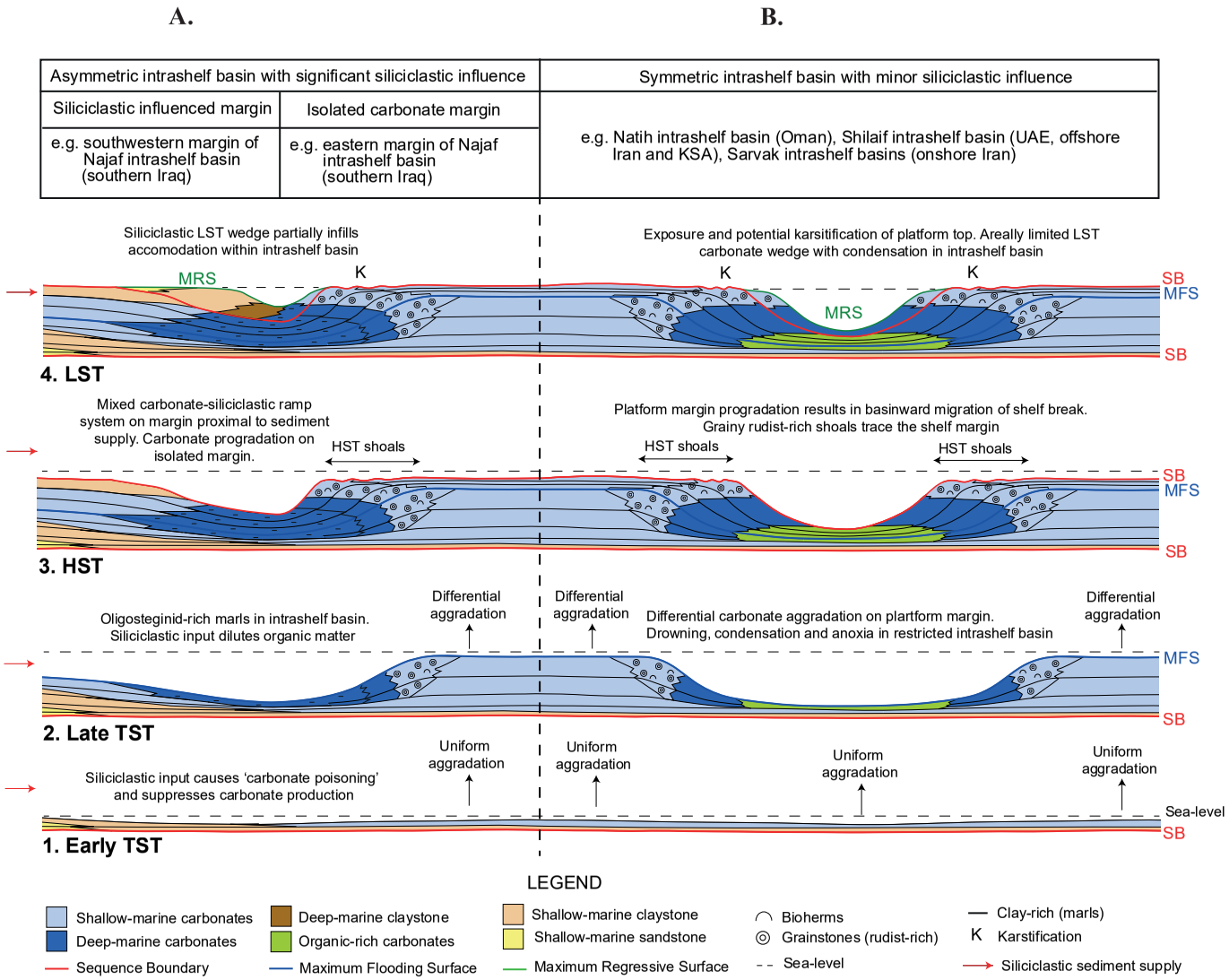

Fig. 5. Conceptual model for the development of Cenomanian intrashelf basins within a single depositional sequence: (A) Development of an asymmetric intrashelf basin in a scenario where there is significant siliciclastic influx, e.g. adjacent to the Arabian Shield hinterland. This is broadly representative of the Najaf Basin (southern Iraq). The model builds on the "Migratory Carbonate Suppressed Belt" model of Davies *et al.* (2002, 2019). (B) Development of a symmetric intrashelf basin in a scenario with there is only minor siliciclastic influence, e.g. within the interior of the Arabian Platform. This is broadly representative of the Natih Basin (Oman), the Shiliaf Basin (UAE, offshore Iran and KSA) and the Sarvak Basins (Iran). The model is modified after Razin *et al.* (2010). TST = Transgressive Systems Tract; HST = Highstand Systems Tract; LST = Lowstand Systems Tract.

during the early Cenomanian, but only sparse information for the Cenomanian Mahliban, Fahad and Maostsi Formations is available for this area and descriptions date back to van Bellen *et al.* (1959). The dip-orientated well correlations in Figs 7 and 8, which are based on wireline log profiles and observed thickness changes, tend to challenge the interpretations of Aqrawi and Horbury (2008). The correlations show that the sections in wells such as Safawi-1, Shawiya-1 and Ubaid-1 (Fig. 7), as well as Mileh Thathar-1, Samarra-1 and Fallujah-1 (Fig. 8), represent a mixed carbonate-siliciclastic homoclinal ramp succession on the western margin of the basin. This interpretation results in a significant reduction in the areal extent of the Najaf intrashelf basin (Figs 11 and 12) relative to that depicted in previous studies (Aqrawi and Horbury, 2008; Aqrawi *et al.*, 2010).

It is also noteworthy that proximal to distal accommodation change across the Najaf Basin is more subtle than that in contemporaneous intrashelf basins in the UAE and Oman. In addition, there is also no evidence for the presence of organic-rich intervals in deeper-water facies in the Najaf Basin, probably due to dilution attributed to an increased siliciclastic input. This contrasts with the age-equivalent, organic-rich Shilaif Formation and the Natih E which are important source rocks.

The K120 highstand is characterized by strong progradation of the shelf margins of the early Cenomanian intrashelf basins (Fig. 11b). Carbonate clinoforms are observed on seismic data from Oman in the Natih E Member and record the partial infill of the intrashelf basin (Droste and Van Steenwinkel, 2004; Grélaud *et al.*, 2006, 2010; Homewood *et al.*, 2008). Progradational shelf margins are also documented in the Shilaif Basin (Burchette and Briton, 1985; Burchette, 1993; Wharton, 2015; Vahrenkamp *et al.*, 2015; Perrotta *et al.*, 2017; Franco *et al.*, 2018; Lü *et al.*, 2018) (Fig. 6) and in intrashelf basins in Khuzestan, SW Iran (Vincent *et al.*, 2015; Navidtalab *et al.*, 2020; Kalanat *et al.*, 2021) (Fig. 9).

A shallowing-upward trend from deeper-water basinal facies to platform-margin packstones and grainstones is observed in well sections from the eastern margin of the Najaf Basin during the K120 HST (see Dehluran field well, Fig. 8). Progradation of the platform margin is inferred to have filled accommodation within the northern segment of the basin (see wells Kifl-1 and Afaq-1, Fig. 8).

In Fars Province, SW Iran, the K120 sequence is absent at a composite unconformity related to uplift and non-deposition across the Qatar-Fars Arch (Vincent *et al.*, 2015) (Fig. 13A). By contrast, a thick sequence of shallow-water carbonates is interpreted within the K120 sequence in Khuzestan, SW Iran (e.g. at the Ahwaz field) (Kazem Zadeh, 2016).

Middle Cenomanian (K130)
(Figs 11c, 12c and 13c, d)

The base of the middle Cenomanian is regarded to have coincided with a significant global sea-level low (e.g. Hancock, 2004). On the Arabian Plate, this sea-level low (K130 LST) is expressed as a regional exposure surface in platform locations (Hollis, 2011; van Buchem *et al.*, 2011). In Oman, a relative sea-level fall of ~30 m is estimated based on the depths of incisions into the top of the Natih E (Grélaud *et al.*, 2006, 2010; Homewood *et al.*, 2008).

In the Shilaif intrashelf basin (Fig. 12c), the reduced areal extent of the carbonate factory during the lowstand (Fig. 11c) resulted in less carbonate being shed from the margins into the basin centre. Therefore, the lowstand is typically represented by a relatively thin interval of deep-marine carbonates, marls and shales or by a condensed submarine hardground (Fig. 6). Forced regressive carbonate wedges similar to those observed within the Aptian Shu'aiba Formation (e.g. Yose *et al.*, 2010; Maurer *et al.*, 2013) are in general not well documented in the Cenomanian of the Arabian Plate but shallow-marine carbonate lowstand deposits are recognized in the Natih E of Oman (Droste and Van Steenwinkel, 2004; Grélaud, 2005; Grélaud *et al.*, 2006, 2010; Homewood *et al.*, 2008). The lowstand deposits offlap progradational highstand packages and infill remaining accommodation space (Fig. 10c). Thus the middle Cenomanian isopach thick in the Natih E intrashelf basin in Oman is related to lowstand infill (Fig. 13c).

Relative sea-level lows and the onset of transgressions in intrashelf basins on the Arabian Plate are often associated with shaly or marly facies rich in oligosteginids ("calcispheres") (Razin *et al.*, 2010). Oligosteginids are tiny spherical or oval microfossils, of uncertain origin, but typically regarded as calcareous dinoflagellate cysts (Wendler *et al.*, 2010a). Oligosteginid facies are recognized in intrashelf basin successions in the Ahmadi Formation in Iraq (Aqrawi and Horbury, 2008), the Natih Formation of Oman (e.g. Kennedy and Simmons, 1991), the Sarvak Formation of Iran (e.g. Adams *et al.*, 1967; Kalanat and Vaziri-Moghaddam, 2019) and the Derdere Formation of SE Turkey (e.g. Simmons *et al.*, 2020). Sea-water temperature and salinity may locally control oligosteginid abundance, but nutrient supply appears to be a key factor (Dias-Brito, 2000) which is why oligosteginids can be associated with shelf-margin to upper slope environments (Adams *et al.*, 1967; Flügel, 2010) such as the margin of the Garau intrashelf basin in Iran (Adams *et al.*, 1967). However, high nutrient flux can occur in other settings, such as homoclinal ramps proximal to major fluvial sources (e.g. Ahmadi Formation of the Najaf Basin, Iraq). As such, it seems likely that oligosteginid abundance can

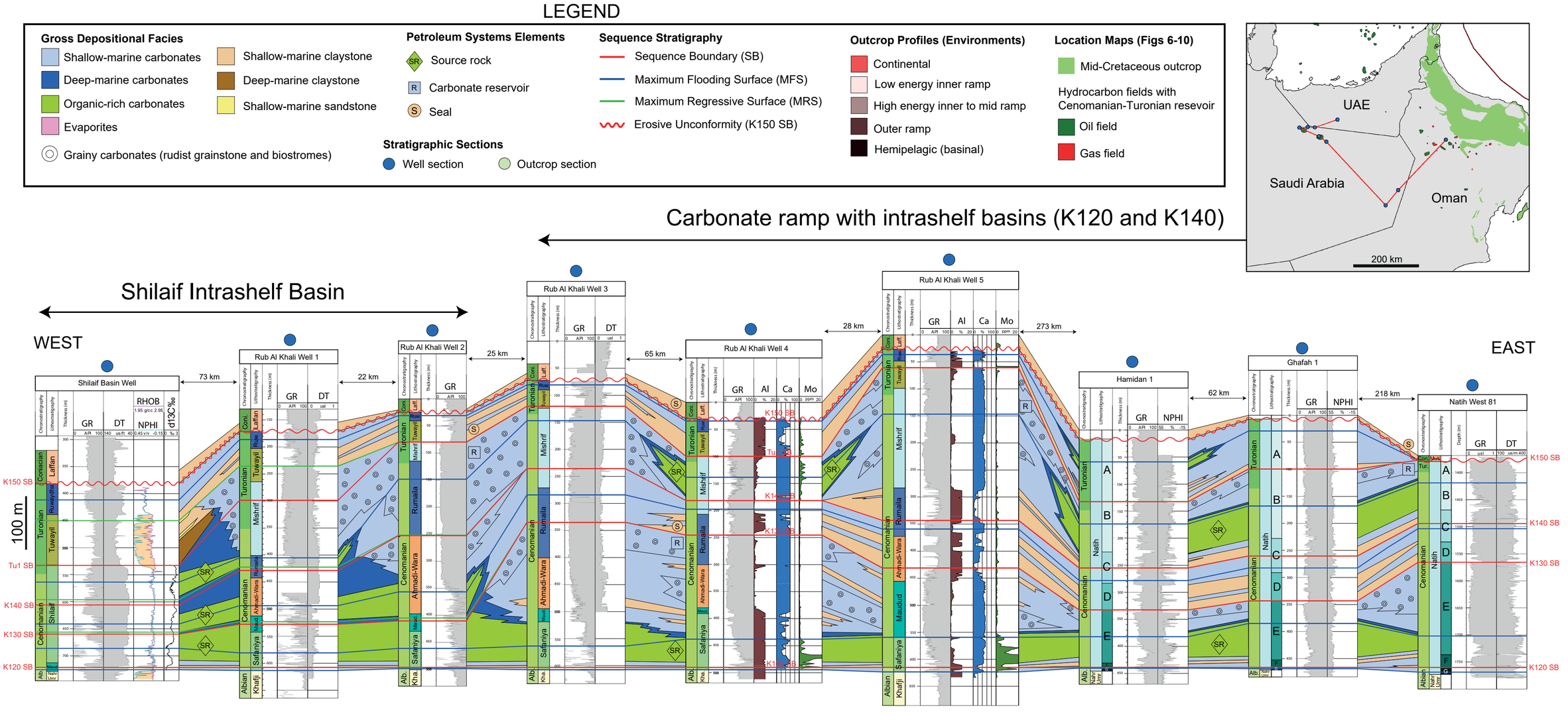

Fig. 6. Regional well correlation across the southern part of the Arabian Plate. The eastern segment of the correlation extends across depositional strike from Oman to the Rub' Al Khali area of Saudi Arabia. The western segment of the correlation extends across depositional dip into the Shilaif intrashelf basin in the UAE. The correlation highlights the distribution of petroleum systems elements within a sequence stratigraphic, palaeogeographic and morphological framework. The Al (%) log is a proxy for siliciclastic content, while the Mo (ppm) log is a proxy for anoxia. Well data is derived from van Buchem (2002), Homewood *et al.* (2008), Craigie (2015) and Perrotta (2017). Lithostratigraphic terms are taken from the original author and in some instances are diachronous with the sequence stratigraphy. The chronostratigraphy provided is based on the application of the sequence stratigraphic model.

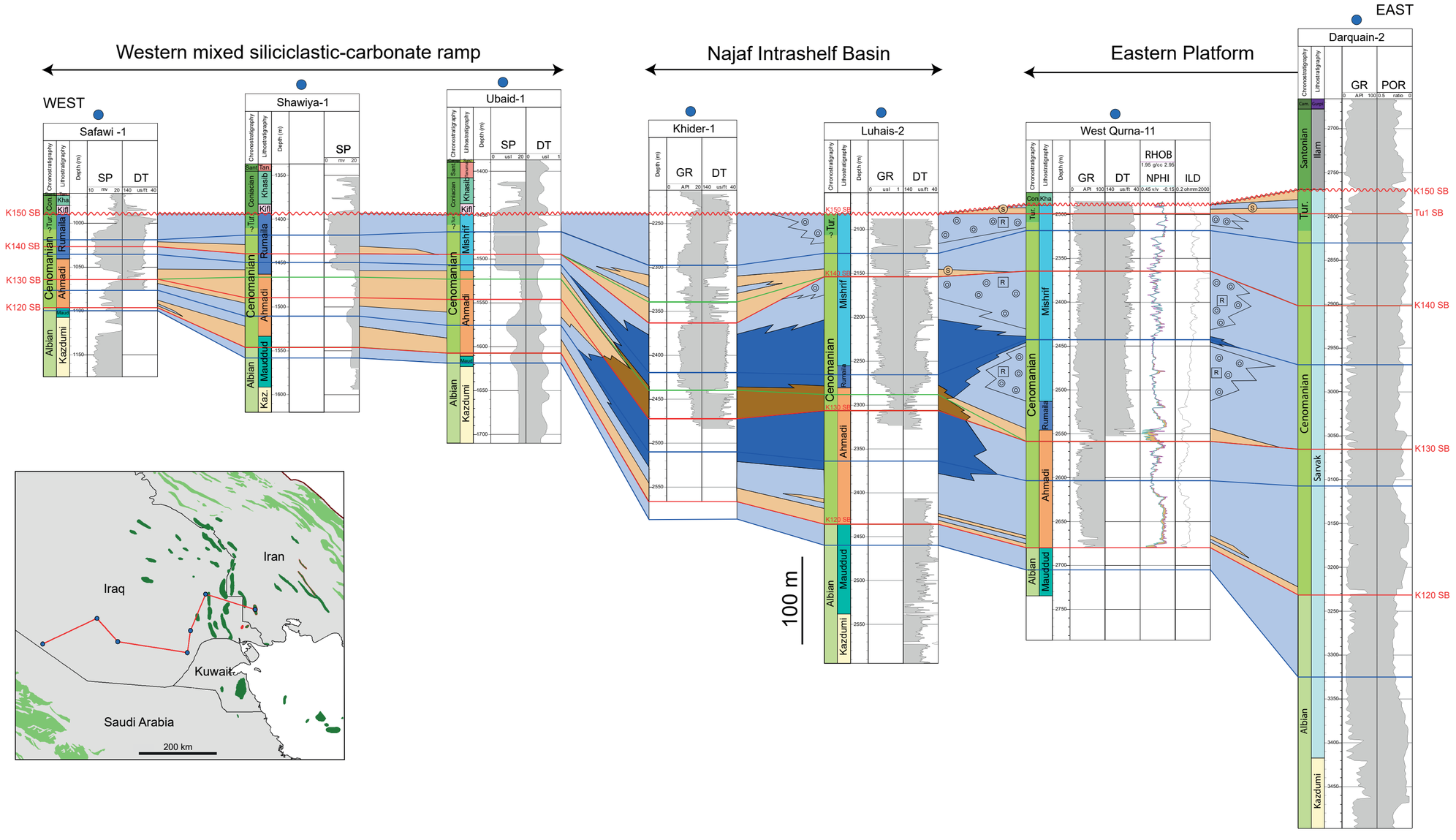

Fig. 7. Regional well correlation through southern Iraq and SW Iran. From east to west, the correlation extends across depositional dip from the platform interior in the Dezful Embayment of Iran, through the Mishrif oilfield trend within the eastern platform margin of SE Iraq, into the southern part of the Najaf intrashelf basin in southern Iraq and onto the mixed siliciclastic-carbonate ramp on the western margin proximal to the Arabian Shield. Well data is derived from Aqrawi and Horbury (2008), Zeinalzadeh and Sajjadian (2009), Grabowski Jr (2014) and Saleh and Awadessian (2019). Lithostratigraphic terms are taken from the original author and in some instances are diachronous with the sequence stratigraphy. The chronostratigraphy provided is based on the application of the sequence stratigraphic model. See Fig. 6 for legend.

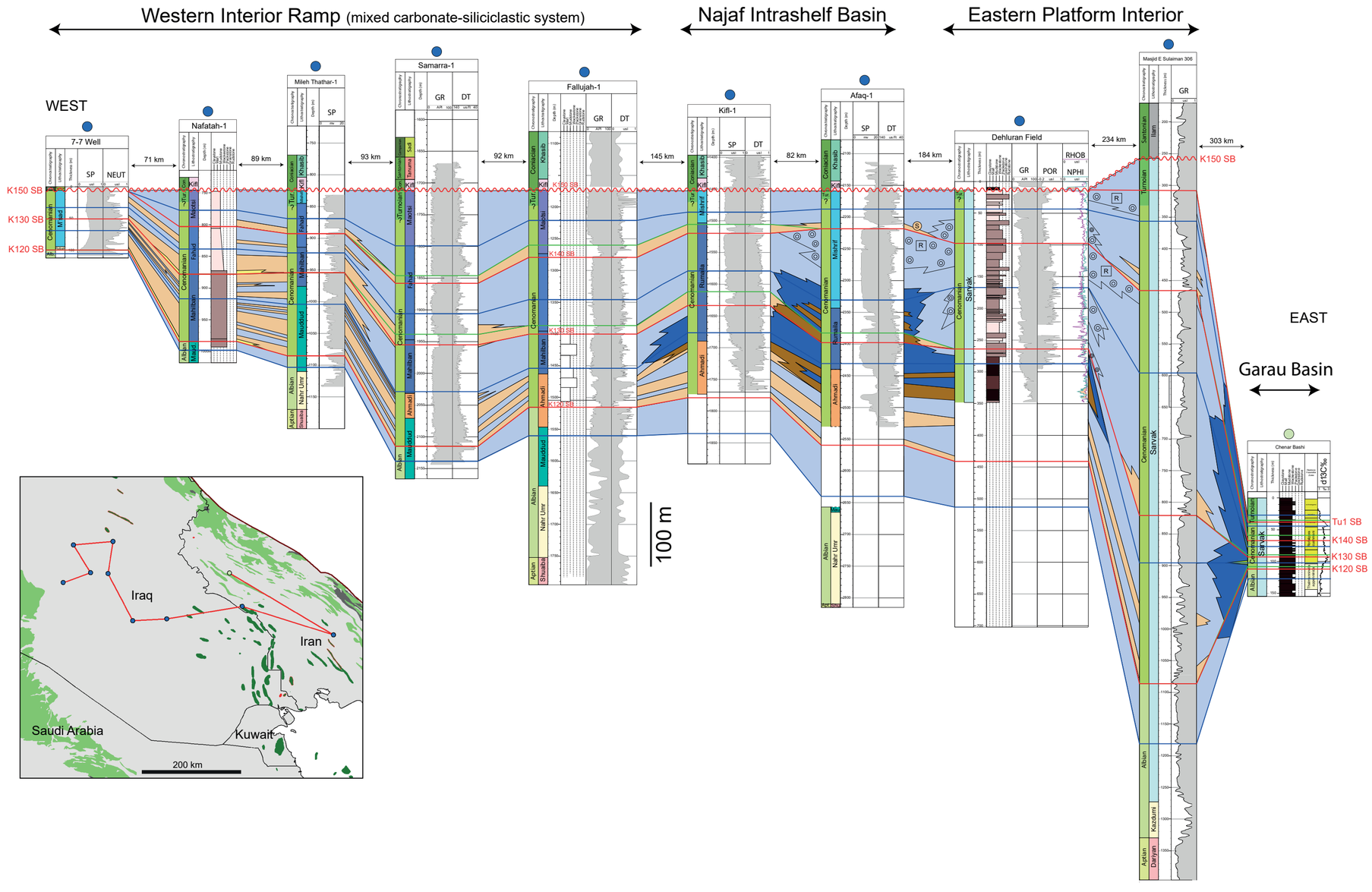

Fig. 8. Regional well correlation through western Iraq, central Iraq and SW Iran. From east to west, the correlation extends across depositional strike from the Garau Basin in Iran, through the platform interior of Iran and the eastern platform margin of SE Iraq, into the northern part of the Najaf intrashelf basin and finally across the interior ramp of the western margin towards the Rutbah High in the Western Desert of Iraq. Well data is derived from Gayara and Al-Sheikhly (1988), Taghavi *et al.* (2006), Aqrawi and Horbury (2008), Grabowski Jr (2014) and Navidtalab *et al.* (2019). Lithostratigraphic terms are taken from the original author and in some instances are diachronous with the sequence stratigraphy. The chronostratigraphy provided is based on the application of the sequence stratigraphic model. See Fig. 6 for legend.

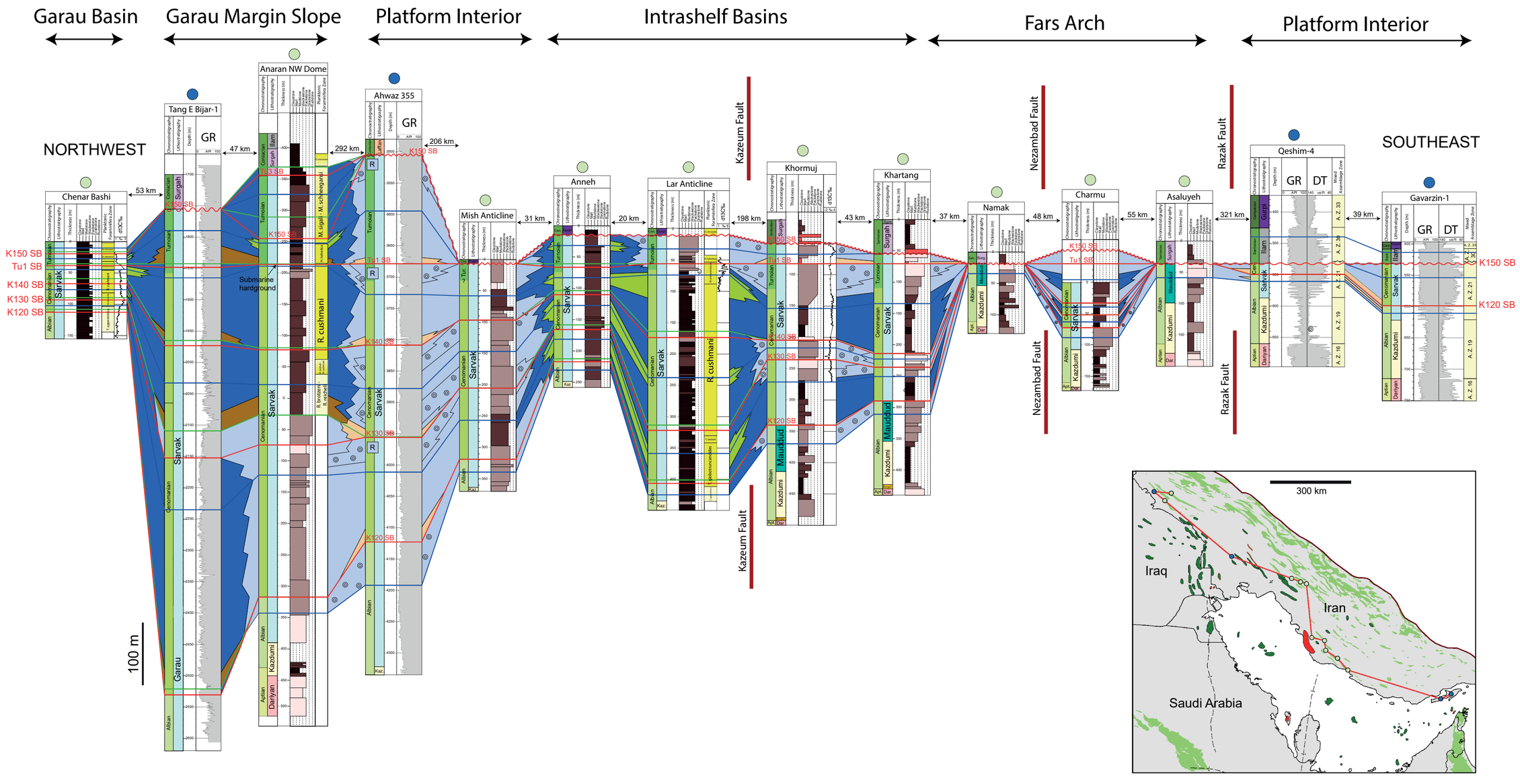

Fig. 9. Northwest to southeast regional correlation through Iran. The correlation is comprised of a mixture of logged outcrop sections and subsurface well sections. The correlation highlights variability in the thickness of sequences related to palaeogeographic setting, and the preservation of sequences related to structural domain and tectonic overprint. Data is derived from Sharp *et al.* (2010), Piryaei *et al.* (2011), Mehmandosti *et al.* (2013), Vincent *et al.* (2015), Kazem Zadeh (2016), Kalanat and Vaziri-Moghaddam (2019), Navidtalab *et al.* (2019), Navidtalab *et al.* (2020), Shoghi *et al.* (2020), and Kalanat *et al.* (2021). Lithostratigraphic terms are taken from the original author and in some instances are diachronous with the sequence stratigraphy. The chronostratigraphy provided is based on the application of the sequence stratigraphic model. See Fig. 6 for legend.

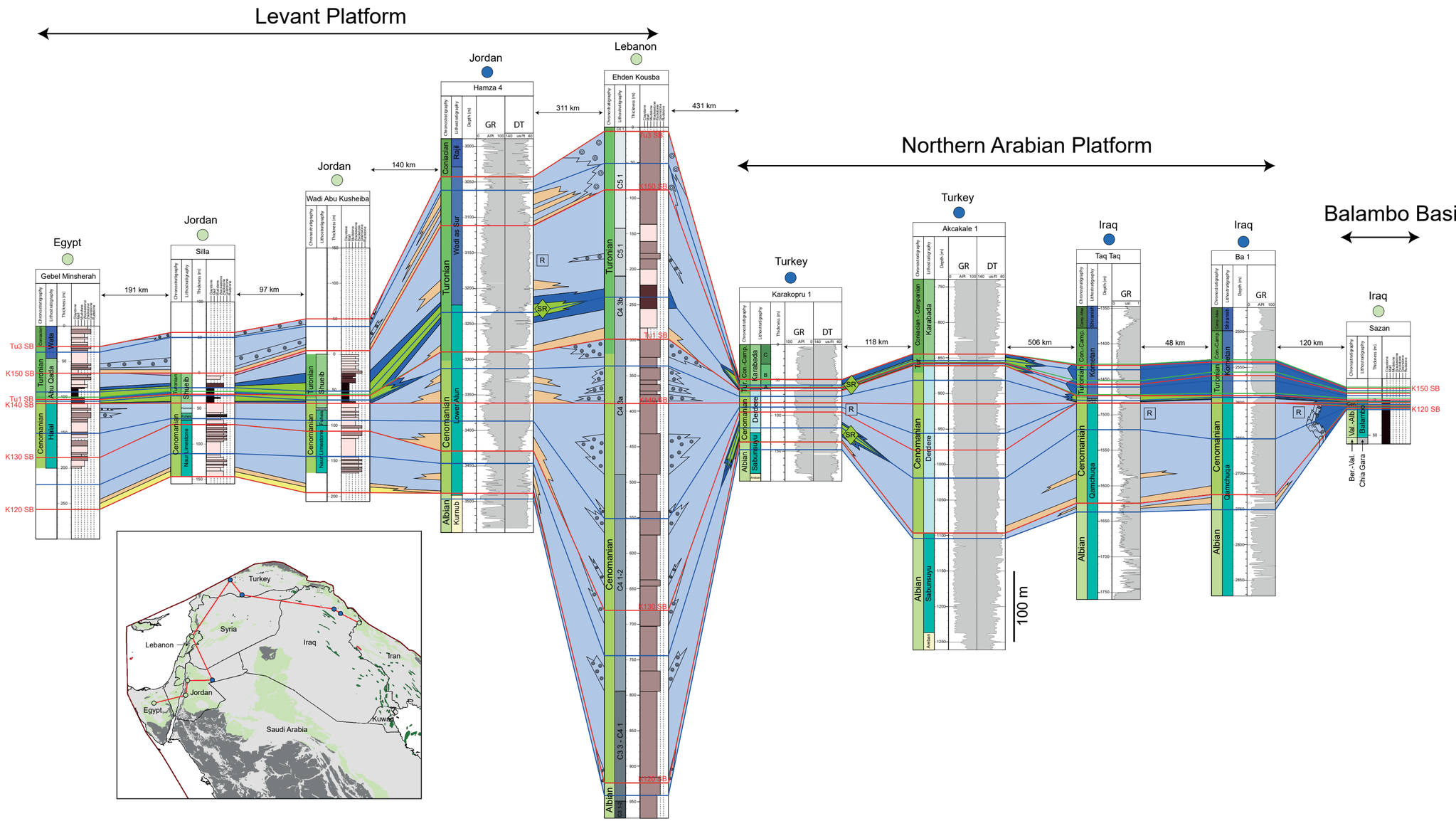

Fig. 10. West to east regional correlation through the northern part of the Arabian Plate across Egypt, Jordan, Lebanon, SE Turkey and northern Iraq. The correlation comprises a mixture of logged outcrop sections and subsurface well sections. The correlation highlights the drowning of the mid-Cretaceous carbonate platform in the late Cenomanian – Turonian. Data is derived from Saint-Marc (1981), Andrews (1992), Coskun (1996), Bauer *et al.* (2003), Schulze *et al.* (2004), Kent (2010), Garland *et al.* (2010), Al-Qayim *et al.* (2016), and Sarraj and Mohialdeen (2020). Lithostratigraphic terms are taken from the original author and in some instances are diachronous with the sequence stratigraphy. The chronostratigraphy provided is based on the application of the sequence stratigraphic model. See Fig. 6 for legend.

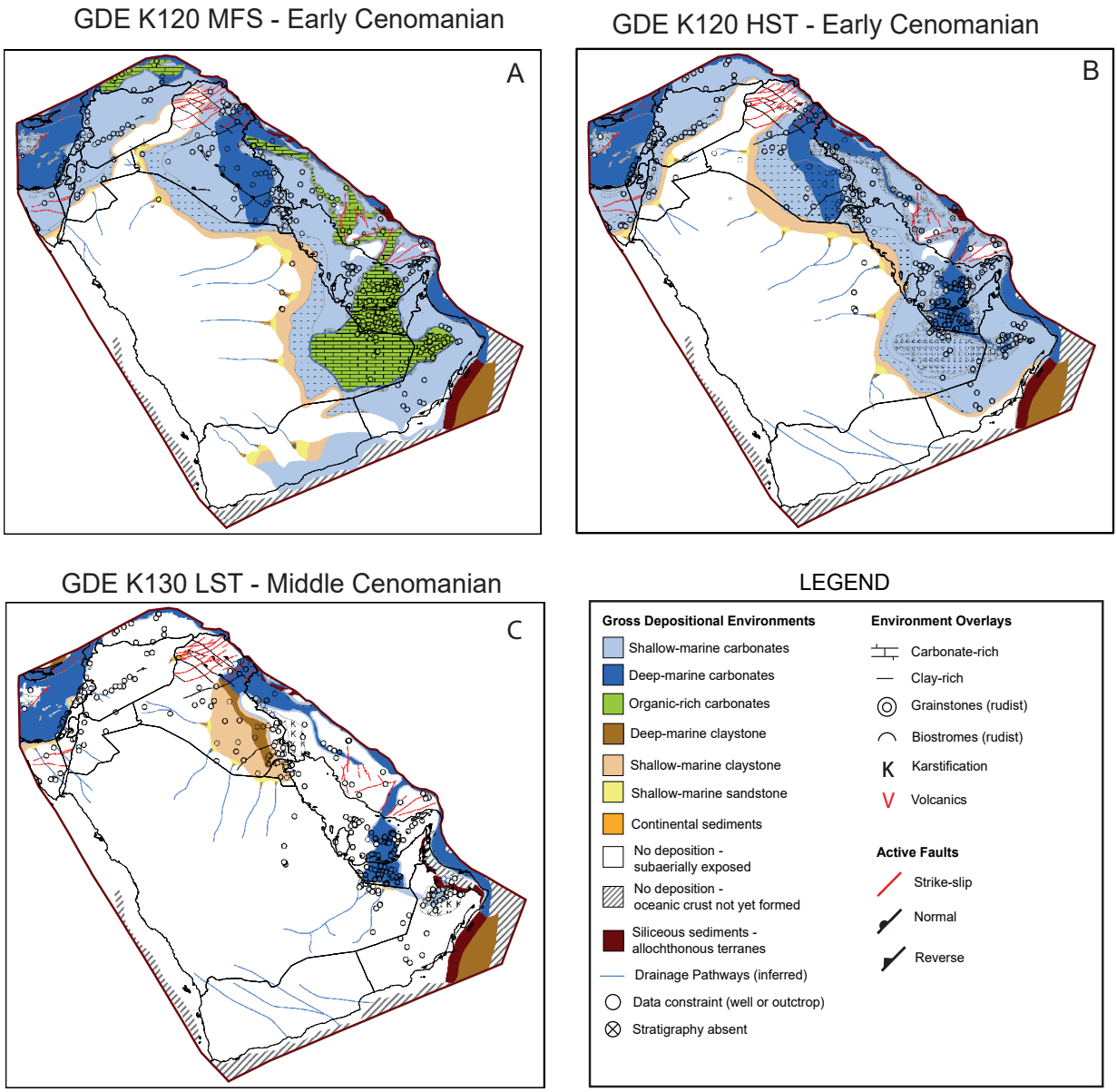

Fig. 11. Gross depositional environment maps covering a full cycle of relative sea-level change within the early-middle Cenomanian. The map surfaces provide a snapshot of the palaeogeography and depositional facies across the Arabian Plate for a specific time-slice within the sequence stratigraphic model related to: (A) the Maximum Flooding Surface (MFS), (B) the Highstand Systems Tract (HST), and (C) the Lowstand Systems Tract (LST). Note that the GDE maps show the depositional extent of facies which may not necessarily equate to the preservation extent.

occur across a range of depositional settings that may transcend the gross depositional facies used within this study.

In Oman, onshore Iran and SW Saudi Arabia, the K130 is a low accommodation sequence in which intrashelf basin facies are not developed (van Buchem *et al.*, 2002; Vincent *et al.*, 2015) (Fig. 12c). Alternating cycles of fine-grained siliciclastics and carbonates within the middle Cenomanian can be correlated with some confidence across the carbonate ramp system which extended across Oman and eastern Saudi Arabia (Fig. 6). Reasons for the absence of intrashelf basin facies within the K130 sequence in the southernmost Arabian Plate are not clear, but may be related to partial suppression of the carbonate factory due to increased siliciclastic supply following the K130 LST. Alternatively, it could be related to the relatively slow rate of sea-level change during the K130 TST which enabled the carbonate system to keep pace with sea-level rise, resulting in relatively uniform aggradation across the platform.

Because the aggradation of platform carbonates during the K130 transgression was relatively uniform, the Shilaif intrashelf basin retained its early Cenomanian configuration into the middle Cenomanian (Fig. 12c). Aggradational rudist grainstone shoals are recognized

along the margin of the basin in the UAE (Burchette, 1993; Burchette and Briton, 1985; Perrotta *et al.*, 2017; Lü *et al.*, 2018) and Saudi Arabia (Wharton, 2015). Carbonate shoals may have developed on topographic highs distal to the Shilaif basin margin, for example in the Umm Al Dalkh field in the UAE (Burchette, 1993; Neo, 1996; Basu *et al.*, 2015) (Fig. 13d).

Late Cenomanian – earliest Turonian (K140) (Figs 11d and 12e, f)

In the southern part of the Arabian Plate in Oman, eastern Saudi Arabia and onshore Iran, the late Cenomanian – earliest Turonian K140 sequence resembles the early Cenomanian K120 sequence in that it is characterized by the development of platform to intrashelf basin relief during a rapid, high-amplitude transgression with the accumulation of organic-rich sediments in intrabasinal depressions (van Buchem *et al.* 2011). In Oman, the K140 sequence is associated with a phase of intrashelf basin development, with the deposition of organic-rich carbonates with TOC contents of up to 14 wt% in the Natih B (van Buchem *et al.*, 2002). A positive $\delta^{13}C$ isotope excursion characteristic of the Cenomanian–Turonian boundary event is identified at the base of the Natih A (Wohlwend *et al.*, 2016) (Fig. 4). This was contemporaneous with the renewed development of intrashelf basins in SW Iran and the recognition of a $\delta^{13}C$ isotope excursion within basinal facies of the Sarvak Formation (Vincent *et al.*, 2015; Kalanat and Vaziri Moghaddam, 2019) (see Fig. 9, Khormuj and Chenar Bashi outcrops). This excursion is also recognized in the upper part of the Shilaif Formation in the UAE (Vahrenkamp *et al.*, 2015; Hennhoefer *et al.*, 2019; Perrotta *et al.*, 2017) (see Fig. 6, Shilaif Basin well).

The development of an intrashelf basin to the SW of the established Shilaif basin platform margin is inferred to have taken place in the Rub' Al Khali area of Saudi Arabia (Fig. 12d). Here, organic-rich intrashelf basin facies are interpreted to occur based on elevated gamma-ray log responses within carbonate-rich intervals associated with elevated contents of molybdenum (Craigie, 2015) (see Fig. 6, Rub' al Khali well 4). These facies follow a similar stratigraphic pattern to that observed within the Natih A-B intrashelf basin in Oman (van Buchem *et al.*, 2002; Droste and Van Steenwinkel, 2004) (see Fig. 6; Natih West 81 well). A thick sequence of rudist bank carbonates identifiable on the K140 sequence isopach (see Fig. 6, Rub' al Khali well 5 and Fig. 13e) separates the Rub' al Khali intrashelf basin in Saudi Arabia from the Shilaif intrashelf basin in the UAE (Craigie, 2015). Newell and Hennington (1983) described organic-rich carbonates with TOC contents of 10 wt% in the 'lower Mishrif' below the Cenomanian–Turonian boundary, which is likely to correlate with the K140 sequence.

In southern Iraq, accommodation within the Najaf intrashelf basin appears largely to have been infilled by the K140 sequence, resulting in a homoclinal ramp morphology in this area during the late Cenomanian to earliest Turonian. Lagoonal facies with isolated grain-rich carbonate shoals in the Mishrif Formation are widespread on the isolated eastern basin margin (Aqrawi *et al.*, 2010a, b; Mahdi *et al.*, 2013; Mahdi and Aqrawi, 2014; Cantrell *et al.*, 2020). An overall shallowing trend within the Mishrif Formation and its equivalents is interpreted across southern Iraq. The $\delta^{13}C$ isotope excursion characteristic of the OAE2 event has been identified within the upper part of the Mishrif Formation (mA unit) in the Rumaila field (Ryder *et al.,* 2013; Lehmann *et al.*, 2017), and is stratigraphically above deeper-water intrashelf basin facies (Zhu *et al.*, 2016). Based on the application of the age-constrained sequence model used in this study, we infer that the uppermost part of the Mishrif Formation above the $\delta^{13}C$ isotope excursion may extend into the earliest Turonian. However, it should be noted that there is no documented biostratigraphic evidence to unequivocally support a Turonian age for the Mishrif Formation in Iraq.

In the western and central parts of the Najaf area, the Mishrif Formation (and lateral equivalents) is overlain by the Kifl Formation (Figs 7 and 8) which consists of interbedded carbonates and anhydrite (Aqrawi and Horbury, 2008; Grabowski Jr, 2014). The age and depositional environment of the Kifl Formation is contentious. The formation is conventionally placed below the mid-Turonian unconformity (e.g. Aqrawi *et al.*, 2010; Mahdi and Aqrawi, 2014; Grabowski Jr, 2014). Deposition of the Kifl Formation has been interpreted to have occurred in an isolated, restricted basin (e.g. Aqrawi and Horbury, 2008; Aqrawi *et al.*, 2010a), or alternatively in an evaporitic lagoon behind the Mishrif shelf margin (e.g. Al-Naqib, 1967; Grabowski Jr, 2014). The alternative interpretation presented here assigns the Kifl Formation to above the mid-Turonian regional unconformity (K150 SB). As such, the Kifl Formation is regarded as early transgressive facies at the start of the next tectonostratigraphic megasequence that pre-dates the deposition of the Khasib Formation in the late Turonian to early Coniacian. Given the magnitude and length (~5 Ma) of the mid-Turonian unconformity, it seems unlikely that the predominantly evaporitic Kifl Formation could have been preserved if it was deposited prior to mid-Turonian uplift. It is proposed that the Kifl Formation was deposited within restricted lagoons across a variable topographic surface post mid-Turonian uplift. In the Basrah area, the Kifl Formation is observed between 'obvious' Mishrif and 'obvious' Khasib (Gaddo, 1971), where it is associated with lacustrine and pedogenic facies of very similar

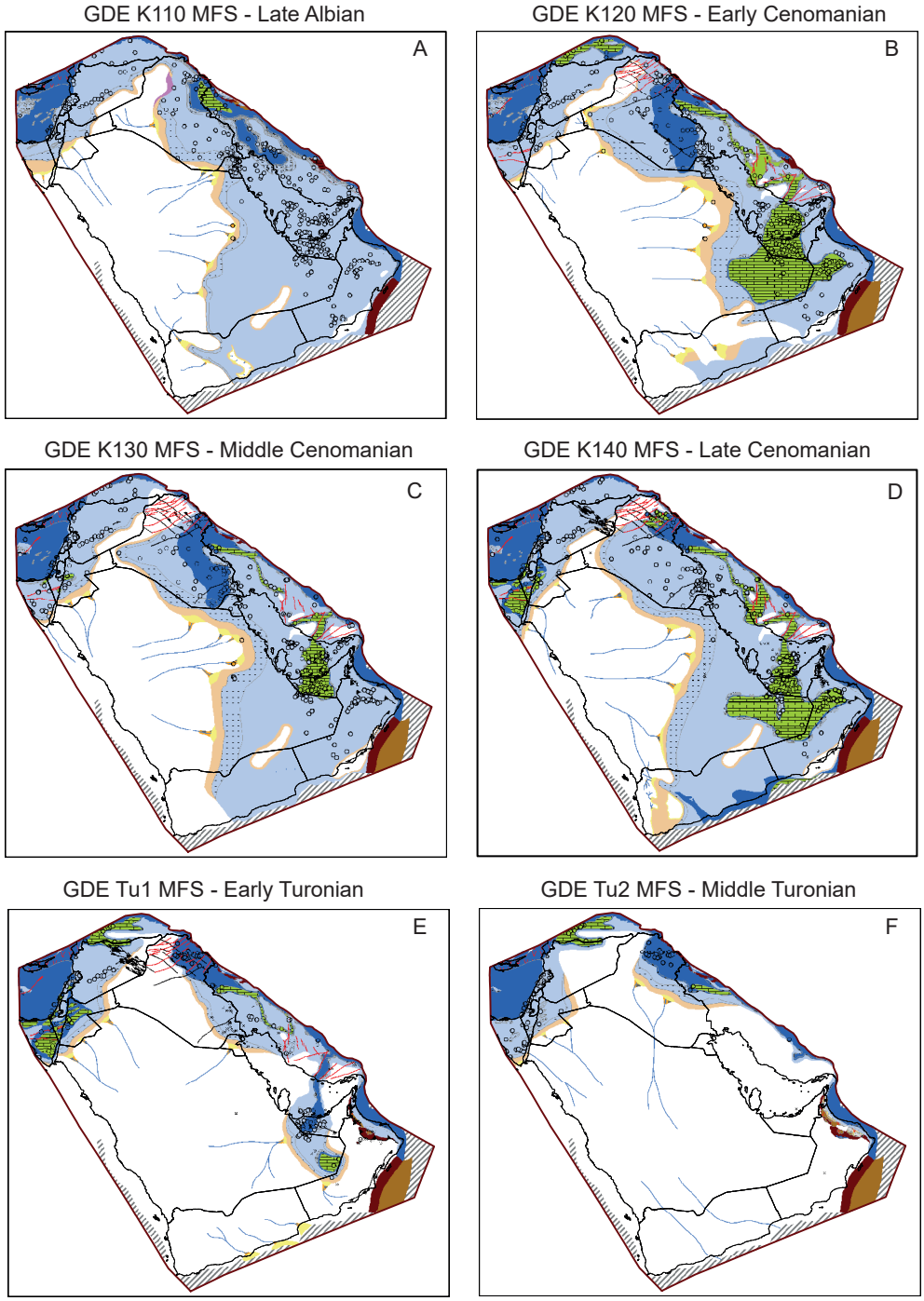

Fig. 12. Maximum Flooding Surface Gross Depositional Environment Maps for the depositional sequences recognized in the late Albian – Turonian. (A) K110 MFS – late Albian; (B) K120 MFS – early Cenomanian; (C) K130 MFS – middle Cenomanian; (D) K140 MFS – late Cenomanian; (E) Tu1 MFS – early Turonian; (F) Tu2 MFS – middle–late Turonian. Note that the GDE maps show the depositional extent of facies which may not necessarily equate to the preservation extent.

character to the Laffan Formation in Iran (A. Horbury and B.Vincent, *pers. comm*., 2022), which although Coniacian in age, rest with clear unconformity above eroded Cenomanian (Vincent *et al.*, 2015).

Early-middle Turonian (Tu1) (Fig. 12e)

The Tu1 SB is superimposed with the mid-Turonian K150 SB across large parts of the Arabian Plate, forming a tectonically-enhanced, compound sequence boundary (Figs 6, 7, 8, 9 and 14). Turonian sequences in the southern and eastern Arabian Plate are strongly overprinted by tectonic uplift and show variable preservation (van Buchem *et al.*, 2011). Meteoric diagenesis and karstification associated with the composite mid-Turonian unconformity is recognized regionally within carbonate platforms (Jordan *et al.*, 1985; van Buchem *et al.*, 2002; Hollis, 2011; Chen *et al.*, 2021).

In southwest Iran, the Sarvak Formation probably extends into the Turonian (Omidvar *et al.*, 2014) and the Tu1 SB is recognized as an intra-Sarvak disconformity and karstified surface (Rahimpour-Bonab *et al.*, 2013; Mehrabi and Rahimpour-Bonab, 2014; Hajikazemi *et al.*, 2017; Malekzadeh *et al.* 2020) (see Fig. 9, Ahwaz 355 well). It should be noted that unequivocal biostratigraphic evidence for a Turonian age for the uppermost Sarvak platform is lacking, although this is not the case in more open-marine facies of the Sarvak Formation (Sharp *et al.*, 2010; Schlagintweit and Simmons, 2022). Zone 29 of Wynd, (1965) within the upper Sarvak platform (the *Valvulammina–Dicyclina* Assemblage Zone), was renamed the *Moncharmontia apenninica –Nezzazatinella – Dicyclina* Assemblage Zone by Omidvar *et al.* (2014) with the observation that this is Turonian in age, mainly because of the presence of *Moncharmontia apenninica*. However, Schlagintweit and Yazdi-Moghadam (2021) have convincingly shown that *M. apenninica* can occur in Cenomanian strata, leaving the age of this zone open to question. As such it is possible that the intra-Sarvak disconformity assigned to the Cenomanian–Turonan boundary (Rahimpour-Bonab *et al.*, 2013; Mehrabi and Rahimpour-Bonab, 2014; Hajikazemi *et al.*, 2017; Malekzadeh *et al.* 2020) and recognized in this study as Tu1 SB, could be older. A plausible alternative interpretation could be to recognize this disconformity as the late Cenomanian K140 SB. Sharp *et al.* (2010) recognized signifcant forced regression within the Sarvak Formation in the late Cenomanian in the Anaran area of Lurestan Province but noted that the latest Cenomanian to early Turonian is absent in proximal settings.This implies erosion related to the mid-Turonian unconformity down-cut into the late Cenomanian within platform areas, with the overlying middle-late Turonian stratigraphy assigned to the younger tectonostratigraphic megasequence deposited post mid-Turonian uplift. In distal settings towards the margin of the Garau Basin, the correlative conformity to the mid-Turonian unconformity (K150 SB) is interpreted within the upper part of the Sarvak Formation (see Fig. 9, Anaran NW Dome outcrop) with the latest Cenomanian to earliest Turonian inferred to be absent or possibly condensed at a submarine hardgound (Sharp *et al.*, 2010).

In the UAE, the Tu1 LST is recorded within the Tuwayil Formation and represents a significant change within the Shilaif intrashelf basin fill from carbonates to siliciclastics (see Fig. 6, Shilaif basin well) (Azzam, 1995). An early Turonian age for the Tuwayil Formation is inferred from its stratigraphic position above the Cenomanian–Turonian boundary event $\delta^{13}C$ isotope excursion documented in the upper sequence of the Shilaif Formation (K140 sequence) (Vahrenkamp *et al.*, 2015; Perrotta *et al.*, 2017; Hennhoefer *et al.*, 2019) (see Fig. 6, Shilaif basin well). The Tuwayil Formation consists of siliciclastic mudstones with shoreface and shallow-marine sandstones (Azzam, 1995) which filled the majority of the remaining accommodation space within the intrashelf basin (Al-Zaabi *et al.*, 2010; Vahrenkamp *et al.*, 2015; Franco *et al.*, 2018). The switch from carbonates to siliciclastics is related to regional Turonian uplift and erosion of the Arabian Shield hinterland (Al-Zaabi *et al.*, 2010; Franco *et al.*, 2018; Davies *et al.*, 2019). Reactivation of deep-seated basement structures in the SW UAE channelled the Tuwayil siliciclastics within the intrashelf basin (Azzam, 1995; Al-Zaabi *et al.*, 2010).The initial phase of Tuwayil Formation siliciclastic deposition was coincident with carbonate progradation along the margins of the Shilaif Basin (e.g. Al-Zaabi *et al.*, 2010; Franco *et al.*, 2018). Carbonate lowstand wedges have been identified in some wells (see Fig. 6, Rub' Al Khali well 1), but are areally restricted and only extend a short distance into the intrashelf basin with most of the accommodation being infilled by siliciclastics.

Early-middle Turonian carbonates of the Ruwaydah Formation (Tu1 MFS) overlie the siliciclastics of the Tuwayil Formation (Vahrenkamp *et al.*, 2015; Franco *et al.*, 2018; Van Laer *et al.*, 2019) (Fig. 6). The Ruwaydah Formation consists of planktonic foraminiferal and oligosteginid-rich wackestones in central Abu Dhabi, indicating deposition within a deeper-water environment (Al Zaabi *et al.*, 2010; Taher and Al Zaabi, 2015). High energy, peloidal shoal facies have been reported at the platform margin, while lower energy wackestones, packstones and mudstones characterize the platform interior (Al Zaabi *et al.*, 2010) (Fig. 12e).

Middle – late Turonian (Tu2) (Fig. 12f)

There is no evidence for the preservation of middle-late Turonian stratigraphy in the southern part of the Arabian Plate. As only a single depositional sequence (Tu1 sequence) within the Ruwaydah Formation is recognised (Al-Zaabi *et al.*, 2010; Vahrenkamp *et al.*, 2015; Van Laer *et al.*, 2019), a hiatus spanning the middle-late Turonian (Tu2 sequence) is inferred prior to the deposition of the Laffan Formation (and regional equivalents) in the early Coniacian (K150 sequence) (Fig. 12f). This is consistent with the occurrence of regional uplift and erosion across the southern part of the Arabian Plate at this time (Sharland *et al.*, 2001).

The Tu2 sequence is recognized within a distal setting towards the margins of the Garau Basin in Lurestan Province, SW Iran (see Fig. 9, Anaran NW Dome outctop) (Sharp *et al.*, 2010) that was presumably isolated from mid-Turnonain uplift and hence records an apparently continous marine succession through the mid-late Turonian. A complete succession of Turonian stratigraphy is also recognized

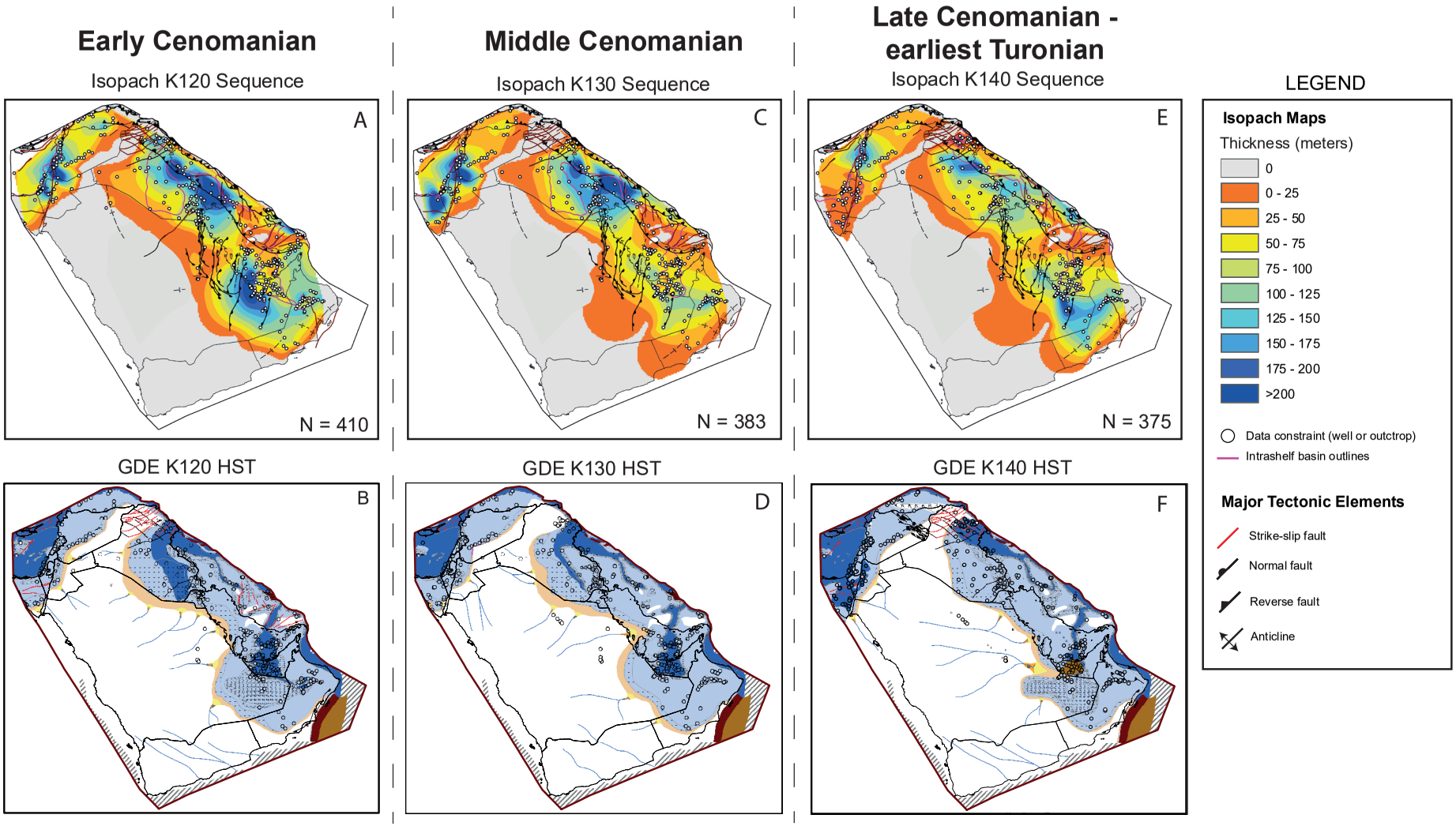

Fig. 13 (above). Isopach maps for the three Cenomanian sequences. Highstand Gross Depositional Environment Maps for each depositional sequence are shown (below) for palaeogeographic context. (A, B) K120 sequence – early Cenomanian; (C, D) K130 sequence – middle Cenomanian; (E, F) K140 sequence – late Cenomanian. Intrashelf basins are typically associated with condensation and sediment thins, while platform margins are typically associated with carbonate aggradation and sediment thicks. Note that there is tectonic overprint across structural highs and salt domes, particularly in Fars Province in Iran.

along the northern margin of the plate (see Table 2). Outcrops in the onshore Levant, particularly the well-documented sections in Jordan (e.g. Powell and Moh'd, 2011), provide a type-section for the Turonian of the Arabian Plate. In Jordan, a prominent salina/sabkha gypsum bed at the top of the Shueib Formation (see Fig. 10, Silla outcrop) (Schulze *et al.*, 2005; Powell and Moh'd, 2011) marks the culmination of significant regression and the mid-Turonian K150 SB. This surface is contemporaneous with the major erosional unconformity noted across much of the Arabian Plate.

DISCUSSION

Evolution of Accommodation Space across the Arabian Plate

There are large variations in the preserved thickness of Cenomanian–Turonian stratigraphy across the Arabian Plate (Fig. 14). In platform settings in Oman, Saudi Arabia, UAE and Iraq, the Cenomanian–Turonian is typically 300-500 m thick (Figs 6, 7 and 8). However, in SW Iran the thickness of the interval varies from >800 m in Khuzestan Province (e.g. at the Ahwaz field; Kazem Zadeh, 2016) to 0 m in parts of Fars Province (Vincent *et al.*, 2015) (Fig. 9).

Comparing sequence isopach maps and GDE maps (Fig. 13) demonstrates the evolution of accommodation space across the Arabian Plate. Changes in accommodation space are due to the interplay between relative sea-level change, palaeogeographic setting and tectonic regime. Across the majority of the plate, palaeogeographic trends began to differentiate in the early Cenomanian from an expansive and relatively flat carbonate ramp system in the late Albian (K110). An exception to this occurred in the Garau Basin in SW Iran and NE Iraq, interpreted as a re-entrant of NeoTethys which was inherited from the Albian and which was maintained throughout the Cenomanian–Turonian. As a result, a complete, deep-water Cenomanian–Turonian succession is preserved in the basin although it is only ~100 m thick (Fig. 14) (Navidtalab *et al.*, 2019).

In general, the Cenomanian sequences were deposited on the passive Arabian Plate margin during relatively quiescent tectonic conditions. The composite thickness of the Cenomanian across much of the plate was controlled by differential rates of carbonate aggradation in response to relative sea-level changes and the development of condensed intrashelf basin successions (Razin *et al.*, 2010, 2017). For instance, the Cenomanian is relatively thin (<200 m) in the Shilaif Basin compared to the platform margin succession (>400 m). However, the Turonian succession in the intrashelf basin is thicker (100-200 m) than the corresponding platform succession (<100 m) as the remaining accommodation space was largely infilled by siliciclastics of the Tuwayil Formation (Tu1 LST) (Fig. 6).

In SW Iran, regional transects demonstrate significant changes in the thickness and preservation of the Cenomanian–Turonian depositional sequences, as well as variations in the palaeogeography (Figs 9 and 14). There is a partial correlation between the development of Cenomanian intrashelf basins in Iran and the occurrence of WNW-ESE and ENE-WSE trending basement faults such as the Sarvestan, Nezambad and Kazerun faults in Fars Province (Figs 9, 11 and 12) (Navidtalab *et al.*, 2020; Kalanat *et al.*, 2021). There is a regional differentiation between the southern Fars Province and the area to the north of the Kazerun Fault. Significant subsidence occurred to the north during the Aptian and Albian (van Buchem *et al.*, 2010), a trend that continued into the Cenomanian where a very thick sequence of shallow-water Sarvak Formation was accommodated in the Ahwaz area (e.g. Kazem Zadeh, 2016). During the Albian there was no evidence for differential tectonic subsidence in southern Fars Province, where the Cenomanian is relatively thin to completely absent and was influenced by salt tectonics (Vincent *et al.*, 2015).

Palaeohighs reactivated in the Cenomanian (e.g. Gad-e-Safid and Gachsaran) are recognized within the Dezful Embayment (Mehrabi and Rahimpour-Bonab, 2014). Variability in the intensity and duration of karstification at unconformity surfaces assigned to the mid-Cenomanian (K130 SB), Cenomanian–Turonian boundary (probable Tu1 SB) and mid-Turonian (K150 SB) has been associated with the presence of these palaeohighs (Mehrabi and Rahimpour-Bonab, 2014). Mehrabi and Rahimpour-Bonab (2014) related the reactivation and uplift of these structural highs during the Cenomanian to compression associated with the transition from a passive margin to an active margin along the eastern periphery of the Arabian Plate. However, the mid-Cenomanian (K130 SB) and Cenomanian–Turonian boundary (probable Tu1 SB) unconformities pre-date the transition to an active margin which occurs within the mid-Turonian (K150 SB) (Sharland *et al.*, 2001). As such, it seems likely that only the mid-Turonian unconformity is associated with the compressional phase that occurred as a precursor to obduction in the Late Cretaceous (Searle *et al.*, 2014).

An alternative interpretation for the presence of active highs and horst-graben architecture during the Cenomanian invokes an extensional regime that occurred prior to Turonian inversion (Navidtalab *et al.*, 2020; Kalanat *et al.*, 2021). Extension along basement structures gave rise to troughs while contemporaneous salt movements created structural highs. The influence of local salt movement on the thickness of the Cenomanian–Turonian stratigraphy was also recognized by Vincent *et al.* (2015), and

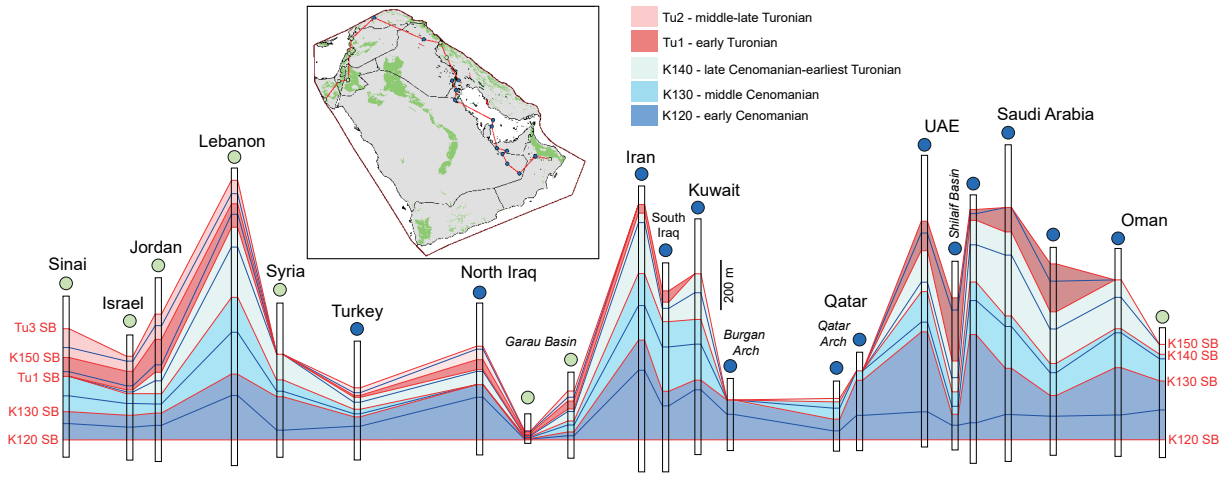

Fig. 14. Mega-regional correlation highlighting the thickness and preservation of Cenomanian–Turonian sequences across the Arabian Plate. Thickness changes are principally related to palaeogeographic setting, while preservation is related to the structural domain and tectonic overprint. Note the absence of late Cenomanian and Turonian sequences across basement-cored structural highs such as the Burgan Arch and the Qatar Arch.

halokinesis implies that there was structural control on the development of at least some Cenomanian intrashelf basins in Iran. Regional extension here is compatible with plate-wide studies that indicate a transtensional regime in the mid-Cretaceous elsewhere in Africa-Arabia (Guiraud and Bosworth, 1997).

However, not all intrashelf basins in onshore Iran necessarily had structural control. Razin *et al.* (2010) documented the development of an intrashelf basin in the High Zagros related solely to differential aggradation of a carbonate platform in response to relative seal-level rise, with no tectonic subsidence. The timing of intrashelf basin development during the Cenomanian in Iran and Oman is contemporaneous, which may imply a regional control linked to the rate and magnitude of relative sea-level change.

Turonian Uplift and Tectonic Overprint

The Turonian sequences were deposited within an active margin compressional phase and hence the thickness of these sequences has a strong tectonic overprint. In the southern and eastern parts of the Arabian Plate, the composite Turonian unconformity (K150 SB) locally cuts down and truncates older Cenomanian sequences (Fig. 14). For instance, the upper part of the K140 sequence is truncated in parts of Oman (van Buchem *et al.*, 2011) (see Fig. 6, Natih West-81 well), while the Cenomanian K120, K130 and K140 sequences show variable preservation in the eastern Mishrif Platform in the UAE and Iran (Jordan *et al.*, 1985; Videtich *et al.*, 1988; Pascoe *et al.*, 1995; Piryaei *et al.*, 2011). Long-lived basement-cored structural features were reactivated and preferentially uplifted as a result of Turonian compression. The late Cenomanian (K140) and the entire Turonian (Tu1 and Tu2) is absent across the Qatar Arch in offshore Qatar (van Buchem *et al.*, 2014), while the early Cenomanian (K120) subcrops beneath the unconformity across the Burgan Arch in Kuwait (Davies *et al.*, 2002) (Fig. 14). There is also considerable truncation of the Cenomanian to early Turonian stratigraphy along the Safaniyah-Nowrooz-Hendijan Arch in the northern Arabian Gulf (Al-Laboun, 1977; Baniasad *et al.*, 2021). The Mishrif Formation is absent from the area around the Lekhwair Arch in SE UAE (Franco *et al.*, 2018), indicating erosion into the Albian or the underlying succession. In parts of Fars Province in SW Iran, the Cenomanian and Turonian are absent within outcrop sections along the structural trend of the Qatar-Fars Arch (Vincent *et al.*, 2015) (see Fig. 9, Namak and Asaluyeh outcrops).

Mid-Turonian uplift and erosion clearly has a strong regional control on the preserved thickness of the Cenomanian stratigraphy as reflected in the mega-regional correlation of the Cenomanian–Turonian sequences (Fig. 14). However, in Fars Province, variable preservation beneath the mid-Turonian unconformity is limited to the Cenomanian and does not extend into the Albian, which is stratigraphically complete with limited thickness variation (Vincent *et al.*, 2015). This suggests that the absence of Cenomanian stratigraphy at outcrop sections in Fars Province may be related to non-deposition during the Cenomanian across an active structural high that formed an extension to the Qatar-Fars Arch (Vincent *et al.*, 2015) as opposed to subsequent erosion during mid-Turonian uplift. In the latter case, a more pronounced erosive profile that cuts down into the Albian stratigraphy would be expected. Further evidence for a syn-depositional structural control on Cenomanian facies and thickness variations in SW Iran was documented by Navidtalab *et al.* (2020) and Kalanat *et al.* (2021) (*see previous discussion*).

IMPLICATIONS FOR PETROLEUM HABITAT

Distribution of Petroleum Systems Elements

The sequence stratigraphic model presented here provides a framework within which to predict the distribution of petroleum systems elements within the Cenomanian–Turonian succession across the Arabian Plate. The distribution of petroleum systems elements can often be directly related to the palaeogeography and morphology of the depositional systems, giving confidence to predictions in areas where there is little data control for the purposes of near-field and frontier exploration.

Source Rocks

The majority of hydrocarbons reservoired within the Cenomanian–Turonian stratigraphic interval are derived from older source rocks. However, Cenomanian –Turonian source rocks are significant in parts of the Arabian Plate and charge (or at least contribute to) mid -Cretaceous reservoirs. The distribution of these source rocks is in general controlled by the development of intrashelf basins in which there was bottom-water anoxia. Within symmetric intrashelf basins (Fig. 5B), organic-rich carbonates and marls are associated with the late TST as intrashelf basin morphology developed (Razin *et al.*, 2010; 2017). However in asymmetric intrashelf basins, the input of siliciclatics has the potential to dilute the organic matter content in deep-water shales and marls, suppressing the development of source rock intervals as demonstrated in the Najaf basin in southern Iraq (Fig. 5A).

Organic-rich carbonates and marls charge Cenomanian–Turonian reservoirs in Oman (Terken, 1999), the UAE (van Lear *et al.*, 2019), Saudi Arabia (Newell and Hennington, 1983) and offshore Iran (Bordenave, 2014; Hosseiny *et al.*, 2016). Organic-rich carbonates are also recognized within Cenomanian–Turonian deep-water facies in the northern part of the plate. Thus self-sourcing mid-Cretaceous petroleum systems have been reported in both Turkey (Demirel *et al.*, 2001) and Jordan (Lüning and Kuss, 2014). For instance at the Hamzeh oilfield in Jordan, late Cenomanian – early Turonian source rocks of the Shueib Formation charge a mid-Turonian carbonate reservoir in the Wasi As Sir Formation (Lüning and Kuss, 2014) (see Fig. 10; Hamzeh 4 well).

Organic-rich carbonates within the Shilaif and Natih Formations are regarded as emerging unconventional resource plays in the UAE (van Lear *et al.*, 2019) and Oman (Mohsin *et al.*, 2018). The maximum extent of these source rocks within each depositional sequence can be represented by the MFS Gross Depositional Environment (GDE) maps (Fig. 12) which are the basis for source presence screening.

Reservoirs

Cenomanian – Turonian carbonates with high primary reservoir quality typically occur within rudist bioherm and shoal facies which were deposited adjacent to the margins of intrashelf basins (Burchette and Briton, 1985; Burchette, 1993; Mahdi *et al.*, 2013; Perrotta *et al.*, 2017). These facies are preferentially developed within HSTs (Fig. 5), and potential reservoir fairways are therefore present within the HST of each depositional system as rudist biostromes and shoal environments tracked the progradation of shelf margins. Progradational belts can be captured within each depositional sequence on the HST GDE map (Fig. 13), which is the basis for reservoir presence screening.

Seal

The Cenomanian–Turonian petroleum system is bounded by a Late Cretaceous top seal across large parts of the Arabian Plate which overlies the mid-Turonian unconformity (K150 SB) and which typically consists of a claystone or fine-grained carbonate unit within the K150 sequence (van Buchem *et al.*, 2011). In the UAE, claystones within the Coniacian Laffan Formation form an effective top seal for both structural and stratigraphic traps (Al-Zaabi *et al.*, 2010), including those with a subcrop component (Franco *et al.*, 2018). Fine-grained siliciclastic and tight carbonate units may also form intraformational seals. Claystones are typical of the LST in asymmetric intrashelf basins and the early TST within platform settings (van Buchem *et al.*, 2002; Razin *et al.*, 2010; 2017) (Fig. 5). Important intra-reservoir seals include siliciclastic units within the lower and upper members of the Ahmadi Formation in Kuwait and SE Iraq (Youssef *et al.*, 2019) (Figs 7 and 8), the Natih C and Natih D in Oman (van Buchem *et al.*, 2002) (Fig. 6), the Ahmadi-Wara and Rumaila Formations in Kuwait and Saudi Arabia (Alsharhan *et al.*, 2014; Youssef *et al.*, 2014, 2019; El Gezeery *et al.*, 2015), the Khatiyah Formation in Qatar (van Buchem *et al.*, 2014), and the Tuwayil Formation in the UAE and Saudi Arabia (Lü *et al.*, 2018) (Fig. 6).

Fine-grained, tight carbonates can also constitute lateral seals for stratigraphic traps and may result from either depositional facies changes or diagenetic processes. For instance, a change in depositional facies from rudist-rich grainy carbonates to micritic lagoonal carbonates could facilitate a stratigraphic trapping opportunity, with lagoonal carbonates forming the lateral seal. However, such stratigraphic traps are in general subtle and difficult to predict.

Controls on Carbonate Reservoir Quality

Reservoir quality within Cenomanian–Turonian carbonate reservoirs on the Arabian Plate is complex. Carbonate facies deposited across a wide range of depositional environments may exhibit high porosity

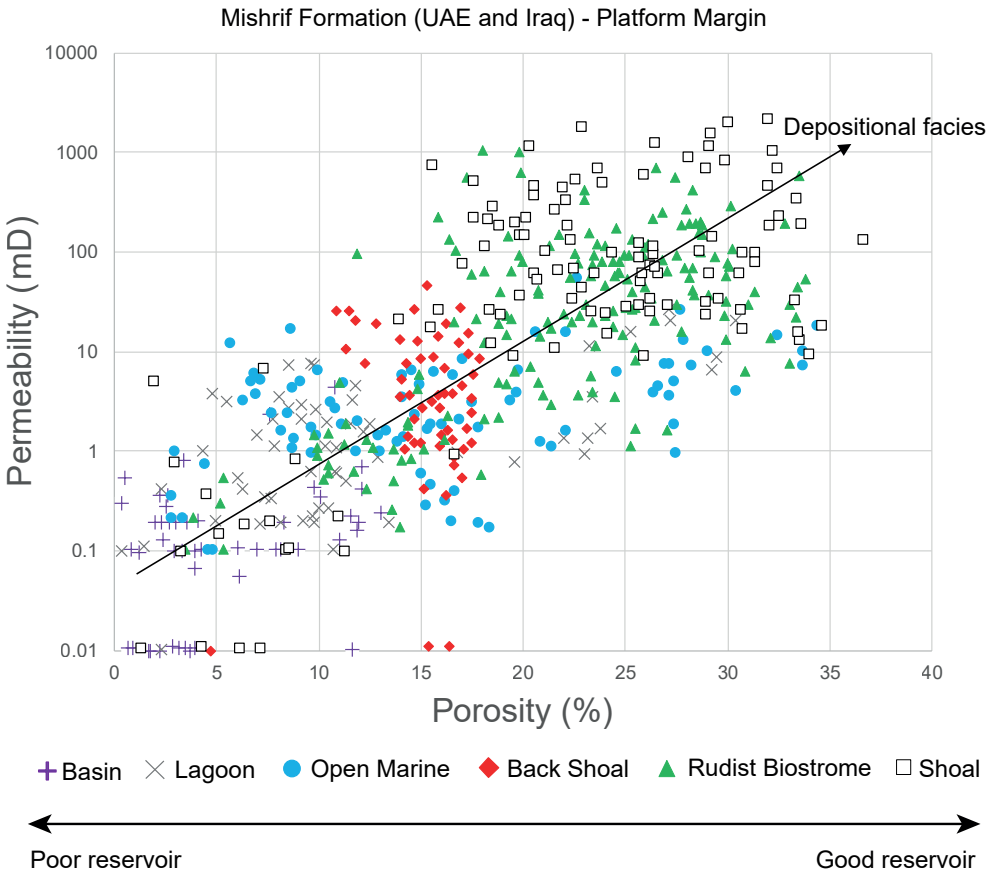

Fig. 15. Porosity – permeability plots for the Mishrif Formation. Data is compiled from various publications including Aqrawi *et al.* (1998) and Perrotta *et al.* (2017). Data from the Mishrif Formation demonstrates a primary control on reservoir quality related to depositional facies in platform margin settings.

but heterogenous permeability (Burchette and Britton, 1985; Jordan *et al.*, 1985; Hollis, 2011) and a particular porosity value may be associated with a range of permeabilities spanning 2-3 orders of magnitude (e.g. <1 to >1000s of mD). Porosity systems can be variable as the carbonates often display ubiquitous micropores together with primary macropores (inter- and intraparticle) and secondary dissolution pores creating a dual or triple porosity system (Hollis, 2011). Fracturing, dolomitization and large-scale karstification are added complexities which may be superimposed on an already heterogenous pore system (Sharp *et al.*, 2010; Hollis, 2011).

The prediction of reservoir quality in Cenomanian–Turonian carbonates at a regional scale is therefore challenging. However, there is a general association between the distribution of grainy, rudist-rich carbonate facies and high reservoir quality (Hollis, 2011). Dissolution of rudist bioclasts results in the development of relatively large biomoulds (up to 1 mm diameter) which provide the majority of the primary macroporosity within the carbonates (Hollis, 2011). These macropores are likely to be more interconnected than micropores, and hence rudist-rich biostrome and shoal facies have significantly higher permeability than basinal or platform interior facies assuming all other factors are equal. This is demonstrated in Fig. 15 which shows porosity-permeability data taken from the Mishrif Formation in platform margin locations in Iraq (Aqrawi *et al.*, 1998) and the UAE (Perrotta *et al.*, 2017). This control on reservoir quality is to some extent predictable at a regional scale from GDE maps, as rudist-rich facies mostly occur along the margins of intrashelf basins. However, there is complexity in the facies' detailed distribution (e.g. Mahdi and Aqrawi, 2014; Lü *et al.*, 2018) as localized rudist buildups can also occur within intrashelf basins (Burchette, 1993; Neo, 1996; Basu *et al.*, 2015) and in back shoals in the platform interior (Lü *et al.*, 2018). Reworking of fragmented rudist material to form grainstones and rudstones both downslope as calciturbidites and into platform interior settings as sand sheets (probably due to storm events) may also occur. Indeed, the latter may cause difficulties in effective reservoir management, particularly where waterflooding is employed to improve secondary recovery (Cross *et al.*, 2010).

While the distribution of rudist-rich facies is important, it is not necessarily a prerequisite to attain high reservoir quality and there are numerous examples of productive reservoirs which were deposited in platform interior settings. For instance, Sarvak reservoirs in the Zagros fold-and-thrust belt of SW Iran

are interpreted to have been deposited a considerable distance away from the margins of any intrashelf basin (Taghavi *et al.*, 2006). In these instances, diagenesis and/or fracturing may improve reservoir quality and compensate for relatively low primary matrix permeability (Taghavi *et al.*, 2006; Casini *et al.*, 2011; Hollis *et al.*, 2011), and reservoirs with high primary reservoir quality may also be enhanced by these secondary processes (Cantrell *et al.*, 2020; Majeed *et al.*, 2021). Tectonic fracturing may result in a dual permeability system which in turn may promote subsequent dolomitization by providing pathways for hydrothermal fluids (Sharp *et al.*, 2006, 2010; Lapponi *et al.*, 2011). Hydrothermal dolomites commonly enhance reservoir quality but are not stratigraphically predictable (Sharp *et al.*, 2010).

Meteoric diagenesis may also impact upon the quality of Cenomanian–Turonian carbonate reservoirs. Prolonged subaerial exposure as a result of relative sea-level fall and/or tectonic uplift may result in karstification of the tops of carbonate platforms. Karstification beneath major sequence boundaries has been recorded from outcrop, seismic, whole core and stable isotope studies (Burchette and Britton, 1995; Jordan *et al.*, 1995; Botton-Dumay *et al.*, 2002; Grélaud *et al.*, 2006, 2010; Homewood *et al.*, 2010; Rahimpour-Bonab *et al.*, 2013; Hajikazemi *et al.*, 2017; Vincent *et al.*, 2020; Cantrell *et al.*, 2020; Malekzadeh *et al.* 2020; Chen *et al.*, 2021). However, the impact of karstification on reservoir quality is complex and difficult to demonstrate away from outcrop, as karst features are typically much larger in scale than thin sections and core plugs. Depending on the circumstances, karstification has the potential either to enhance reservoir quality through the creation of a secondary permeability network, or degrade reservoir quality as paleosols can infill karst vugs, occlude existing pores and create flow baffles (Hollis, 2011).

Permeability enhancement and permeability reduction can occur at different depths within the same karstified reservoir, creating intervals with very heterogenous permeability (Botton-Dumay *et al.*, 2002). Preferential dissolution of rudist debris beneath karst surfaces may create very high permeability (>100 mD) zones that enable early breakthrough of formation waters (Hollis *et al.*, 2010), resulting in complications for reservoir development and management. The following factors should be important when considering karst and its impact upon reservoir quality: duration of exposure; relief; magnitude of relative sea-level change; nature of the exposed substrate; climate; depth to water table; the presence and fill of incised valleys (e.g. sand or shale); clay infiltration of caves, fissures and dolines; grain mineralogy and propensity to dissolution (aragonite vs high Mg vs low Mg calcite allochems); differential cementation; salt movement; and whether soils or coaly swamps are present (Burchette and Britton, 1995; Grelaud *et al.*, 2006, 2010; Ghabeishavi *et al.*, 2009; Cross *et al.*, 2010; Sharp *et al.*, 2010; Burchette *et al.*, 2010; Hollis, 2011; Deville de Periere *et al.*, 2017; Assadi *et al.*, 2018; Xiao *et al.*, 2020).

The likelihood of encountering karst features varies within the Albian–Turonian succession. The most significant karstified surface is the composite mid-Turonian unconformity (K150 SB) which resulted from tectonic uplift and a relatively long duration of exposure (up to 3 Ma) across a highly variable topographic profile. This surface is recognized regionally and is associated with dissolution features, vugs and brecciated cavities, vadose cements, dolines, paleosols, bauxites, incised channels and channel fills at various locations across the southern part of the Arabian Plate (Videtich *et al.*, 1988; Burchette and Britton, 1995, Jordan *et al.*, 1995; Botton-Dumay *et al.*, 2002; Droste and Van Steenwinkel, 2004; Zarasvandi *et al.*, 2008; Sharp *et al.*, 2010; Hollis, 2011; Deville de Periere *et al.*, 2017; Assadi *et al.*, 2018).

Another significant karstified surface occurs at the base of the middle Cenomanian K130 SB and results from a widely recognized relative sea-level fall (e.g. Hancock, 2003; van Buchem *et al.*, 2011). A regional exposure surface occurs beneath the K130 SB in platform locations (Hollis, 2011; van Buchem *et al.*, 2011), with evidence of channel incision in Oman (Grélaud *et al.*, 2006, 2010; Homewood *et al.*, 2008). Disconformities with associated karst features have been reported, at least locally, for all recognized sequence boundaries within the Cenomanian–Turonian interval. For instance, karst features are documented at the top of the Mauddud Formation in Kuwait beneath the K120 SB (Cross *et al.*, 2010; Vincent *et al.*, 2020) and at the "Mishrif Disconformity" in southern Iraq beneath the K140 SB (Mahdi *et al.*., 2013; Mahdi and Aqrawi, 2014; Cantrell *et al.*, 2020). A Cenomanian–Turonian boundary disconformity within the Sarvak Formation in Iran is also recognized (Rahimpour-Bonab *et al.*, 2013; Mehrabi and Rahimpour-Bonab, 2014; Hajikazemi *et al.*., 2017; Malekzadeh *et al.*, 2020), but in this study we assign it to the early Turonian Tu1 SB although we acknowledge that this surface could potentially be older (*see previous discussion*).

Exploration Opportunities in Stratigraphic Traps

As the Arabian Plate is a mature petroleum province with few large-scale structural prospects remaining undrilled, exploration opportunities within the Cenomanian–Turonian petroleum system predominantly consist of stratigraphic traps. Exploration of this play requires a detailed understanding of depositional facies changes which can be achieved within the sequence

stratigraphic framework proposed in this study. GDE maps provide the basis for play screening, as they characterize depositional facies variations through the full cycle of relative sea-level change and show the spatial distribution of petroleum systems elements. Furthermore, field or prospect scale reservoir studies are more valuable when they can be placed within the context of a regional model. There is considerable value to be gained from analogues elsewhere on the Arabian Plate, but only if they can be identified and understood within a regionally consistent framework.

Recent discoveries reported in stratigraphic traps such as the Eridu field, SE Iraq (Lukoil, 2017), and the Mishrif discoveries on the western margin of the Shilaif intrashelf basin in the UAE (Lü *et al.*, 2018; Jaya *et al.*, 2020; Xiao *et al.*, 2020), highlight the remaining potential within the stratigraphic play. At the Eridu field, the limited information available (Lukoil, 2017) suggests that the Mishrif reservoir comprises an isolated rudist biostrome, and this appears to be similar to the stratigraphic trapping mechanism at the Dujaila field (Sadooni, 2005; Khawaja *et al.*, 2021) as illustrated by Mahdi and Aqrawi (2014).

Recent exploration and appraisal wells in the UAE emphasise the complexity of the stratigraphic play as the oil-water contact is not structurally controlled, with water-bearing reservoirs located up-dip from oil discoveries (Lü *et al.*, 2018; Jaya *et al.*, 2020). Controls on the stratigraphic trapping mechanism are not well understood, and there is considerable uncertainty regarding the configuration, volumes and connectivity of the oil pools (Jaya *et al.*, 2020). Diagenetic processes may account for the trapping mechanism (Jaya *et al.*, 2020) although this has not been demonstrated.

It is possible that stratigraphic traps with a similar configuration could result from variations in primary depositional facies. Thus shoal and biostrome facies with well-developed, interconnected macropores may be oil saturated, while adjacent open platform or lagoonal facies with ubiquitous micropores at the same depths within a common structure may have high irreducible water saturations. For example, there are a number of oilfields in the Dezful Embayment (SW Iran) (e.g. Abteymur) and southern Iraq (e.g. Nahr Umr) where interpreted oil-water contacts are shallowest on the crests, deepest on the flanks, and at intermediate depths in-between. Petrophysical analyses indicate a single free-water level across these fields. While fault compartmentalization has been proposed to explain these observations, even though faulting has not been identified on seismic data, a viable alternative model places microporous rocks at the crests of the structures and macroporous rocks on the flanks.

In examples from the Sarvak and Mishrif Formations, the distribution of pore systems can be a consequence of sequence stratigraphic layering. However, lateral facies changes such as those observed on the margins of the Shilaif Basin (Lü *et al.*, 2018; Jaya *et al.*, 2020) may produce similar results with thick transition zones in more crestal areas and deeper, more abrupt oil-water contacts on the flanks. Thus, deeper, dry oil with a negligible water cut is recovered from flank wells rather than from crestal locations in such fields (e.g. Abteymur, SW Iran). Hydrodynamically inclined oil-water contacts due to Oligocene tectonic tilting has been identified in the Al-Shaheen field, offshore Qatar (van Buchem *et al.*, 2014), and the Sirri fields, offshore Iran (Bashari, 2021), and thus should be considered elsewhere.

The charging mechanism for the discoveries on the western margin of the Shilaif Basin in the UAE relies on lateral migration (>100 km) from the thermally mature Shilaif kitchen (Xiao *et al.*, 2020). A karstified exposure surface between the Mishrif Formation reservoir and the Tuwayil Formation top-seal (corresponding to the Tu1 SB) may have acted as a carrier bed for the laterally migrating hydrocarbons (Xiao *et al.*, 2020). This emphasizes the importance of characterizing the extent and nature of karstified surfaces which may potentially act both as carrier beds and thief zones to breached traps. The latter mechanism may explain exploration failures in offshore eastern Abu Dhabi (Burchette and Britton 1985) and offshore Iran (Baniasad *et al.*, 2021).

Screening for Subcrop Traps

Variable preservation beneath the mid-Turonian regional unconformity (K150 SB) results in a Cenomanian –Turonian subcrop across the southern and central parts of the Arabian Plate. In areas where grainy rudist-rich and/or karstified carbonates are truncated by the unconformity, and the unconformity is overlain by an effective seal, there is a high potential for a subcrop play (Fig. 16) (Simmons and Davies, 2016). Burchette and Britton (1985) emphasised the importance of bottom seal integrity to create a configuration where bottom and top seals merge at the unconformity surface, preventing continued migration up-dip. Unlike diagenetic traps and updip porosity pinch-outs which are complex but localized phenomena, the potential for subcrop stratigraphic traps can be predicted at a regional scale. Numerous hydrocarbon accumulations in the Cenomanian–Turonian succession have a subcrop component which is either solely responsible for trapping or complements an existing trap. Examples include the Fateh field, UAE (Jordan *et al.*, 1985; Videtich *et al.*, 1988; Pascoe *et al.*, 1995), the Natih field, Oman (van Buchem *et al.*, 2002), the Sirri A, B, C and D fields offshore Iran (Farzadi, 2006; Ghajari *et al.*, 2013), and the Al Shaheen and Guiriel fields, offshore Qatar (Botton-Dumay *et al.*, 2002; van Buchem *et al.*, 2014; Deville de Periere *et*

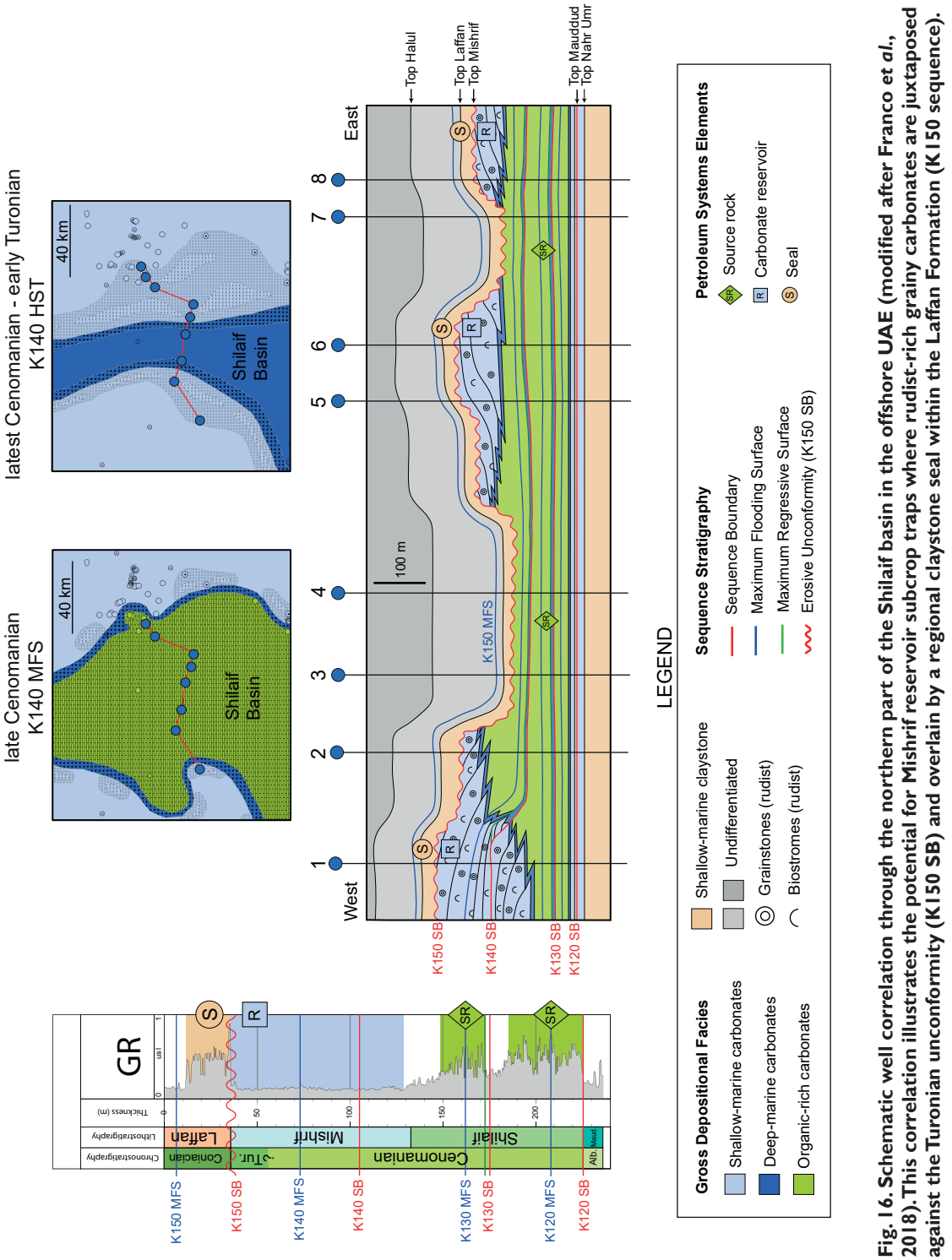

Fig. 16. Schematic well correlation through the northern part of the Shilaif basin in the offshore UAE (modified after Franco *et al.*, 2018). This correlation illustrates the potential for Mishrif reservoir subcrop traps where rudist-rich grainy carbonates are juxtaposed against the Turonian unconformity (K150 SB) and overlain by a regional claystone seal within the Laffan Formation (K150 sequence).

al., 2017). This play concept has also been under recent appraisal in offshore UAE (e.g. Franco *et al.*, 2018).

GDE maps can be used to screen for this subcrop play. By mapping the preservation limits on each GDE map surface, the maps can be processed to give the subcrop extent within each sequence. The HST maps (Fig. 13) can be used to assess the extent of potential reservoir facies beneath the subcrop based on the prediction of either high primary reservoir quality (grainstone or bioherm facies) or secondary reservoir enhancement (karstification). The results of the subcrop screening (Fig. 17) show trends which are consistent with the distribution of fields producing from Cenomanian–Turonian reservoirs, many of which have a subcrop component. The trends include (Fig. 17):

1. The Mishrif trend in SE Iraq which is associated with giant and supergiant fields such as Rumaila and

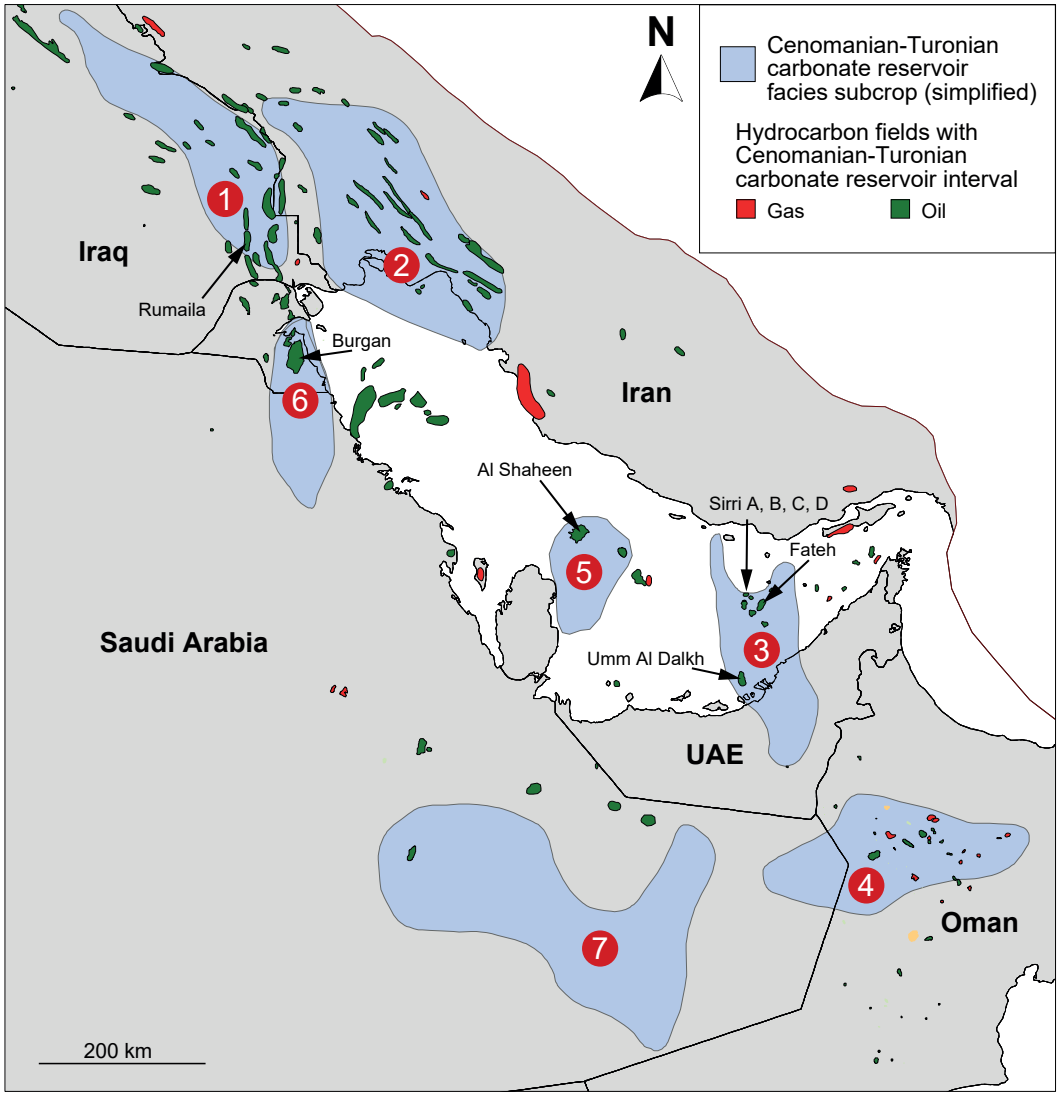

Fig. 17. Map showing the simplified and generalized extent of potential carbonate reservoirs within Cenomanian – Turonian subcrop beneath the regional Turonian unconformity. Overlay shows oil and gas fields with a carbonate reservoir interval of Cenomanian–Turonian age. Note that the screening output reconciles with prolific reservoir trends (labelled), many of which have a subcrop component: (1) the Mishrif trend of SE Iraq; (2) the Sarvak trend of the Dezful Embayment, Iran; (3) the Mishrif trend on the Eastern Platform, UAE; (4) the Natih trend of northern Oman; (5) the Mishrif trend, offshore flank of the Qatar Arch; (6) the Mishrif trend, Burgan Arch and Safaniyah-Nowrooz-Hendijan Arch, Kuwait and PNZ; (7) exploration opportunities within the Rub' Al Khali area of Saudi Arabia.

Majnoon and which accounts for ~30% of Iraq's oil reserves (Mahdi *et al.*, 2013). In this trend, high primary reservoir quality occurs in shoals and patch reefs.

2. The Sarvak trend in the Dezful Embayment, SW Iran, where the reservoir properties of platform interior facies have been significantly enhanced as a result of karstification related to sea-level fall and Turonian uplift (Rahimpour-Bonab *et al.*, 2013; Malekzadeh *et al.*, 2020). Sarvak reservoirs account for >20% of Iranian oil reserves (Bordenave and Hegre, 2010) in fields such as Azadegan, Ahwaz and Gachsaran.

3.The Mishrif trend on the eastern margin of the Shilaif Basin, UAE, which includes giant and supergiant fields such as Fateh (Jordan *et al.*, 1985; Videtich *et al.*, 1988; Pascoe *et al.*, 1995), Umm al Dalkh (Neo, 1996) (UAE) and the Sirri A, B, C and D fields, offshore Iran (Farzadi, 2006; Ghajari *et al.*, 2013). This trend is characterized by excellent primary reservoir quality in shelf margin shoals and biostromes, with reservoir quality further enhanced through karstification beneath the mid-Turonian unconformity.

4. The Natih trend in northern Oman, including fields such as Fahud and Natih, where reservoir quality is significantly enhanced as a result of karstification beneath the mid-Turonian unconformity (K150 SB) (van Buchem *et al.*, 2002).

5. The Mishrif trend offshore Qatar, where differential erosion on the flanks of the Qatar Arch has generated a subcrop profile with karstification of

micritic, microporous platform top carbonates (e.g. Deville de Periere *et al.*, 2017; Botton-Dumay *et al.*, 2002).

6. The Mishrif trend across southern Kuwait and the Partioned Neutral Zone. Differential truncation beneath the mid-Turonian unconformity here was illustrated by Al-Laboun (1987) along the Safaniyah-Nowrooz-Hendijan Arch and by Davies *et al.* (2002) along the flanks of the Burgan Arch.

The subcrop screening also highlights significant exploration opportunities away from known fields. For instance, there are high-graded areas within the Rub' Al Khali of Saudi Arabia (7). This area is more frontier, but the results of this screening process predict high primary reservoir quality with the potential for karstification beneath the Turonian unconformity.

CONCLUSIONS

Based on data sourced from the published literature and the application of a well-dated and -documented sequence stratigraphic model, a high resolution sequence stratigraphic analysis has been made of the Cenomanian–Turonian interval of the Arabian Plate. This model has achieved a stratigraphic resolution that is beyond previously published maps, and is illustrated with palaeogeographic maps, isopach maps and regional well log and outcrop correlations.

This high resolution time framework has allowed illustration at the scale of the Arabian Plate of (i) large-scale patterns of sedimentation including the initiation and infill of intrashelf basins, (ii) the significant palaeogeographic changes that occurred within individual 3rd order depositional sequences, and (iii) the impact of local tectonics on facies patterns and depocentre shifts. This proves the point that a regional – plate-wide – sequence stratigraphic approach is essential in order to understand and predict stratigraphic architecture and with that reduce risk in exploration. The regionally consistent framework facilitates and underpins the entire exploration workflow from well interpretation and correlation to GDE mapping and play screening.

The distribution of petroleum systems elements within the Cenomanian–Turonian succession is closely related to the palaeogeography of the depositional systems and particularly to the style and evolution of intrashelf basins. The configuration of petroleum systems elements differs between symmetric intrashelf basins which were isolated from siliciclastic input (e.g. the Shilaif and Natih Basins) and asymmetric intrashelf basins where there was a significant siliciclastic influence on the inboard basin margin (e.g. the Najaf Basin). Symmetric intrashelf basins are characterized by source rock development in the transgressive systems tract, while rudist-rich carbonate reservoirs track the progradational shelf margins during highstands. Intraformational claystone seals are typical of the early TST within platform settings and record shoreline retrogradation across the top of the exposed platform.

Asymmetric intrashelf basins are typically not associated with source rock development due to siliciclastic dilution. Rudist-rich carbonates with reservoir potential may occur on the outboard margin but are suppressed on the siliciclastic-prone inboard margin. There is high potential to encounter claystone seals resulting from siliciclastic input during the lowstand and its subsequent retrogradation across the homoclinal ramp during the TST.

The sequence attributed plate-scale dataset used in this study is unique and offers some important new insights into the evolution of accommodation space. In SW Iran, the preserved thickness of the Cenomanian–Turonian interval varies from >800 m in Khuzestan to 0 m in parts of Fars Province, and was principally controlled by tectonics. Notwithstanding local tectonic overprint, three Cenomanian sequences can be correlated with confidence at the scale of the Arabian Plate. Within each sequence, significant thickness changes may be related to palaeogeographic variations, with condensation occurring in intrashelf basins and differential aggradation on carbonate platforms. The development of intrashelf basins may have occurred during relative tectonic quiescence as a response to eustatic variations (e.g. in Oman), or in more tectonically active areas undergoing extension (e.g. Fars Province, Iran).

Tectonic overprint related to the mid-Turonian unconformity (K150 SB) is evident in the southern part of the Arabian Plate and impacts the preservation of early Turonian and in some cases Cenomanian sequences. The expression of the uplift is variable, as demonstrated by the presence of a relatively thick and complete Turonian sequence in the northern Arabian Plate which was deposited contemporaneous to regional uplift in the southern plate. Variable preservation beneath the Turonian unconformity results in a subcrop trap play. This play has exploration potential across large parts of the Arabian Plate where rudist-rich, karstified carbonates occur beneath the unconformity and are overlain by a regional-scale claystone seal.

ACKNOWLEDGEMENTS

Halliburton is thanked for permission to publish. Thandeka Mlambo and Sophie Evans are acknowledged for their assistance with stratigraphic interpretation, as is Andy Horbury for insightful discussions concerning the Najaf Basin. The authors are grateful to journal referees Hossain Rahimpour-Bonab (University of

Tehran) and Andy Horbury (Cambridge Carbonates) for the significant improvements they made to early drafts of this manuscript.

Data availability statement

Data is exclusively derived from public domain resources.

Author contributions

AB: Conceptualization (equal); Investigation (lead); Writing – Original Draft Preparation (lead);
FvB and **MS**: Conceptualization (equal); Investigation (support); Original Draft Preparation (support); Writing – Review & Editing (equal);
RD: Writing – Original Draft Preparation (support); Writing – Review & Editing (equal).

Declaration of competing interest

The authors declare that they have no known competing financial interests or personal relationships that could have appeared to influence the work reported in this paper

REFERENCES

ABEED, Q., LEYTHAEUSER, D. and LITTKE, R., 2012. Geochemistry, origin and correlation of crude oils in Lower Cretaceous sedimentary sequences of the southern Mesopotamian Basin, southern Iraq. *Organic Geochemistry*, **46**, 113-126.

ADAMS T.D., KHALILI, M. and KHOSROVI SAID, A., 1967. Stratigraphic significance of some oligosteginid assemblages from Lurestan Province, northwest Iran. *Micropaleontology*, **13**, 55-67.

AL-AMERI, T.K. and ZUMBERGE, J., 2012. Middle and Upper Jurassic hydrocarbon potential of the Zagros Fold Belt, North Iraq. *Marine and Petroleum Geology*, **36**, 13-34.

AL-ANZI, M.S.H., 1995. Stratigraphy and structure in the Bahrah Field, Kuwait. In: AL-HUSSEINI, M. I., (Ed.), Geo'94. The Middle East Petroleum Geosciences, **2**. Selected Middle East Papers from the Middle East Geoscience Conference, April 1994, Bahrain, 53-64.

AL-ANZI, H., and TOURQUI, H., 2019. Facies Architecture, Paleoenvironment, and Reservoir Quality of the Mid-Cretaceous Wara Member, Arabian Gulf, Offshore Saudi Arabia. Siliciclastic Reservoirs of the Arabian Plate. *AAPG Memoir*, **116**, 289-316.

AL-LABOUN, A. A. 1977. The depositional framework of the Wara-Mauddud-Burgan formations in northeastern Arabia: M.Sc. thesis, University of Tulsa, Tulsa, Oklahoma, 95 p.

AL-KHAFAJI, A.J., HAKIMI, M.H. and NAJAF, A.A., 2018. Organic geochemistry characterisation of crude oils from Mishrif reservoir rocks in the southern Mesopotamian basin, South Iraq: Implication for source input and paleoenvironmental conditions. *Egyptian Journal of Petroleum*, **27**, 117-130

AL-NAQIB, K.M., 1967. Geology of the Arabian Peninsula; southwestern Iraq. USGS - Professional Paper 560-G, U.S. Government Printing Office, 54 pp.

AL-QAYIM, B., QADIR, F.M. and ALBEYATI, F., 2010. Dolomitization and porosity evaluation of the Cretaceous Upper Qamchuqa (Mauddud) Formation, Khabbaz oil field, Kirkuk area, northern Iraq. *GeoArabia*, **15**, 49-76.

AL-QAYIM, B., HUSSEIN, S., QADER, F.M., AL-HAKARI, S.H., SHUKOR, B., SARDAR, Z., AHMED, S. and ABDULLAH, H., 2016. Integrated stratigraphic study of the Cretaceous petroleum-potential succession, Sulaimani area, Kurdistan, Iraq. Special Issue, GeoKurdistan II (39-50). *Journal of Zankoy Sulaimani (JZS-A)*, **8**, 391-418.

AL-SAGRI, K.E.A. 2015. Linking the Timing of Deposition and Organic Matter Richness of the Gulneri Formation of Northern Iraq to the Global Oceanic Anoxic Event 2 (OAE 2): Implications to better constrain the Depositional Models of Iraqi's Oil Source Beds and their Timing of Deposition. *Iraqi Journal of Science*, **56**, 2007-2023.

AL-ZAABI, M., TAHER, A., AZZAM, I. and WITTE, J., 2010. Geological Overview of the Middle Cretaceous Mishrif Formation in Abu Dhabi. Abu Dhabi International Petroleum Exhibition and Conference, November 2010, Abu Dhabi, UAE. Society of Petroleum Engineers (SPE), 1-20.

ALIPOUR, M., ALIZADEH, B., MIRZAIE, S. and CHEHRAZI, A., 2021. Basin and petroleum system analysis in the southeastern Persian Gulf basin: a 2D basin modeling approach. *Journal of Petroleum Exploration and Production Technology*, **11**, 4201-4214.

ALSHARHAN, A.S., STROHMENGER, C.J., ABDULLAH, F.H. and AL SAHLAN, G., 2014. Mesozoic stratigraphic evolution and hydrocarbon habitats of Kuwait. In: MARLOW, L., KENDALL, C. and YOSE, L. (Eds), Petroleum Systems of the Tethyan Region. *AAPG Memoir*, **106**, 541-611.

ANDREWS, I. J., 1992. Cretaceous and Palaeogene lithostratigraphy in the subsurface of Jordan. *Subsurface Geology Bulletin*, 1-60. Natural Resources Authority, The Hashemite Kingdom of Jordan,

AQRAWI, A.A.M. and HORBURY, A.D., 2008. Predicting the Mishrif Reservoir quality in the Mesopotamian Basin, southern Iraq. GEO 2008, 8th Middle East Geoscience Conference, Manama, Bahrain, 1-39.

AQRAWI, A.A.M. and KHAIWKA, M.H., 1989. Microfacies analysis of Rumaila Formation and equivalents (Cenomanian) in Mesopotamian Basin, a statistical approach. *Journal of the University of Kuwait. Science*, **16**, 143-152.

AQRAWI, A.A.M., MAHDI, T.A., SHERWANI, G.H. and HORBURY, A. D., 2010a. Characterisation of Mid-Cretaceous Mishrif Reservoir of the Southern Mesopotamian Basin, Iraq. AAPG GEO 2010 Middle East Geoscience Conference & Exhibition, Manama, Bahrain, March 2010. *AAPG Search and Discovery* 50264, 1-35.

AQRAWI, A.A. M., GOFF, J.C., HORBURY, A.D. and SADOONI, F.N., 2010b. The Petroleum Geology of Iraq. Scientific Press Ltd (UK), pp. 424

AQRAWI, A.A.M., THEHNI, T.A., SHERWANI, G.H. and KAREEM, B.M.A., 1998. Mid-Cretaceous rudist-bearing carbonates of the Mishrif Formation: an important reservoir sequence in the Mesopotamian Basin, Iraq. *Journal of Petroleum Geology*, **21**, 57-82.

ASSADI, A., HONARMAND, J., MOALLEMI, S.A and IRAJ, A.-F., 2018. An integrated approach for identification and characterization of palaeo-exposure surfaces in the upper Sarvak Formation of Abadan Plain, SW Iran. *Journal of African Earth Sciences*, **145**, 32-48.

AZAR, J.H., NABI-BIDHENDI, M., JAVAHERIAN, A. and PISHVAIE, M.R., 2009. Integrated seismic attributes to characterize a widely distributed carbonate clastic deposit system in Khuzestan Province, SW Iran. *Journal of Geophysics and Engineering*, **6**, 162-171.

AZZAM, I.N., 1995. Sequence stratigraphy of Middle Cretaceous siliciclastic sandstone (Tuwayil Formation) in west Abu Dhabi: a model approach to oil exploration. In: AL-HUSSEINI, M.I. (Ed.), Geo'94. The Middle East Petroleum Geosciences, **1**. Selected Middle East Papers from the Middle East Geoscience Conference, April 1994, Bahrain, 155-165.

BANIASAD A., LITTKE, R., FROIDL, F., GROHMANN, S. and SOLEIMANY, B., 2021. Quantitative hydrocarbon generation and charge risk assessment in the NW Persian Gulf: A 3D

basin modeling approach. *Marine and Petroleum Geology*, **126**, 104900.

BASHARI, A., 2021. Hydrodynamic activity in the Mishrif reservoirs: an approach to characterize Sarvak Formation, in eastern part of the Persian Gulf. *Iranian Journal of Petroleum Geology*, **19**, 45-57.

BASU, S., FOLLOWS, E., SINGHAL, M., TURKI, A. and ABBAS, F., 2015. Mishrif Rock Typing: Robust Reservoir Analysis. Abu Dhabi Intl. Petroleum Exhibition &Conference, November, Abu Dhabi, UAE. *SPE Conference Paper* no. 177764-MS, 1-9.

BAUER, J., KUSS, J. and STEUBER, T., 2003. Sequence architecture and carbonate platform configuration (Late Cenomanian-Santonian), Sinai, Egypt. *Sedimentology*, **50**, 387-414.

BEIN, A. 1976. Rudistid Fringing Reefs of Cretaceous Shallow Water Carbonate Platform of Israel. *AAPG Bulletin*, **60**, 258-272.

BORDENAVE, M.L. and HUC, A.Y., 1995. The Cretaceous source rocks in the Zagros foothills of Iran. *Revue de l'Institut Francais du Petrole et Annales des Combustibles Liquides*, **50**, 727-752.

BORDENAVE, M.L. and HEGRE, J.A., 2010. Current distribution of oil and gas fields in the Zagros Fold Belt of Iran and contiguous offshore as the result of the petroleum systems. In: LETURMY, P. and ROBIN, C. (Eds), Tectonic and Stratigraphic Evolution of Zagros and Makran during the Mesozoic-Cenozoic. *Geol. Soc. Lond. Spec. Publ.*, **330**, 291-353.

BORDENAVE, M.L., 2014. Petroleum Systems and Distribution of the Oil and Gas Fields in the Iranian Part of the Tethyan Region. In: MARLOW, L., KENDALL, C.C.G. and YOSE, L.A. (Eds), Petroleum Systems of the Tethyan Region. *AAPG Memoir*, **106**, 505-540

BOTTON-DUMAY, R., MANIVIT, T., MASSONNAT, G. and GAY, V., 2002. Karstic High Permeability Layers: Characterization and Preservation While Modelling Carbonate Reservoirs. Abu Dhabi International Petroleum Exhibition and Conference, Abu Dhabi, United Arab Emirates, October 2002. Society of Petroleum Engineers (SPE), 1-16.

BUCHBINDER, B., BENJAMINI, C. and LIPSON-BENITAH, S., 2000. Sequence development of Late Cenomanian-Turonian carbonate ramps, platforms and basins in Israel. *Cretaceous Research*, **21**, 813-843.

BUDAY, T., 1980, The Regional Geology of Iraq, **1**: Stratigraphy and Paleogeography. Publications of Geological Survey of Iraq, Baghdad, pp. 445

BURCHETTE, T.P., 1993. Mishrif Formation (Cenomanian-Turonian), southern Arabian Gulf: carbonate platform growth along a cratonic basin margin. In: SIMO, J.A., SCOTT, R.W. and MASSE, J.P. (Eds), Cretaceous Carbonate Platforms. *AAPG Memoir*, **56**, 185-199.

BURCHETTE, T.P. and BRITTON, S.R., 1985. Carbonate facies analysis in the exploration for hydrocarbons: a case history from the Cretaceous of the Middle East. In: BRENCHLEY, P.J. and WILLIAMS, B.P.J. (Eds), Sedimentology: recent developments and applied aspects. *Geol. Soc. Lond. Spec. Publ.*, **18**, 311-338.

CANTRELL, D.L., SHAH, R.A., OU, J., XU, C., PHILLIPS, C., LI, X.L. and HU, T.M., 2020. Depositional and diagenetic controls on reservoir quality: Example from the upper Cretaceous Mishrif Formation of Iraq. *Marine and Petroleum Geology*, **118**, 104415.

CASINI, G., GILLESPIE, P.A., VERGÉS, J., ROMAIRE, I., FERNÁNDEZ, N., CASCIELLO, E., SAURA, E., MEHL, C., HOMKE, S., EMBRY, J.-C., AGHAJARI, L. and HUNT, D.W., 2011. Sub-seismic fractures in foreland fold and thrust belts: insight from the Lurestan Province, Zagros Mountains, Iran. *Petroleum Geoscience*, **17**, 263-282.

ÇELIKDEMIR, M.E., DULGER, S., GORUR, N., WAGNER, C. and UYGUR, K., 1991. Stratigraphy, sedimentology, and hydrocarbon potential of the Mardin Group, south-east Turkey. In: SPENCER, A. M. (Ed.), Generation, Accumulation and Production of Europe's Hydrocarbons. *EAPG Spec. Publ.* **1**, 439-454.

CHEN, P., GUO, L., LI, C. and TONG, Y., 2021. Karstification characteristics of the Cenomanian-Turonian Mishrif Formation in the Missan Oil Fields, southeastern Iraq, and their effects on reservoirs. *Frontiers of Earth Science*, 1-11.

COSKUN, B., 1996. Tectonic controls on the evolution of porosity in the Cretaceous Mardin Group Carbonates, Adiyaman Oilfields, SE Turkey. *Journal of Petroleum Geology*, **19**, 445-460.

CRAIGIE, N.W., 2015. Applications of chemostratigraphy in Cretaceous sediments encountered in the North Central Rub' al-Khali Basin, Saudi Arabia. *Journal of African Earth Sciences*, **104**, 27-42.

CROSS, N., GOODALL, I., HOLLIS, C., BURCHETTE, T., AL-AJMI, H.Z.D., JOHNSON, I.G., MUKHERJEE, R., SIMMONS, M. and DAVIES, R., 2010. Reservoir description of a mid Cretaceous siliciclastic-carbonate ramp reservoir: Mauddud Formation in the Raudhatain and Sabiriyah fields, North Kuwait. *GeoArabia*, **15**, 17-50.

DATTA, K., AL-ENEZI, B., ABDULLAH, F., BURMAN, K., AL-ENEZI, H., FILAK, J., LE GUERROUÉ, E., MURAT, B., ROUSSE, S. and PEYSSON, A., 2011. New sequence stratigraphic model for the Burgan, Mauddud and Wara formations of Greater Burgan field, Kuwait. *AAPG Search and Discovery* Article 40858

DATTA, K., YASER, M., GOMEZ, E., MA, Y.Z., FILAK, J.-M., AL-NASHEET, A. and ORTEGON, L.D.T., 2019. Capturing Multiscale Heterogeneity in Paralic Reservoir Characterization: A Study in Greater Burgan Field, Kuwait. In: AL ANZI, H.R., RAHMANI, R.A., STEEL, R.J. and SOLIMAN O.M. (Eds), Siliciclastic Reservoirs of the Arabian Plate. *AAPG Memoir*, **116**, 261-288.

DAVIES, R.B., CASEY, D.M., HORBURY, A.D., SHARLAND, P.R. and SIMMONS, M.D., 2002. Early to mid-Cretaceous mixed carbonate-clastic shelfal systems; examples, issues and models from the Arabian Plate. *GeoArabia*, **7**, 541-598.

DAVIES, R.B., SIMMONS, M.D., JEWELL, T.O. and COLLINS, J., 2019. Regional Controls on Siliciclastic Input into Mesozoic Depositional Systems of the Arabian Plate and Their Petroleum Significance. In: AL ANZI, H.R., RAHMANI, R.A., STEEL, R.J. and SOLIMAN O.M. (Eds), Siliciclastic reservoirs of the Arabian plate. *AAPG Memoir* **116**, 103-139.

DEHYADEGARI, E., 2019. Geochemistry and origins of Sarvak oils in Abadan plain: oil-oil correlation and migration studies. *Energy Sources*, **43**, 716-726.

DEMIREL, I.H. and GUNERI, S., 2000. Cretaceous Carbonates in the Adiyaman Region, SE Turkey: An assessment of Burial History and Source-rock Potential. *Journal of Petroleum Geology*, **23**, 91-106.

DEMIREL, I.H., YURTSEVER, T.S. and GUNERI, S., 2001. Petroleum systems of the Adiyaman region, Southeastern Anatolia, Turkey. *Marine and Petroleum Geology*, **18**, 391-410.

DEVILLE DE PERIERE, M., DURLET, C., VENNIN, E., CALINE, B., BOICHARD, R. and MEYER, A., 2017. Influence of a major exposure surface on the development of microporous micritic limestones – Example of the Upper Mishrif Formation (Cenomanian) of the Middle East. *Sedimentary Geology*, **353**, 96-113.

DIAS-BRITO, D., 2000. Global stratigraphy, palaeobiogeography and palaeoecology of Albian–Maastrichtian pithonellid calcispheres: impact on Tethys configuration. *Cretaceous Research*, **21**, 315-349.

DROSTE, H., 2010. High-resolution seismic stratigraphy of the Shu'aiba and Natih formations in the Sultanate of Oman: implications for Cretaceous epeiric carbonate platform systems. In: VAN BUCHEM, F.S.P., GERDES, K.D. and ESTEBAN, M. (Eds), Mesozoic and Cenozoic carbonate systems of the Mediterranean and the Middle East: stratigraphic and diagenetic reference models. *Geol. Soc.*

Lond. Spec. Publ., **329**, 145-162.
DROSTE, H. and VAN STEENWINKEL, M., 2004. Stratal geometries and patterns of platform carbonates: the Cretaceous of Oman. In: EBERLI, G.P., MASAFERRO, J.L. and SARG, J.F. (Eds), Seismic Imaging of Carbonate Reservoirs and Systems. *AAPG Memoir* **81**, 185-206.
EL GEZEERY, T.M., EBAID, A., ISMAEL, A., SILAMBUCHLVAN, J.K., PADHY, G.S., ABDUL-LATIF, A., DAS, O., AL-ANEZI, K., ELSHERIF, A.I. and AHMED, A.M., 2015. High Resolution Sequence Stratigraphy and Seismic Data Integration Aid on Achieving Successful Horizontal Wells in Challenging Wara and Upper Burgan Reservoirs of Minagish Field, Kuwait. SPE Kuwait Oil and Gas Show & Conference, October, Mishref, Kuwait. SPE Conference Paper no. SPE-175334-MS, 1-27.
FAROUK, S., AHMAD, F. and POWELL, J.H., 2017. Cenomanian–Turonian stable isotope signatures and depositional sequences in northeast Egypt and central Jordan. *Journal of Asian Earth Sciences*, **134**, 207-230.
FARZADI, P., 2006. The development of Middle Cretaceous carbonate platforms, Persian Gulf, Iran: constraints from seismic stratigraphy, well and biostratigraphy. *Petroleum Geoscience*, **12**, 59-68.
FLÜGEL, E., 2010. Microfacies of carbonate rocks: Analysis, Interpretation and Application. Springer, pp. 984
FORBES, G.A., JANSEN, H.S.M. and SCHREURS, J., 2010. Lexicon of Oman Subsurface Stratigraphy. *GeoArabia Special Publication*, **5**, pp. 371
FRANCO B.J., CELENTANO, M.A., POPA, D.M., TAHER, A. and AL-SHEHHI, M., 2018. Stratigraphic Traps Generation in Abu Dhabi as a Consequence of Ensuing Late Cretaceous Plate Collision and Obduction at the Eastern Arabian Plate Margin. Abu Dhabi International Petroleum Exhibition & Conference held in Abu Dhabi, UAE, 12-15 November 2018. Society of Petroleum Engineers (SPE), 1-12.
GADDO, J.Z.H., 1971. The Mishrif Formation paleoenvironment in the Rumaila/Tuba/Zubair region of South Iraq. *Journal of the Geological Society of Iraq*, **4**, 1-12.
GALE, A.S., MUTTERLOSE, J., BATENBURG, S., GRADSTEIN, F.M., AGTERBERG, A.S., OGG, J.G. and PETRIZZO, M.R., 2020. The Cretaceous Period. In: GRADSTEIN, F.M., OGG, J.G., SCHMITZ, M.D. and OGG, G.M. (Eds), Geologic Time Scale 2020. Elsevier, 1023-1086.
GARLAND, C.R., ABALIOGLU, I., AKCA, L., CASSIDY, A., CHIFFOLEAU, Y., GODAIL, L., GRACE, M.A.S., KADER, H.J., KHALEK, F., LEGARRE, H., NAZHAT, H.B. and SALLIER, B., 2010. Appraisal and development of the Taq Taq field, Kurdistan region, Iraq. In: VINING, B.A. and PICKERING, S.C. (Eds), Petroleum Geology: From Mature Basins to New Frontiers. Proc. 7th Petroleum Geology Conference. *Geol. Soc. Lond. Petroleum Geology Conference Series*, **7**, 801-810..
GAYARA, A.D. and AL-SHEIKHLY, S.S.J., 1988. Cenomanian Stratigraphy and Sedimentology in Western Iraq. *Journal of the Geological Society of Iraq*, **21**, 85-90.
GERTSCH, B., KELLER, G., ADATTE, T., BERNER, Z., KASSAB, A.S., TANTAWY, A.A.A., EL-SABBAGH, A.M. and STUEBEN, D., 2010. Cenomanian-Turonian transition in a shallow water sequence of the Sinai, Egypt. *International Journal of Earth Sciences (Formerly Geologische Rundschau)*, **99**, 165-182.
GHABEISHAVI, A., VAZIRI-MOGHADDAM, H. and TAHERI, A., 2009. Facies distribution and sequence stratigraphy of the Coniacian–Santonian succession of the Bangestan Palaeo-high in the Bangestan Anticline, SW Iran. *Facies*, **55**, 243-257.
GHABEISHAVI, A., MOGHADDAM, H.V., TAHERI, A. and TAATI, F., 2010. Microfacies and depositional environment of the Cenomanian of the Bangestan anticline, SW Iran. *Journal of Asian Earth Sciences*, **37**, 275-285.
GHAJARI, A., KAMALI, M. and MORTAZAVI, S.A., 2013. A Comprehensive Study of Laffan Shale Formation in Sirri Oil Fields, offshore Iran: Implications for Borehole Stability. *Journal of Petroleum Science and Engineering*, **107**, 50-56.
GRABOWSKI Jr., G.J., 2014. Iraq. In: MARLOW, L., KENDALL, C.C.G. and YOSE, L.A. (Eds), Petroleum Systems of the Tethyan Region. *AAPG Memoir*, **106**, 379-468.
GRELAUD, C., 2005. Enregistrement stratigraphique des phases d'emersion sur les plates-formes carbonates (Stratigraphic record of the phases of emersion of the platform carbonates). Université Michel de Montaigne Bordeaux 3.
GRELAUD, C., RAZIN, P. and HOMEWOOD, P., 2010. Channelized systems in an inner carbonate platform setting: differentiation between incisions and tidal channels (Natih Formation, Late Cretaceous, Oman). In: VAN BUCHEM, F.S.P., GERDES, K.D. and ESTEBAN, M. (Eds), Mesozoic and Cenozoic carbonate systems of the Mediterranean and the Middle East: stratigraphic and diagenetic reference models. *Geol. Soc. Lond., Spec. Publ.* **329**, 163-186.
GRELAUD, C., RAZIN, P., HOMEWOOD, P.W. and SCHWAB, A.M., 2006. Development of Incisions on a Periodically Emergent Carbonate Platform (Natih Formation, Late Cretaceous, Oman). *Journal of Sedimentary Research (formerly Journal of Sedimentary Petrology)*, **76**, 647-669.
GUIRAUD, R. and BOSWORTH, W., 1997. Senonian basin inversion and rejuvenation of rifting in Africa and Arabia: synthesis and implications to plate-scale tectonics. *Tectonophysics*, **282**, 39-82.
HADDAD, S.N.S. and AMIN, M.A., 2007. Mid-Turonian-early Campanian sequence stratigraphy of northeast Iraq. *GeoArabia*, **12**, 135-176.
HAJIKAZEMI, E., AL-AASM, I.S. and CONIGLIO, M., 2017. Diagenetic history and reservoir properties of the Cenomanian-Turonian carbonates in southwestern Iran and the Persian Gulf. *Marine and Petroleum Geology*, **88**, 845-857.
HAQ, B.U., 2014. Cretaceous Eustasy Revisited. *Global and Planetary Change*, **113**, 44-58.
HANCOCK, J.M., 2004. The mid-Cenomanian eustatic low. *Acta Geologica Polonica*, **54**, 611-627.
HARRIS, P.M., FROST, S.H., SEIGLIE, G.A. and SCHNEIDERMANN, N., 1984. Regional unconformaties and depositional cycles, Cretaceous of the Arabian Peninsula. In: SCHLEE, J.S. (Ed.), Interregional Unconformaties and Hydrocarbon Accummulations. *AAPG Memoir*, **36**, 67-80.
HENNHOEFER, D., AL SUWAIDI, A., BOTTINI, C., HELJA, E. and STEUBER, T., 2019. The Albian to Turonian carbon isotope record from the Shilaif Basin (United Arab Emirates) and its regional and intercontinental correlation. *Sedimentology*, **66**, 536-555.
HOLLIS, C., 2011. Diagenetic controls on reservoir properties of carbonate successions within the Albian–Turonian of the Arabian Plate. *Petroleum Geoscience*, **17**, 223-241.
HOLLIS, C., VAHRENKAMP, V., TULL, S., MOOKERJEE, A., TABERNER, C. and HUANG, Y., 2010. Pore system characterisation in heterogeneous carbonates: An alternative approach to widely-used rock-typing methodologies. *Marine and Petroleum Geology,* **27**(4), 772-793.
HOMEWOOD P., RAZIN, P., GRELAUD, C., DROSTE, H., VAHRENKAMP, V., METRAUX, M. and MATTNER, J., 2008. Outcrop sedimentology of the Natih Formation, northen Oman: A field guide to selected outcrops in the Adam Foothills and Al Jabal al Akhdar areas. *GeoArabia*, **13**, 39-120.
HOSSEINY, E., RABBANI, A.R. and MOALLEMI, S.A., 2016. Source rock characterization of the Cretaceous Sarvak Formation in the eastern part of the Iranian sector of Persian Gulf. *Organic Geochemistry*, **99**, 53-66.
JAMES, G.A. and WYND, J.G., 1965. Stratigraphic Nomenclature of the Iranian Oil Consortium Agreement Area. *AAPG Bulletin*, **49**, 2182-2245.
JASSIM, S.Z. and BUDAY, T., 2006. Late Tithonian-Early Turonian Megasequence AP8. In: JASSIM, S. Z. and GOFF, J.C. (Eds), Geology of Iraq. Dolin, Prague and Moravian Museum, Brno, Czech Republic, pp 124-139
JAYA, S., MENHALI, H.A., AL SHKEILI, F. and SHASHANKA, A.,

2020. A Novel Approach, Determining Oil Pockets Size in a Very Complex Combination of Structural and Stratigraphic Traps of Middle Cretaceous Formation in Onshore Abu Dhabi. Abu Dhabi International Petroleum Exhibition & Conference, Abu Dhabi, UAE, November 2020. Society of Petroleum Engineers (SPE), 1-9.

JORDAN, C.F., CONNALLY, R.C. and VEST, H. A., 1985. Middle Cretaceous Carbonates of the Mishrif Formation, Fateh Field, Offshore Dubai, UAE. In: ROEHL, P.O. and CHOQUETTE, P.W. (Eds), Carbonate Petroleum Reservoirs, 425-442. New York, Springer-Verlag.

KALANAT, B. and VAZIRI-MOGHADDAM, H., 2019. The Cenomanian/Turonian boundary interval deep-sea deposits in the Zagros Basin (SW Iran): Bioevents, carbon isotope record and palaeoceanographic model. *Palaeogeography, Palaeoclimatology, Palaeoecology*, **533**, 109238.

KALANAT, B., VAZIRI-MOGHADDAM, H. and BIJANI, S., 2021. Depositional history of the uppermost Albian-Turonian Sarvak Formation in the Izeh Zone (SW Iran). *International Journal of Earth Sciences (Formerly Geologische Rundschau)*, **110**, 305-330.

KARIM, K.H. and TAHA, Z.A., 2009. Tectonical history of Arabian platform during Late Cretaceous An example from Kurdistan region, NE Iraq. *Iranian Journal of Earth Sciences*, **1**, 1-14.

KAZEM ZADEH, M., 2016. Biostratigraphy, facies and sequence stratigraphy of the Sarvak Formation in the Ahwaz Oil Field, North Dezful Embayment Zone. *Journal of Stratigraphy and Sedimentology Researches*, **32**, 53-72.

KENNEDY, W.J. and SIMMONS, M.D., 1991. Mid-Cretaceous ammonites and associated microfossils from the Central Oman Mountains. *Newsletters on Stratigraphy*, **25**, 127-154.

KENT. W.N., 2010. Structures of the Kirkuk Embayment, northern Iraq: Foreland structures or Zagros Fold Belt structures? *GeoArabia*, **15**, 147-188.

KHAWAJA, A.M. and THABIT, J.M., 2021. Interpretation of 3D Seismic Reflection Data to Reveal Stratigraphic Setting of the Reservoir of Mishrif Formation in Dujaila Oil Field, Southeast of Iraq. *Iraqi Journal of Science*, **62**, 2250-2261.

LAPPONI, F., CASINI, G., SHARP, I., BLENDINGER, W., FERNÁNDEZ, N., ROMAIRE, I. and HUNT, D., 2011. From outcrop to 3D modelling: a case study of a dolomitized carbonate reservoir, Zagros Mountains, Iran. *Petroleum Geoscience*, **17**, 283-307.

LEHMANN, C., GARDNER, J.A., TOTTON, K., OLATOKE, O.J. and TOUGH, K., 2017. The Margin of the Mishrif Platform, Rumaila Field, Southern Iraq. AAPG Annual Convention and Exhibition, Houston, Texas, April 2017. Abstract no. 90291,

LIPSON-BENITAH, S., FLEXER, A., ROSENFIELD, A., HONIGSTEIN, A., CONWAY, B. and ERIS, H., 1990. Dysoxic sedimentation in the Cenomanian-Turonian Daliyya formation, Israel. In: HUC, A.Y. (Ed.), Deposition of Organic Facies. *AAPG Studies in Geology*, **30**, 27-39.

LOUTFI, G., S.M. BASLAIB and M. ABU HAMD, 1987, Cenomanian Stratigraphic Traps in Western Abu Dhabi, UAE. Proceedings of the 5th Society of Petroleum Engineers Middle East Oil Conference, Bahrain 1987. Society of Petroleum Engineers (SPE).

LU, M., AL SUWAIDI, S.K., JI, Y., SWAIN, A.S.S., AL SHEHHI, M., LUO, B., MAO, B., JIA, M., ZI, D., ZHU, J. and JI, Y., 2018. Hydrocarbon accumulation model of upper Cretaceous Mishrif Formation and oilfield discovery in western Abu Dhabi. Abu Dhabi International Petroleum Exhibition and Conference, Abu Dhabi, November, 2018. Society of Petroleum Engineers (SPE), 1-11.

LUKOIL., 2017. A Gift from Ancient Sumer. *Oil Journal*, 311.

LÜNING, S. and KUSS, J., 2014. Petroleum Geology of Jordan. In: L. Marlow, C.C.G. Kendall and L.A. Yose (Eds), Petroleum Systems of the Tethyan Region. *AAPG Memoir* **106**, 217-240..

MAHDI, T. A. and AQRAWI, A.A.M., 2014. Sequence stratigraphic analysis of the mid-Cretaceous Mishrif Formation, southern Mesopotamian Basin, Iraq. *Journal of Petroleum Geology*, **37**, 287-312.

MAHDI, T. A., AQRAWI, A.A.M., HORBURY, A. D. and SHERWANI, G. H., 2013. Sedimentological characterization of the mid-Cretaceous Mishrif reservoir in southern Mesopotamian Basin, Iraq. *GeoArabia*, **18**, 139-174.

MAJEED, A.J., AL-MUKHTAR, A., ABOOD, F.A. and ALSHARA, A.K., 2021. Numerical study of the natural fracture using dual porosity-dual permeability model for Rumaila Field, southern Iraq. *Arabian Journal of Geosciences*, **14**, 1828.

MALEKZADEH, H., DARAEI, M. and BAYET-GOLL, A., 2020. Field-scale reservoir zonation of the Albian–Turonian Sarvak Formation within the regional-scale geologic framework: A case from the Dezful Embayment, SW Iran. *Marine and Petroleum Geology*, **121**, 104586.

MAURER, F., VAN BUCHEM, F.S.P., EBERLI, G.P., PIERSON, B.J., RAVEN, M.J., LARSEN, P.H., AL-HUSSEINI, M.I. and VINCENT, B., 2013. Late Aptian long-lived glacio-eustatic lowstand recorded on the Arabian Plate. *Terra Nova*, **25**, 87-94.

MEHMANDOSTI, E.A., ADABI, M.H. and WOODS, A.D., 2013. Microfacies and Geochemistry of the Middle Cretaceous Sarvak Formation in Zagros Basin, Izeh Zone, SW Iran. *Sedimentary Geology*, **293,** 9-20.

MEHRABI, H. and RAHIMPOUR-BONAB, H., 2014. Paleoclimate and tectonic controls on the depositional and diagenetic history of the Cenomanian – early Turonian carbonate reservoirs, Dezful Embayment, SW Iran. *Facies*, **60**, 147-167.

MEISTER, C. and PIUZ, A., 2015. Cretaceous ammonites from the Sultanate of Oman (Adam foothills). *GeoArabia*, ***20***, 19-74. MILLER, K.G., KOMINZ, M.A., BROWNING, J.V., WRIGHT, J.D., MOUNTAIN, G.S., KATZ, M.E., SUGARMAN, P.J., CRAMER, B.S., CHRISTIE-BLICK, N. and PEKAR, S.F., 2005. The Phanerozoic Record of Global Sea Level Change. *Science*, **310**, 1293-1298.

MILLER, K.G., WRIGHT, J.D. and BROWNING, J.V., 2005, Visions of ice sheets in a greenhouse world, *Marine Geology*, **217,** 215-231.

MOGHADDAM, I., 2017. The microbiostratigraphy and depositional history of the Turonian-Santonian Surgah Formation at the Northern Flank of the Kuh-e Sepid Anticline, Lorestan Basin. *Iranian Journal of Earth Sciences*, **9**, 75-83.

MOHSIN, L., ALSHUKAILI, A., MAHESH, A.L., LEWIS, R.E., STRAPOC, D., BONDABOU, K., PISHARAT, M., AL GHAFRI, A.M.D., FORNASIER I. and PERALTA, J., 2018. Natih B Carbonate Source Rock: Resource Assessment to Production Test. SPWLA 59th Annual Logging Symposium, London, UK, June 2018. SPWLA Conference Paper no. SPWLA-2018-GG.

MÜLAYIM, O., MANCINI, E., CEMEN, I., and YILMAZ, O. I., 2016. Upper Cenomanian - Lower Campanian Derdere and Karababa formations in the Çemberlitaş oil field, southeastern Turkey: their microfacies analyses, depositional environments, and sequence stratigraphy. *Turk. J. Earth Sci.,* **25**, 46-63,

MÜLAYIM, O., YILMAZ, O.I., SARI, B., TASLI, K. and WAGREICH, M., 2020. Cenomanian–Turonian drowning of the Arabian Carbonate Platform, the Inişdere section, Adıyaman, SE Turkey. In: WAGREICH, M., HART, M.B., SAMES, B. and YILMAZ, I.O. (Eds), Cretaceous Climate Events and Short-Term Sea-Level Changes. *Geol. Soc. Lond. Spec. Publ.* **498**, 189-210.

MURRIS, R.J., 1980. Hydrocarbon Habitat of the Middle East. In MIALL, A.D. (Eds.), Facts and Principles of World Petroleum Occurrence. *Canadian Society of Petroleum Geologists – Memoir*, **6**, 765-800.

NAVIDTALAB, A., RAHIMPOUR-BONAB, H., NAZARI-BADII, A. and SARFI, A., 2014. Challenges in deep basin

sequence stratigraphy: A case study from the Early–Middle Cretaceous of SW Zagros. *Facies*, **60**, 195-215.

NAVIDTALAB, A., HEIMHOFER, U., HUCK, S., OMIDVAR, M., RAHIMPOUR-BONAB, H., AHARIPOUR, R. and SHAKERI, A., 2019. Biochemostratigraphy of an upper Albian–Turonian succession from the southeastern Neo-Tethys margin, SW Iran. *Palaeogeography, Palaeoclimatology, Palaeoecology*, **533**, 109255.

NAVIDTALAB, A., SARFI, M., ENAYATI-BIDGOLI, A. and YAZDI-MOGHADAM, M., 2020. Syn-depositional continental rifting of the Southeastern Neo-Tethys margin during the Albian–Cenomanian: evidence from stratigraphic correlation. *International Geology Review*, **62**, 1698-1723.

NEO, S., 1996. The Structural Origin and Relating Geological Framework of the Upper Mishrif Formation in a Mishrif-Reservoired Oil Field, Offshore Abu Dhabi. Proc. 7th Abu Dhabi International Petroleum Exhibition and Conference, Abu Dhabi. Society of Petroleum Engineers (SPE), 233-243.

NEWELL, K.D. and HENNINGTON, R.D., 1983. Potential Petroleum Source-Rock Deposition in the Middle Cretaceous Wasia Formation, Rub'Al Khali, Saudi Arabia. Proc. Society of Petroleum Engineers 3rd Middle East Oil Technical Conference and Exhibition, March 1983, Bahrain. Society of Petroleum Engineers (SPE), 151-160.

OMIDVAR, M., MEHRABI, H., SAJJADI, F., BAHRAMIZADEH-SAJJADI, H., RAHIMPOUR-BONAB, H. and ASHRAFZADEH, A., 2014. Revision of the foraminiferal biozonation scheme in Upper Cretaceous carbonates of the Dezful Embayment, Zagros, Iran: Integrated palaeontological, sedimentological and geochemical investigation. *Revue de Micropaléontologie*, **57**, 97-116.

ÖZKAN, R. and ALTINER, D., 2019. The Cretaceous Mardin Group carbonates in southeast Turkey: Lithostratigraphy, foraminiferal biostratigraphy, microfacies and sequence stratigraphic evolution. *Cretaceous Research*, **98**, 153-178.

PASCOE, R.P., EVANS, N. and HARLAND, T., 1995. The generation of unconformities within the Mishrif and Laffan Formations of Dubai and adjacent areas: applications to exploration and production. In: AL-HUSSEINI, M. I. (Eds), Geo'94. The Middle East Petroleum Geosciences, **2.** Selected Middle East Papers from the Middle East Geoscience Conference, April 1994, Bahrain, 749-760.

PERROTTA, S., ZAMPETTI, V., CHARRI, G., KRAYENBUEHL, T., BRAUN, M., FRANCO, B.J., NEVES F. and SAAD AL KOBAISI, A., 2017. Seismic Stratigraphy and Depositional Evolution of the Mishrif Formation in Western Onshore Abu Dhabi. SPE Abu Dhabi International Petroleum Exhibition & Conference, November, Abu Dhabi, UAE. Society of Petroleum Engineers (SPE), 1-13.

PHILIP, J., BORGOMANO, J. and AL-MASKIRY, S., 1995. Cenomanian - Early Turonian carbonate platform of Northern Oman: stratigraphy and palaeo environments. *Palaeogeography, Palaeoclimatology, Palaeoecology*, **119**, 77-92.

PIRYAEI, A., REIJMER, J.J.G., BORGOMANO, J. and VAN BUCHEM, F.S.P., 2011. Late Cretaceous tectonic and sedimentary evolution of the Bandar Abbas area, Fars region, southern Iran. *Journal of Petroleum Geology*, **34**, 157-180.

PIRYAEI, A., REIJMER, J.J.G., VAN BUCHEM, F.S.P., MOGHADAM, M.Y., SADOUNI, J. and DANELIAN, T., 2010. The influence of Late Cretaceous tectonic processes on sedimentation patterns along the northeastern Arabian plate margin (Fars Province, SW Iran). In: LETURMY, P. and ROBIN, C. (Eds), Tectonic and Stratigraphic Evolution of Zagros and Makran during the Mesozoic-Cenozoic. *Geol. Soc. Lond. Spec. Publ.,* **330**, 211-251.

PITMAN, J.K., STEINSHOUER, D. and LEWAN, M.D., 2004. Petroleum generation and migration in the Mesopotamian Basin and Zagros Fold Belt of Iraq: results from a basin-modeling study. *GeoArabia*, **9**, 41-72.

PIUZ, A. and VICEDO, V., 2020. New Cenomanian "nummoloculinas" of the Natih Formation of Oman. *Cretaceous Research*, **107,** 104224.

PIUZ, A., MEISTER, C. and VICEDO, V., 2014. New Alveolinoidea (Foraminifera) from the Cenomanian of Oman. *Cretaceous Research*, **50**, 344-360.

POINAR, G., LAMBERT, J.B. and WU, Y., 2004. NMR analysis of amber in the Zubair Formation, Khafji oilfield (Saudi Arabia - Kuwait): coal as an oil source rock? *Journal of Petroleum Geology*, **27**, 207-209.

POWELL, J. H. and MOH'D, B.K., 2011. Evolution of Cretaceous to Eocene alluvial and carbonate platform sequences in central and south Jordan. *GeoArabia*, **16**, 29-82.

RAHIMPOUR-BONAB, H., MEHRABI, H., NAVIDTALAB, A., OMIDVAR, M., ENAYATI-BIDGOLI, A.H., SONEI, R., SAJJADI, F., AMIRI-BAKHTYAR, H., ARZANI, N. and IZADI-MAZIDI, E., 2013. Palaeo-Exposure Surfaces in Cenomanian – Santonian Carbonate Reservoirs in the Dezful Embayment, SW Iran. *Journal of Petroleum Geology*, **36**, 335-362.

RAZIANI, M., VAHIDINIA, M. and SADEGHI, A., 2018. Paleoecology of Turonian-Santonian on the basis of planktonic foraminifera in the type section of Surgah Formation, Kabir-kuh anticline, South of Ilam. *Sedimentary Facies*, **11**, 229-249.

RAZIN, P., GRÉLAUD, C. and VAN BUCHEM, F., 2017. The mid-Cretaceous Natih Formation in Oman: A model for carbonate platforms and organic-rich intrashelf basins. *AAPG Bulletin*, **101**, 515-522.

RAZIN, P., TAATI, F. and VAN BUCHEM, F.S.P., 2010. Sequence stratigraphy of Cenomanian–Turonian carbonate platform margins (Sarvak Formation) in the High Zagros, SW Iran: an outcrop reference model for the Arabian Plate. In: VAN BUCHEM, F.S.P., GERDES, K.D. and ESTEBAN, M. (Eds), Mesozoic and Cenozoic carbonate systems of the Mediterranean and the Middle East: stratigraphic and diagenetic reference models. *Geol. Soc. Lond. Spec. Publ.*, **329**, 187-218.

ROBERTSON, A.H.F. and SEARLE, M.P., 1990. The northern Oman Tethyan continental margin: stratigraphy, structure, concepts and controversies. In: ROBERTSON, A.H.F., SEARLE, M.P. and RIES, A.C. (Eds.), The geology and tectonics of the Oman region. *Geol. Soc. Lond. Spec. Publ.*, **49**, 3-25.

RYDER, K., LEHMANN, C., VINCENT, B. and MORRIS, P., 2013. Enhanced Stratigraphic Resolution of the Mishrif Formation by Integrating Biostratigraphy and Chemostratigraphy, Rumaila Field, South Iraq. 2nd EAGE Workshop on Iraq, 1-2.

SADOONI, F.N., 2005. The nature and origin of Upper Cretaceous basin-margin rudist buildups of the Mesopotamian Basin, southern Iraq, with consideration of possible hydrocarbon stratigraphic entrapment. *Cretaceous Research*, **26**, 213-224.

SAINT-MARC, P. 1981. Lebanon. In: REYMENT, R.A. and BENGTSON, P. (Eds), Aspects of Mid-Cretaceous Regional Geology. IGCP International Geoscience Programme Project (Formerly International Geological Correlation Programme Project), **58**, 103-131.

SALEH, A.H. and AWADEESIAN, A.M.R., 2019. Sequence Stratigraphy for Optimize Development Strategy, Ahmadi Carbonates, Case Study, South Iraq Oil Fields. *Iraqi Journal of Science*, **60**, 4, 819-829.

SARRAJ, R.H.A. and MOHIALDEEN, I.M.J., 2020. Sedimentology, palynofacies and hydrocarbon generation potential of the Cretaceous Balambo Formation from Zagros Fold-Thrust Belt, Kurdistan, NE Iraq. *Arabian Journ. Geosciences*, **13**, 1-26.

SCHLAGINTWEIT, F. and SIMMONS, M., 2022. Developing best practice in micropalaeontology: examples from the mid-Cretaceous of the Zagros Mountains. *Acta Palaeontologica Romaniae,* **18**, 63-84.

SCHLAGINTWEIT, F. and YAZDI-MOGHADAM, M., 2020, *Orbitolinopsis cenomaniensis* n. sp., a new larger benthic foraminifera (Orbitolinidae) from the middle-?late

Cenomanian of the Sarvak Formation (SW Iran, Zagros Zone): a regional marker taxon for the Persian Gulf area and Oman. *Revue de micropaléontologie*, **67**, 100413.

SCHLAGINTWEIT, F. and YAZDI-MOGHADAM, M., 2021. *Moncharmontia* De Castro 1967, benthic foraminifera from the middle-upper Cenomanian of the Sarvak Formation of SW Iran (Zagros Zone): a CTB survivor taxon. *Micropaleontology*, **67**, 19-29.

SCHULZE, F., MARZOUK, A. M., BASSIOUNI, M.A., and KUSS, J., 2004. The late Albian–Turonian carbonate platform succession of west-central Jordan: stratigraphy and crises, *Cretaceous Res*., **25**, 709-737, 2004.

SCHULZE, F., KUSS, J. and MARZOUK, A., 2005. Platform configuration, microfacies and cyclicities of the upper Albian to Turonian, west-central Jordan. *Facies*, **50**, 505-527.

SCOTESE, C.R., 2021. An Atlas of Phanerozoic Paleogeographic Maps: The Seas Come in and the Seas Go Out. *Annual Review of Earth and Planetary Sciences*, **49**.

SCOTT, R.W., SCHLAGER, W., FOUKE, B. and NEDERBRAGT, S.A., 2000. Are Mid-Cretaceous Eustatic Events Recorded in Middle East Carbonate Platforms? In: ALSHARHAN, A.S. and SCOTT, R.W. (Eds), Middle East models of Jurassic/ Cretaceous carbonate systems. *SEPM Special Publications*, **69**, 77-88.

SEARLE, M.P., CHERRY, A.G., ALI, M.Y. and COOPER, D.J.W., 2014. Tectonics of the Musandam Peninsula and northern Oman Mountains: from ophiolite obduction to continental collision. *GeoArabia*, **19**, 135-174.

SFIDARI, E., ZAMANZADEH, S.M., DASHTI, A., OPERA A. and TAVAKKOL, M.H., 2016. Comprehensive source rock evaluation of the Kazhdumi Formation, in the Iranian Zagros Foldbelt and adjacent offshore. *Marine and Petroleum Geology*, **71**, 26-40.

SHARLAND, P. R., ARCHER, R., CASEY, D.M., DAVIES, R.B., HALL, S., HEWARD, A., HORBURY, A. and SIMMONS, M.D., 2001. Arabian Plate Sequence Stratigraphy. *GeoArabia Special Publication* **2**, Gulf PetroLink, pp. 1-387.

SHARP, I., GILLESPIE, P., LONOY, A., HORN, S. and MORSALNEZHAD, D., 2006. Outcrop Characterization of Fractured Cretaceous Carbonate Reservoirs, Zagros Mountains, Iran. International Oil Conference and Exhibition in Mexico, 31 August-2 September, Cancun, Mexico. Society of Petroleum Engineers (SPE), 1-19.

SHARP, I., GILLESPIE, P., MORSALNEZHAD, D., TABERNER, C., KARPUZ, R., VERGES, J., HORBURY, A., PICKARD, N., GARLAND, J. and HUNT, D., 2010. Stratigraphic architecture and fracture-controlled dolomitization of the Cretaceous Khami and Bangestan groups: an outcrop case study, Zagros Mountains, Iran. In: VAN BUCHEM, F.S.P., GERDES, K.D. and ESTEBAN, M. (Eds), Mesozoic and Cenozoic carbonate systems of the Mediterranean and the Middle East: stratigraphic and diagenetic reference models. *Geol. Soc. Lond. Spec. Publ*., **329**, 343-396.

SHOGHI, J., BAHRAMIZADEH-SAJJADI, H., NICKANDISH, A. B. and ABBASI, M., 2020. Facies modelling of synchronous successions - A case study from the mid Cretaceous of NW Zagros, Iran. *Journal of African Earth Sciences,* **162**, 1-19.

SIMMONS, M. and DAVIES, R., 2016. Arabian Plate Sequence Stratigraphy Revisited: Mega-Sequences AP9 and AP10. Sixth Arabian Plate Geology Workshop. European Association of Geoscientists and Engineers (EAGE), 1-4.

SIMMONS, M.D. and HART, M.B., 1987. The biostratigraphy and microfacies of the Early to mid-Cretaceous carbonates of Wadi Mi'aidin, central Oman Mountains. In: Hart, M.S. (Ed.), Micropalaeontology of Carbonate Environments, 176-207.

SIMMONS, M.D., WHITTAKER, J.E. and JONES, R.W., 2000. Orbitolinids from Cretaceous sediments of the Middle East - A revision of the F.R.S. Henson and Associates Collection. In: Hart, M. B., Kaminski, M. A. and Smart, C.W. (Eds), Proceedings of the fifth international workshop on agglutinated Foraminifera. *Gryzbowski Found. Spec. Pub*., **7**, 411-437

SIMMONS, M.D., SHARLAND, P.R., CASEY, D.M., DAVIES, R.B. and SUTCLIFFE, O.E., 2007. Arabian Plate sequence stratigraphy: Potential implications for global chronostratigraphy. *GeoArabia*, **12**, 101-130.

SIMMONS, M.D., VICEDO, V., YILMAZ, I., HOŞGÖR, I., MÜLAYIM, O. and SARI, B., 2020. Micropalaeontology, biostratigraphy, and depositional setting of the mid-Cretaceous Derdere Formation at Derik, Mardin, south-eastern Turkey. *Journal of Micropalaeontology*, **39**, 203-232.

SIMMONS, M.D., MILLER, K.G., RAY, D.C., DAVIES, A., VAN BUCHEM, F.S.P., GRÉSELLE, B., 2020. Phanerozoic Eustasy. In: GRADSTEIN, F.M., OGG, J.G., SCHMITZ, M. D., OGG, G.M. (Eds), Geologic Time Scale 2020. Elsevier, 357-400.

SMITH, A.B., SIMMONS, M.D. and RACEY, A., 1990. Cenomanian echinoids, larger foraminifera and calcareous algae from the Natih Formation, central Oman Mountains. *Cretaceous Research*, **11**, 29-69.

SOROKA, W.L., AL-SHEKAILI, F.S., STROHMENGER, C.J., SATTAR, M.A., AL-AIDAROUS, A. and SUMAIDAA, S.B., 2005. Reservoir facies prediction of the Mishrif Formation, Upper Cretaceous, UAE. International Petroleum Technology Conference, Doha, Qatar, November 2005. Paper IPTC-10426-MS.

STAMPFLI, G.M. and BOREL, G.D., 2002. A plate tectonic model for the Paleozoic and Mesozoic constrained by dynamic plate boundaries and restored synthetic oceanic isochrons. *Earth and Planetary Science Letters*, **196**, 17-33.

STEUBER, T. and BACHMANN, M., 2002. Upper Aptian–Albian Rudist Bivalves from Northern Sinai, Egypt. *Palaeontology*, **45**, 725-749.

STROHMENGER, C.J., MITCHELL, J.C., FELDMAN, H.R., LEHMANN, P.J., BROOMHALL, R.W., PATTERSON, P.E., AL-SAHLAN, G., DEMKO, T.M., WELLNER, R.W., McCRIMMON, C.G. and AL-AJMI, N., 2006. Sequence stratigraphy and reservoir architecture of the Burgan and Mauddud Formations (Lower Cretaceous), Kuwait. Giant Hydrocarbon Reservoirs of the World. *AAPG Memoir*, **88**, 213-245.

TAGHAVI, A.A., MORK, A. and EMADI, M.A., 2006. Sequence stratigraphically controlled diagenesis governs reservoir quality in the carbonate Dehluran Field, southeast Iran. *Petroleum Geoscience*, **12**, 115-126.

TAHER, A., AZZAM, I., ABDULLA, N.A. and WITTE, J., 2010. Mishrif Diagenetic Trapping Potential in Western Onshore Abu Dhabi. Abu Dhabi International Petroleum Exhibition and Conference, 1-4 November 2010, Abu Dhabi, UAE. SPE Conference Paper no. 137900-MS, 1-15.

TAHER, A. and AL ZAABI, M.R., 2015. Wasia Unconventional Oil Exploration Potential in Western Onshore Abu Dhabi. Abu Dhabi International Petroleum Exhibition and Conference, 9-12 November, Abu Dhabi, UAE.

TERKEN, J. M. J., 1999. The Natih Petroleum System of North Oman. *GeoArabia*, **4**, 157-180.

TSCHOPP, R. H., 1967. The general geology of Oman. 7th World Petroleum Congress *Proceedings,* **2**, 231-242.

VAHRENKAMP, V. C., 2013. Carbon-isotope signatures of Albian to Cenomanian (Cretaceous) shelf carbonates of the Natih Formation, Sultanate of Oman. *GeoArabia*, **18**, 65-82.

VAHRENKAMP, V., FRANCO, B.J., POPA D. and BARATA, J., 2015. Development and infill of the Late Albian to Turonian Shilaif Intrashelf Basin at the eastern margin of the giant Mesozoic Arabian carbonate platform: Basin architecture and time stratigraphy. International Petroleum Technology Conference Paper, v. IPTC-18488-MS, 1-9.

VAN BELLEN R.C., DUNNINGTON H.V., WETZEL R. and MORTON D.M. 1959. Iraq. Lexique Stratigraphique Internationale, Asie 3 (10a), 1-333.

VAN BUCHEM, F.S.P., RAZIN, P., HOMEWOOD, P.W., PHILIP,

J.M., EBERLI, G.P., PLATEL, J.-P., ROGER, J., ESCHARD, R., DESAUBLIAUX, G.M.J., BOISSEAU, T., LEDUC, J.-P., LABOURDETTE, R. and CANTALOUBE, S., 1996. High resolution sequence stratigraphy of the Natih Formation (Cenomanian / Turonian) in Northern Oman: Distribution of Source Rocks and Reservoir Facies. *GeoArabia*, **1**, 65-91.

VAN BUCHEM, F.S.P., RAZIN, P., HOMEWOOD, P.W., OTERDOOM, W.H. and PHILIP, J., 2002. Stratigraphic organization of carbonate ramps and organic-rich intrashelf basins: Natih Formation (middle Cretaceous) of northern Oman. *AAPG Bulletin*, **86**, 21-53.

VAN BUCHEM, F.S.P., BAGHBANI, D., BULOT, L.G., CARON M., GAUMET, F., HOSSEINI, A., KEYVANI, F., SCHROEDER, R., SWENNEN, R., VEDRENNE, V. and VINCENT, B., 2010. Barremian-Lower Albian sequence stratigraphy of southwest Iran (Gadvan, Dariyan and Kazhdumi formations) and its comparison with Oman, Qatar and the United Arab Emirates. In: VAN BUCEHM, F.S.P., AL-HUSSEINI, M.I., MAURER, F. and DROSTE, H.J. (Eds), Barremian–Aptian Stratigraphy and Hydrocarbon Habitat of the Eastern Arabian Plate, **2**. *GeoArabia Special Publication* **4**, 503-548.

VAN BUCHEM, F.S.P., SIMMONS, M.D., DROSTE, H.J. and DAVIES, R.B., 2011. Late Aptian to Turonian stratigraphy of the eastern Arabian Plate – depositional sequences and lithostratigraphic nomenclature. *Petroleum Geoscience*, **17**, 211-222.

VAN BUCHEM, F.S.P., SVENDSEN, N., HOCH, E., PEDERSEN-TATALOVIC, R. and HABIB, K., 2014. Depositional History and Petroleum Habitat of Qatar. In: MARLOW, L., KENDALL, C.C.G. and YOSE, L.A. (Eds), Petroleum Systems of the Tethyan Region. *AAPG Memoir*, **106**, 641-678.

VAN LAER, P., LEYRER, K., POVSTYANOVA, M., BAIG, M.Z., MAKARYCHEV, G. and AL-MARZOOQI, H., 2019. Cenomanian Shilaif Unconventional Shale Oil Potential in Onshore Abu Dhabi, UAE. Proceedings of the 7th Unconventional Resources Technology Conference. *AAPG Datapages Miscellaneous Series*, **526**, 1-17.

VAN SIMAEYS, S., JANSZEN, A., HARDY, C., GARNIER, E., SULLIVAN, M.M., FABUEL-PEREZ, I., SPISTO, Y. and TWIGG, T., 2019. Unravelling the Tectono-Stratigraphy of the Eratosthenes Continental Block. 81st EAGE Conference and Exhibition 2019, 1-5.

VICEDO, V. and PIUZ, A., 2017, Evolutionary trends and biostratigraphical application of new Cenomanian alveolinoids (Foraminifera) from the Natih Formation of Oman. *Journal of Systematic Palaeontology*, **15**, 821-850.

VIDETICH, P., MCLIMANS, R.K., WATSON, H.K.S. and NAGY, R.M., 1988. Depositional, Diagenetic, Thermal and Maturation Histories of Cretaceous Mishrif Formation, Fateh Field, Dubai. *AAPG Bulletin*, **72**, 1143-1159.

VINCENT, B., VAN BUCHEM, F.S.P., BULOT, L.G., JALALI, M., SWENNEN, R., HOSSEINI, A.S. and BAGHBANI, D., 2015. Depositional sequences, diagenesis and structural control of the Albian to Turonian carbonate platform systems in coastal Fars (SW Iran). *Marine and Petroleum Geology*, **63**, 46-67.

VINCENT, B., AL-ZANKAWI, O., HAYAT, I., GARLAND, J., GUTTERIDGE, P. and THOMPSON, S., 2020. Unravelling the complexity of thin (sub-seismic) heterogeneous carbonate reservoirs: An integrated study of the Albian Mauddud Formation in the Greater Burgan Area, Kuwait. *Journal of Petroleum Geology*, **43**, 249-276.

WAGNER, P. D., 1990. Geochemical stratigraphy and porosity controls in Cretaceous carbonates near the Oman Mountains. In: H. F. Robertson, M. P. Searle, and A. C. Ries (Eds), The Geology and Tectonics of the Oman Region. *Geol. Soc. Lond. Spec. Publ.*, **49**, 127-137.

WENDLER, J. E., WENDLER, I., HUBER, B., and MACLEOD, K. G., 2010a. What are calcispheres? Pristine specimens from the Tanzania drilling project provide unprecedented insight into an enigmatic Cretaceous Microfossil Group. Geol. Soc. of America, Abstracts with Program, Boulder, USA, **42,** 131

WENDLER, J.E., LEHMANN, J. and KUSS, J., 2010b. Orbital time scale, intra-platform basin correlation, carbon isotope stratigraphy and sea-level history of the Cenomanian–Turonian Eastern Levant platform, Jordan. In: HOMBERG, C. and BACHMANN, M. (Eds), Evolution of the Levant Margin and Western Arabia Platform since the Mesozoic. *Geol. Soc. Lond. Spec. Publ.*, **341**, 171-186.

WHARTON, S.R., 2015. Seismic chronostratigraphy and basin development at a Mid-Cretaceous intrashelf basin margin. *Interpretation*, **3**, SN1-SN20.

WOHLWEND, S., HART, M. and WEISSERT, H., 2016. Chemostratigraphy of the Upper Albian to mid-Turonian Natih Formation (Oman) – how authigenic carbonate changes a global pattern. *The Depositional Record*, **2**, 97-117.

WRIGHT, C.W., KENNEDY, W.J. and GALE, A.S., 2017. The Ammonoidea of the Lower Chalk. Part 7. *Palaeontographical Society (Monograph)*, **171**, 461-571.

WRIGHT, N.M., SETON, M., WILLIAMS, S.E., WHITTAKER, J.M. and MÜLLER, R.D., 2020. Sea level fluctuations driven by changes in global ocean basin volume following supercontinent break-up. *Earth-Science Reviews*, 103293.

WYND, J.G., 1965. Biofacies of the Iranian Oil Consortium Agreement area. Iranian Oil Operating Companies, Geological and Exploration division. Report No. 1082.

XIAO, D., AL SUWAIDI, S.K., JI, Y., BLOOSHI, A.A., LU, M., MAO, D., AL SHEHHI, M., SHASHANKA, A., WANG, L., HU, G., ZHAO, W. and MA, R., 2020. Source Characteristics and Lateral Migration of Middle Cretaceous Petroleum System in Western Abu Dhabi, Insight from Biomarker and Reservoir Investigation. Abu Dhabi International Petroleum Exhibition & Conference, Abu Dhabi, UAE, November 2020. Society of Petroleum Engineers (SPE), 1-10.

YOSE, L.A., STROHMENGER, C.J., AL-HOSANI, I., BLOCH, G. and AL-MEHAIRI, Y., 2010. Sequence-stratigraphic evolution of an Aptian carbonate platform (Shu'aiba Formation), eastern Arabian Plate, onshore Abu Dhabi, United Arab Emirates. In: VAN BUCHEM, F.S.P., AL-HUSSEINI, M.I., MAURER, F. and DROSTE, H. J. (Eds), Barremian-Aptian stratigraphy and hydrocarbon habitat of the eastern Arabian Plate, **2.** *GeoArabia Special Publication* **4**, 309-340.

YOUSSEF, A.H., KADAR, A.P. and KARAM, K.A., 2014. Sequence stratigraphy framework of late early to middle Cenomanian Rumaila and late Cenomanian to earliest Turonian Mishrif formations, onshore Kuwait. International Petroleum Technology Conference, 19-22 January, Doha, Qatar, 1-6.

YOUSSEF, A.H., AL-SAHLAN, G., KADAR, A.P., KARAM, K.A., PACKER, S., STARKIE, S. and STEAD, D., 2019. Sequence stratigraphic framework of the Wara and Ahmadi Formations, onshore Kuwait. *Stratigraphy*, **16**, 1-26.

ZARASVANDI, A., CHARCHI, A., CARRANZA, E.J.M. and ALIZADEH, B., 2008. Karst bauxite deposits in the Zagros Mountain Belt, Iran. *Ore Geology Reviews*, **34**, 521-532.

ZEINALZADEH, A. and SAJJADIAN, V.A., 2009. Investigating source rock zones in the Darkhovain oil field by using petrophysics and rock eval analysis. *Journal of Science (University of Tehran) (JSUT)*, **35**, 3, 63-70.

ZHU, Y., SONG, X., SONG, B., TIAN, C., MA, S., GAO, Y., LI, Y., ZHANG., W., LIU, Z., ZHEN, X., LI, B., WU, S., WEI, C., LIU, B. and YANG, Q., 2016. Typical Reservoir Architecture Models, Thief-zone Identification and Distribution of the Mishrif Carbonates for a Super-giant Cretaceous Oilfield in the Middle East. SPE Asia Pacific Oil & Gas Conference and Exhibition. Society of Petroleum Engineers (SPE), 1-12.

ZIEGLER, M.A., 2001. Late Permian to Holocene Paleofacies Evolution of the Arabian Plate and its Hydrocarbon Occurrences. *GeoArabia*, **6**, 445-504.

Table 2. Descriptions of the depositional sequences documented in this study across the entirety of the Arabian Plate. The descriptions are divided by broad geographic area, sequence and systems tract (where applicable).

Sequence	Systems Tract	Southern Plate (Oman, UAE, Saudi Arabia, Qatar, Bahrain, Kuwait and southern Iraq)	Northern Plate (Northern Iraq, southeast Turkey, Syria, Lebanon, Jordan, Israel and Sinai)	Eastern Plate (Southwest Iran)
Late Albian K110 Sequence (Fig. 12a)	**TST**	Transition from siliciclastic muddy ramp to extensive carbonate platform (van Buchem et al., 2011). Carbonate shoal reservoirs recognized within the Mauddud Formation in Kuwait (Strohmenger et al., 2006; Cross et al., 2010).	Rudist reefs developed along northwestern margin of the plate (Bein, 1976; Steuber and Bachmann, 2002; Gardosh, 2002) (Fig. 10a). In northern Iraq, reservoirs within the Qamchuqa Formation consist of alternating limestones and dolostones (Al-Qayim et al., 2010).	Extensive carbonate platform corresponding to the lower part of the Sarvak Formation (van Buchem et al., 2011). An exception is the Garau Basin in Kermanshah Province in Iran which is differentiated from the Arabian carbonate platform during the Albian (Navidtalab et al., 2019) and formed a long-lived intrashelf basin throughout the mid-Cretaceous (Fig. 12a).
	HST			
Early Cenomanian K120 Sequence (Fig. 12b)	**LST**	Platform exposure and karstification recognized in Kuwait (Vincent et al., 2020). In Oman, there no evidence for subaerial exposure with a marine hardground at the top of the Natih-G (van Buchem et al., 2011).	A karstified surface is recognized in northern Iraq (Al-Qayim et al., 2010) and southeast Turkey (Çelikdemir et al., 1991).	Associated with a major karst surface in Fars Province, Iran, which locally condenses the entire Cenomanian and Turonian interval (Vincent et al., 2015) (see Fig. 9; Namak and Asaluyeh outcrops).
Early Cenomanian K120 Sequence (Fig. 12b)	**TST**	Retrogradation during the early TST is associated with the deposition of fine grained marine siliciclastics, which can form regional seals (van Buchem et al., 2002; Youssef et al., 2019; Davies et al., 2019) (Figs 6, 7 and 8). Platform drowning during the late TST is associated with development of intrashelf basins in Oman, UAE, Saudi Arabia and southern Iraq (van Buchem et al., 2002; Mahdi and Aqrawi, 2014; Vahrenkamp et al., 2015) (Fig. 11b). Organic-rich carbonates deposited within these intrashelf basins are important source rocks (van Buchem et al., 2002; van Laer et al., 2019).	Siliciclastics associated with the retrogradation of the Arabian Shield shoreline during the early TST are recognized in Jordan (Schulze et al., 2005) and Sinai (Bauer et al., 2003). Intrashelf basin development in southeast Turkey is associated with platform drowning during the late TST. The Derdere Formation consists of deeper-water facies in its lowermost parts (Özkan and Altiner, 2019; Simmons et al., 2020) and contains organic-rich carbonate units which have source rock potential (Demirel et al., 2001) (see Fig. 10; Karakopru 1 well).	Characterized by the development of intrashelf basins. Hemipelagic carbonates within the Sarvak Formation are recognized within intrashelf basinal areas in onshore Iran (Razin et al., 2010; Piryaei et al., 2010; Vincent et al., 2015; Navidtalab et al., 2020; Kalanat et al., 2021) (Figs 9 and 12b). Organic-rich carbonates were deposited within the northern portion of the Shilaif intrashelf basin which extends into the Iranian offshore (Hosseiny et al., 2016),
	HST (Fig. 11b)	Associated with the strong progradation of intrashelf basin shelf margins (Droste and Steenwinkel, 2004; Vahrenkamp et al., 2015) (Fig. 11b). Characterized by rudist-rich grainy facies belts with clinoform geometries (Wharton, 2015). These progradational belts have high reservoir potential (Perrotta et al., 2017; Lu et al., 2018).	Extensive carbonate platforms are recognized across the northern part of the Arabian Plate (Buchbinder et al., 2000; Bauer et al., 2003; Schulze et al., 2005; Powell and Moh'd, 2011). The intrashelf basin in southeast Turkey is infilled by carbonate progradation. A shallowing upwards succession is recognized with the Deredere Formation (Çelikdemir et al., 1991; Özkan and Altiner, 2019; Simmons et al., 2020).	Progradational infill of intrashelf basins within the Iranian onshore. High energy rudist-rich grainstone facies are widely recognized (Razin et al., 2010; Vincent et al., 2015) (Fig. 11B).
Middle Cenomanian K130 Sequence (Fig. 12c)	**LST (Fig. 11c)**	Significant relative sea-level fall of ~30 m (as determined from incision into the top of the Natih E in Oman) (Grélaud et al., 2006, 2010; Homewood et al., 2008). A regional subaerial exposure surface marked by karstification within platform areas (Hollis, 2011; van Buchem et al., 2011).	Significant disconformity and hiatus in northern Iraq that corresponds to the break-up of the long-lived Qamchuqa carbonate platform (Ameen and Gharib, 2013). In some areas, this unconformity may be superimposed with older sequence boundaries with a hiatus spanning the Late Albian to Campanian (Packer et al., 2021).	Karstified disconformity within the Sarvak Formation in Iran (Mehrabi and Rahimpour-Bonab, 2014; Malekzadeh et al., 2020).
Middle Cenomanian K130 Sequence (Fig. 12c)	**TST**	Low relief muddy carbonate ramp with alternating carbonate and siliciclastic cycles in platform areas (van Buchem et al., 2002; Droste and Steenwinkel, 2004; Craigie, 2015) (Fig. 7). K130 is a low accommodation depositional sequence in Oman and Saudi Arabia that lacks intrashelf basin development (Figs 12c and 13c). Continuation of deep-marine hemipelagic deposition in long-lived Cenomanian intrashelf basins such as the Shilaif Basin in UAE (Vahrenkamp et al., 2015) and Najaf Basin in southern Iraq (Aqrawi and Horbury, 2008) (Fig. 12c).	A stratigraphic hiatus is recognized within the middle Cenomanian within platform areas of northern Iraq (Ameen and Gharib, 2013; Ghafur et al., 2020) (Fig. 2). Along the northwestern margin of the plate, mixed siliciclastics and shallow marine carbonate facies are recognized within a homoclinal ramp system (El-Araby, 2002; Farouk et al., 2017). There is evidence for local drowning of the carbonate ramp in the Coastal Plain of Israel (Lipson-Benitah et al., 1990; Buchbinder et al., 2000; Gardosh et al., 2008) and the formation of an isolated intrashelf basin in Jordan (Schulze, 2003) (Figs 10 and 12c).	The aerial extent of intrashelf basins in Iran is reduced in the Middle Cenomanian relative to the Early Cenomanian (Piryaei et al., 2010; Razin et al., 2010; Vincent et al., 2015; Kalanat et al., 2021). This follows the regional pattern of low accommodation within the K130 sequence as observed in Oman and Saudi Arabia. The Iranian intrashelf basins that continue into the Middle Cenomanian may have a structural control as they partially coincide with WNW-ESE and ENE-WSE trending basement faults (Navidtalab et al., 2020) (Fig. 12c).
	HST (Fig. 13d)	Relatively stable shelf margins surrounding the Shilaif and Najaf intrashelf basins are characterized by aggradation and minor progradation (Fig. 13d). The K130 HST is a prolific reservoir interval within southeast Iraq associated with rudist grainstone shoals within the Mishrif Formation (Fig. 6) (Aqrawi et al., 2010; Mahdi et al., 2013; Mahdi and Aqrawi, 2014; Yixiang et al., 2016; Cantrell et al., 2020).		
Late Cenomanian - early Turonian K140 Sequence (Fig. 12d)	**LST**	The K140 LST is not typically associated with channel incision or extensive karstification at the regional scale (Hollis, 2011). However, in south-eastern Iraq, meteoric diagenesis and karstification of carbonate reservoirs is recognized beneath the Late Cenomanian 'Mishrif Disconformity' (Mahdi et al., 2013; Mahdi and Aqrawi, 2014; Cantrell et al., 2020).	The transgressive surface is recognized as a drowning unconformity across the northernwestern margin of the plate (Buchbinder et al., 2000; Bauer et al., 2003; Schulze et al., 2005; Gertsch et al., 2008; Wendler et al., 2010b) and in northern Iraq (Karim and Taha, 2009) (Fig. 11).	Exposure surface within the Sarvak Formation in platform successions, but not typically associated with extensive karstification or meteoric diagenesis (Vincent et al., 2015).

Table 2 (*cont.*).

Late Cenomanian - early Turonian K140 Sequence (Fig. 12d)	**TST**	Characterized by the renewed generation of intrashelf basins in Oman and Saudi Arabia (van Buchem et al., 2002; Craigie, 2015) and continuation of hemipelagic deposition in the Shilaif and Najaf intrashelf basins (Fig. 12d).	Platform drowning along the northwestern margin of the plate characterized by the deposition of condensed deep marine ammonite-rich carbonates, marls and black shales (Lipson-Benitah et al., 1990; Buchbinder et al., 2000; Bauer et al., 2003; Schulze et al., 2005; Gertsch et al., 2008; Wendler et al., 2010b) (Fig. 10). In northern Iraq, the K140 sequence is also associated with platform drowning and the deposition of the Dokan and Gulneri formations (Haddad and Amin, 2007) (see Fig. 10; Taq Taq well, and Fig. 12d). The Gulneri Formation consists of organic-rich hemipelagic facies, rich in planktonic foraminifera recording deep-marine conditions within tilted half-graben ramp systems. The Gulneri Formation is assigned to the late Cenomanian based on association with the δ13C isotope excursion characteristic of OAE2 (Al-Sagri, 2015). However, it has also been dated as early Turonian (e.g. Haddad and Amin, 2007). The Deredere Formation in southeast Turkey also records deeper water facies within its uppermost part (K140 sequence) (Özkan and Altiner, 2019; Simmons et al., 2020).	Renewed development of intrashelf basins in onshore Iran (Razin et al., 2010; Vincent et al., 2015) (Fig. 12d). A potential hiatus or extremely condensed section is recognized in the latest Cenomanian to earliest Turonian at the Anaran NW Dome outcrop section on the margin of the Garau Basin (Sharp et al, 2010) (Fig. 9). The latest Cenomanian OAE2 event stratigraphy is not detected at this otherwise stratigraphically complete outcrop.
	HST (Fig. 13f)	Strong progradation of shelf margins filled accommodation within intrashelf basins in Oman and Saudi Arabia (van Buchem et al., 2002; Droste and Steenwinkel, 2004; Vahrenkamp et al., 2015) (Fig. 13f). This highstand sequence is associated with prolific reservoirs intervals within the Natih-A (van Buchem et al., 2002) and Mishrif Formation of UAE (Burchette and Britton, 1995; Vahrenkamp et al., 2015; Franco et al., 2018). In southern Iraq, the Najaf intrashelf basin was infilled with a succession of shallowing upwards carbonates of the Mishrif Formation.		
Early-middle Turonian Tu1 Sequence (Fig. 12e)	**LST**	Tectonically enhanced lowstand associated with meteoric diagenesis and karstification on top of carbonate platforms (van Buchem et al., 2002; Hollis, 2011). The Tu1 SB can be superimposed with the K150 SB to form a composite unconformity result of regional Turonian uplift (van Buchem et al., 2011).In the Shilaif intrashelf basin the Tu1 LST is recorded by thick siliciclastics of the Tuwayil Formation (Al-Zaabi et al., 2010; Vahrenkamp et al., 2015; Franco et al., 2018) (see Fig. 6; Shilaif Basin well).	Typically, a submarine hardground within platform drowning succession (Bauer et al., 2003; Schulze et al., 2005)	Major karstification surface that significantly enhances reservoir quality within the Sarvak Formation (e.g. Ahwaz 355 well; Fig. 9) (Rahimpour-Bonab et al., 2013; Mehrabi and Rahimpour-Bonab, 2014; Hajikazemi et al., 2017; Malekzadeh et al. 2020). A correlative conformity is interpreted at a submarine hardground in deeper-water settings (e.g. Anaran NW Done outcrop; Fig. 9) (Sharp et al., 2010).

Early-middle Turonian Tu1 Sequence (Fig. 12e)	**TST**	Early-middle Turonian carbonates of the Ruwaydha Formation overly siliciclastics of the Tuwayil Formation in the vicinity of the Shilaif Basin (Vahrenkamp et al., 2015; Franco et al., 2018; Van Laer et al., 2019) (Fig. 6). The top of the Natih A in parts of southeast Saudi Arabia may extend into the middle Turonian. The uppermost cycle of organic-rich carbonates recognized in the correlation of Droste and Van Steenwinkel, (2004) is interpreted within the Tu1 sequence, but age constraint cannot be confirmed (see Fig. 6; Hamidan-1 well).	Along the northern margin of the Arabian Plate, deep-marine deposition is recorded during the Tu1 sequence across the drowned carbonate platform in Sinai (Bauer et al., 2003), Israel (Buchbinder et al., 2000), Jordan (Schulze, 2003; Farouk et al., 2017) and Lebanon (Saint-Marc., 1981) (Fig. 12e). In northern Iraq, deep water carbonate facies of the Kometan Formation were deposited during the Turonian within inclined half graben ramp structures (Haddad and Amin, 2007) (Fig. 10). In southeast Turkey, the Karababa-A Member spans the Turonian based on biostratigraphy and carbon isotopes (Mülayim et al., 2020). The Karababa-A Member is an organic-rich carbonate with average TOC of 1.4 wt.% (Demirel and Guneri, 2000) and was deposited within an intrashelf basin or restricted lagoon environment (Çelikdemir et al., 1991) (see Fig. 10 - Karakopru 1 and Akcakale 1 wells, and Fig. 12e).	Within the Dezful Embayment of Iran shallow-marine carbonate deposition may have continued into the early Turonian (e.g. Ahwaz and Marun fields) (see Fig. 9; Ahwaz-355 well). The *Nezzazatinella-Dicyclina* biozone ofWynd, (1965) is recognized within wells from these fields suggesting a possible early Turonian age for the uppermost part of the Sarvak Formation (Rahimpour-Bonab et al., 2013; Omidvar et al., 2014). However, definitive proof of early Turonian Sarvak Formation in platform settings is lacking from the microfauna present (Schlagintweit and Simmons, 2022).
	HST			
Middle-late Turonian Tu2 Sequence (Fig. 12f)	**LST** **TST** **HST**	There is no evidence for the preservation of middle-late Turonian stratigraphy within the southern part of the Arabian Plate. This sequence is absent at the composite Turonian unconformity (K150 SB).	In the onshore Levant, mixed carbonate-siliciclastic ramp systems are documented within the middle-late Turonian (Buchbinder et al., 2000; Bauer et al., 2003; Powell and Moh'd, 2011). High energy carbonate facies are recognized (Saint-Marc, 1981; Bauer et al., 2003; Schulze et al., 2005) (Figs 10 and 12f). In northern Iraq, the middle-late Turonian is represented by deep-marine hemipelagic facies of the Kometan Formation (Haddad and Amin, 2007), while in southeast Turkey, it is represented by organic-rich carbonates of the Karababa-A Member (Mulayim et al., 2020) (Figs 10 and 12f).	Middle-late Turonian stratigraphy in southwest Iran is generally absent at the regional Turonian unconformity. An exception is documented at the Anaran NW Dome outcrop section on the margin of the Garau Basin. At this locality the uppermost part of the Sarvak Formation contains deeper-water micrites and wackestones that span the *M. schneegansi* biozones indicating deposition into the middle-late Turonian on the slope of this long-lived depocenter (Sharp et al., 2010) (Fig. 9).